Air Force Institute of Technology
AFIT Scholar

Theses and Dissertations | Student Graduate Works

3-10-2010

Performance of a Small Internal Combustion Engine Using N-Heptane and Iso-Octane

Cary W. Wilson

Follow this and additional works at: https://scholar.afit.edu/etd

 Part of the Aeronautical Vehicles Commons, and the Propulsion and Power Commons

Recommended Citation
Wilson, Cary W., "Performance of a Small Internal Combustion Engine Using N-Heptane and Iso-Octane" (2010). *Theses and Dissertations*. 2059.
https://scholar.afit.edu/etd/2059

This Thesis is brought to you for free and open access by the Student Graduate Works at AFIT Scholar. It has been accepted for inclusion in Theses and Dissertations by an authorized administrator of AFIT Scholar. For more information, please contact richard.mansfield@afit.edu.

PERFORMANCE OF A SMALL INTERNAL COMBUSTION ENGINE USING N-HEPTANE AND ISO-OCTANE

THESIS

Cary W. Wilson, Captain, USAF

AFIT/GAE/ENY/10-M28

DEPARTMENT OF THE AIR FORCE
AIR UNIVERSITY

AIR FORCE INSTITUTE OF TECHNOLOGY

Wright-Patterson Air Force Base, Ohio

APPROVED FOR PUBLIC RELEASE; DISTRIBUTION UNLIMITED

The views expressed in this thesis are those of the author and do not reflect the official policy or position of the United States Air Force, Department of Defense, or the United States Government. This material is declared a work of the U.S. Government and is not subject to copyright protection in the United States.

AFIT/GAE/ENY/10-M28

PERFORMANCE OF A SMALL INTERNAL COMBUSTION ENGINE USING N-HEPTANE AND ISO-OCTANE

THESIS

Presented to the Faculty

Department of Aeronautics and Astronautics

Graduate School of Engineering and Management

Air Force Institute of Technology

Air University

Air Education and Training Command

In Partial Fulfillment of the Requirements for the

Degree of Master of Science in Aeronautical Engineering

Cary W. Wilson, BS

Captain, USAF

March 2010

APPROVED FOR PUBLIC RELEASE; DISTRIBUTION UNLIMITED

AFIT/GAE/ENY/10-M28

PERFORMANCE OF A SMALL INTERNAL COMBUSTION ENGINE USING N-HEPTANE AND ISO-OCTANE

Cary W. Wilson, BS

Captain, USAF

Approved:

_____//SIGNED//_____	_____
Paul I. King	Date
_____//SIGNED//_____	_____
Frederick R. Schauer	Date
_____//SIGNED//_____	_____
Frederick G. Harmon	Date

Abstract

With the sustained interest in Unmanned Aircraft Systems (UAS) and Micro Air Vehicles (MAV), the military services have a real need for vehicles powered by an internal combustion (IC) engine that can run efficiently on heavy hydrocarbon fuels, especially JP-8 due to established logistics. This thesis concerns the results of running a two horsepower, 4-stroke, spark-ignition engine (FUJI BF34-EI) with both iso-Octane and n-Heptane. Results include the knocking characteristic of this engine with n-Heptane, a comparison of the brake specific fuel consumption (BSFC) of the two fuels in a factory delivered engine configuration with a 17x10 APC propeller loading, a comparison of the heated fuel effects on BSFC and torque of the two fuels and the effects of varied spark timing with n-Heptane on BSFC and torque. It is shown with stock ignition timing and fuel at ambient temperature, n-Heptane exhibits on average less specific fuel consumption than iso-Octane; specifically, an average of 4.1% over the entire engine loading and 12.61% over the stock propeller engine loading. It is concluded that the knocking characteristic of a zero octane number (ON) fuel using a stock configuration in this engine is negligible, thus allowing the USAF to use any ON fuel for this particular engine. Additionally, with spark timing advanced or retarded beyond the stock setting, it is shown to decrease BSFC on average 9.4% with n-Heptane. Lastly, the performance effects of heating n-Heptane up to 344K and iso-Octane up to 311K are shown to be negligible.

Acknowledgments

I would like to thank my academic advisor, Dr. Paul King, and the research sponsor, Dr. Fred Schauer, for allowing me the opportunity to work on this research with them. Thank you Dr. King for the numerous hours spent in your office discussing this research and furthering my understanding of it. Thanks Fred for believing in me in the beginning and letting me work in your lab.

This research would not have been accomplished if it weren't for the help and guidance of several key players that work in D-Bay. Dr. John Hoke and Adam Brown were instrumental in assisting me with the experimental setup and I appreciate their patience in helping me understand many key concepts for this research. Thanks to Dave Burris for writing the LabView program and to Jacob Baranski for his work on the varied spark timing program. I would like to thank Curtis Rice for his always willing lab support, which included anything from helping me find materials to explaining the purpose of circuit board components to me. Also thanks to Justin Goffena for always lending a helping hand.

Lastly, but most importantly, I would like thank my wife. From being covered with homework and class projects in the beginning, to being stuck at the lab for late hours in the end, she has supported me the whole way.

Table of Contents

Page

List of Figures

Page

List of Tables

Page

List of Symbols

Acronyms

AFIT = Air Force Institute of Technology
AFRL = Air Force Research Laboratory
ASTM = American Society for Testing and Materials
ATDC = After Top Dead Center
BDC = Bottom Dead Center
BTDC = Before Top Dead Center
DAQ = Data Acquisition
IC = Internal Combustion
MON = Motor Octane Number
NATO = North Atlantic Treaty Organization
ON = Octane Number
OSD = Office of the Secretary of Defense
RON = Research Octane Number
RPM = Revolutions Per Minute
RZTC = Combustion Branch
TDC = Top Dead Center
UAS = Unmanned Aerial System
UAV = Unmanned Aerial Vehicle
VTD = Vehicle Technology Directorate
USAF = United States Air Force

Subscripts

b = brake
boil = boil
c = clearance
conv = convection
crit = critical
D = diameter
d = displacement
f = formation
fuel = fuel
g = gas
i = inlet
o = outlet
lm = log mean
s = surface

Symbols – [] denotes SI units and {} denotes English units

A = area [cm^2] {in^2}
a = acceleration [cm/s^2] {in/s^2}
b = cylinder bore [cm] {in}
bmep = brake mean effective pressure [Pa] {psi}
bsfc = brake specific fuel consumption [g/hr/kW] {lb/hr/hp}
C_p = constant pressure specific heat [J/(kg*K)] {BTU/(lbm*°R)}
D = diameter [cm] {in}
h = convection coefficient [W/m^2*K] {$BTU/(hr*ft^2*°F)$}
H = enthalpy [kJ/kg] {BTU/lbm}
HHV = combustion higher heating value [kJ/kg] {BTU/lb}
K = thermal conductivity [W/m*K] {BTU/(hr*ft*°F))
L = tube length [cm] {in}
l = rod length [cm] {in}
LHV = combustion lower heating value [kJ/kg] {BTU/lb}
$\dot{m}$ = mass flow rate [kg/s] {lbm/s}
MW = molecular weight [kg/kmol]
N = engine speed [RPM]
Nu = nusselt number
P = power [W] {HP}
p = pressure [atm] {psi}
q = heat transfer rate [W] {BTU/hr}
r = crankshaft radius [cm] {in}
Re = reynolds number
s = piston stroke distance [cm] {in}
T = temperature [K] {°F}
U = piston speed [cm/s] {in/s}
V = volume [cm^3] {in^3}
# = number

Greek Symbols – [] denotes SI units and {} denotes English units

Δ = change in
p = pi [3.14]
ρ = density [g/ml] {lbm/ft^3}
μ = viscosity [Pa-s] {}
θ = crankshaft angle [degrees]
t = torque [N-m] {ft-lb}

PERFORMANCE OF A SMALL INTERNAL COMBUSTION ENGINE USING N-HEPTANE AND ISO-OCTANE

I. Introduction

Overview

Since 1988, the North Atlantic Treaty Organization (NATO) nations have been mandating the single fuel concept, JP8, for use in all military aircraft, vehicles and equipment[1]. The concept is simple; mandate everything to use the same fuel and eliminate the major logistics train, i.e. costs, needed to support many different fuels. In an internal combustion (IC) engine the primary issue with JP-8, a low ON (15-25) [2] heavy fuel with similar characteristics to diesel fuel, is the difficulty in vaporizing the fuel to obtain higher combustion efficiency and improved power specific fuel consumption. The purpose of this paper is to study the effects of using pure hydrocarbon fuels of varied octane ratings in a spark ignition engine. The fuels used will be the limits of the octane number (ON) range: n-Heptane (zero ON) and iso-Octane (100 ON). The engine used in this study is the FUJI BF34-EI, a 33.5cc 4-stroke spark ignition IC engine, factory rated for gasoline. This engine is currently being used in the Army's Silver Fox unmanned aerial system (UAS) platform. Accompanying the single fuel concept, the Office of Secretary of Defense's (OSD) latest Unmanned Aircraft Systems roadmap outlines clear direction, "Develop and field reliable propulsion alternatives to gasoline-powered internal combustion engines"[3]. The directives

from NATO and the OSD are clear; develop platforms from inception to use JP-8 (or other logistically supportable alternatives) or retrofit current platforms in the field to do so. The results in this paper take steps to satisfy these objectives.

Research Objectives

The primary goal of this research is to evaluate the ON effects on a FUJI BF34-EI, small 4-stroke spark ignition engine as preliminary steps to using a military grade JP-8 jet turbine fuel. This primary objective can be split into specific research objectives and tasks needed to be completed for the experimental setup.

1. Research Objectives
    a. Demonstrate that this engine is able to be used as delivered from the factory with n-Heptane.
    b. Compare the BSFC of n-Heptane with iso-Octane over the entire engine loading and specifically for a 17x10 propeller loading.
    c. Show that BSFC can be decreased and torque increased by optimizing the timing with n-Heptane.
    d. Compare the effects of heated fuel on BSFC and torque between n-Heptane and iso-Octane.
2. Tasks needed for the design and fabrication of the dynamometer test stand

a. Complete the design and fabrication of the engine mounting system.
b. Design and fabricate the engine cooling system, engine to dynamometer coupling, engine starting system, throttle control system, fuel heating system and controller and the variable spark timing system.
c. Evaluate the supplied dynamometer.
d. Organize design requirements for the small engine LabView test program.

Organization

Chapter I served as an overview of an Air Force issue corresponding to the research presented in this thesis. Additionally it outlined the objectives of the research. Chapter II will discuss several engineering fundamentals of internal combustion engines, as well as outline brief synopses of other relevant research. In Chapter III, the details of the experimental setup and facility, including test hardware, software and experimental configurations are discussed. Chapter IV will outline the results and analysis of the research. Chapter V will summarize the previous chapters and provide a list of recommended future research and equipment or tasks that need to be conducted.

II. Background

Chapter Overview

This chapter will discuss several fundamental internal combustion engine concepts useful to this particular research, such as the Otto 4-stroke cycle, abnormal combustion (knock and surface ignition) and octane rating. Performance criteria for an IC engine will be discussed and engineering formulas presented. To conclude the chapter, several previous research efforts will be presented with the relevant data discussed.

Internal Combustion Engine Overview

Currently in the aerospace community, internal combustion engines are more a legacy propulsion technology, giving way to turbines, scramjets and ramjets. Conversely, with the ever emergence of small UAS's, the focus has started to come back to IC engines. IC engines, alone or with hybrid's, are undeniably the propulsion choice for a high percentage of today's UAS's. With this fact, some fundamental concepts and issues must be explored and understood.

Engine Types and Operation.

The two most common types of engines used today are the gasoline engine and the diesel engine. Gasoline engines are typically categorized as using an Otto cycle and require a spark plug for the ignition to begin the combustion process. The Otto cycle's foundation lies with the assumption that the combustion event occurs quick enough to happen during the time when the

piston is at top dead center, or in other words during constant volume. In contrast, a Diesel cycle assumes a constant pressure state of combustion. The Diesel cycles are typically associated with diesel fuel engines and rely on auto-ignition to start the combustion process. The Fuji research engine is a gasoline engine, therefore the Otto cycle will be looked at in more detail.

Nicolaus Otto invented the first practical four stroke internal combustion engine in 1876 and called it the “Otto Cycle Engine” [4]. A four stroke cycle refers to one when there is one power stroke per two revolutions of the engine. The pressure-volume diagram of the Otto cycle can be seen in Figure 1. The numbers on the diagram represent the specific event in the four stroke cycle listed in Table 1.

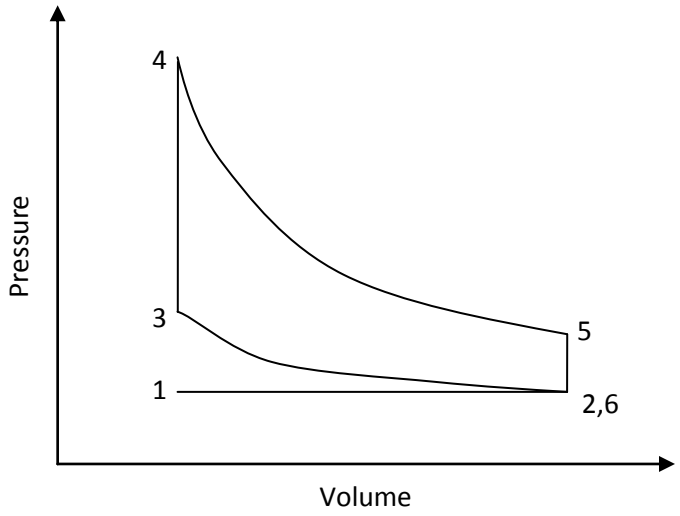

Figure 1. Ideal Otto cycle

During the intake process, the piston is moving toward bottom dead center (BDC) while bringing the fuel/air mixture into the cylinder at atmospheric pressure, therefore increasing the cylinder volume. During the compression

stroke, the piston is moving toward top dead center (TDC) increasing the pressure and decreasing the volume in the cylinder. Now the combustion process takes place while the piston is at TDC with a constant volume and creates a pressure spike.

Table 1. Ideal Otto cycle processes

Cycle Event	Process Name
1 → 2	Intake
2 → 3	Compression
3 → 4	Combustion
4 → 5	Expansion
5 → 6	Heat Rejection
6 → 1	Exhaust

Next is the expansion, or power stroke, where the piston is sent back toward BDC where pressure is decreasing and the cylinder volume is increasing. The exhaust valve is then opened while the piston is at BDC with constant volume and therefore letting heat leave the cylinder and reducing pressure. Finally, the piston approaches TDC again allowing the exhaust to exit the cylinder at atmospheric pressure, with the volume in the cylinder decreasing. It should be noted that this cycle is ideal and due to inefficiencies may not be realistic.

The Fuji engine uses a carburetor to meter the fuel; therefore the fuel is pulled into the air stream which forms a homogenous mixture by the time it is pulled into the cylinder. In order for the engine to operate smoothly, the homogeneous mixture needs to exhibit a controlled burn during combustion. The fuels octane number can affect this greatly and will be discussed in the next section along with issues from uncontrolled burning.

Octane Number.

The octane rating of the fuel is a key parameter when addressing the knock characteristics in a spark ignition engine. In 1927, Graham Edgar created the octane rating system, based on a high and low reference fuel; iso-Octane and n-Heptane, respectfully [4]. The objective was to take a new fuel, test its anti-knock characteristic, and then compare and match it to the characteristics of a blend of the two reference fuels. The corresponding octane rating would then be the percent of iso-octane contained in that particular blend. Today, there are two main methods to test the knock characteristics of the fuels, a research octane number (RON) method and a motor octane number (MON) method. The RON standard was adopted by the American Society for Testing and Materials (ASTM) in 1951. RON is regarded as the more important method due to its operating conditions matching more closely to real world application. The MON standard was adopted by ASTM in 1939 and is regarded as a more stringent method. Table 2 shows the operating conditions for the two methods [5].

Table 2. Operating conditions for two octane number methods

Condition	RON	MON
Inlet Temperature	52°C (125°F)	149°C (300°F)
Inlet Pressure	Atmospheric	
Humidity	0.0036-0.0072 kg/kg dry air	
Coolant Temperature	100°C (212°F)	
Engine Speed	600 RPM	900 RPM
Spark Advance	13° BTDC	19-26° BTDC
Air/Fuel Ratio	Adjusted for maximum knock	

The United States uses an antiknock index, the mean of the RON and MON given by Equation 1, that is currently used to assign a fuel's octane rating[5].

$$Antiknock\ Index = \frac{RON+MON}{2} \quad (1)$$

Abnormal Combustion.

Normal combustion can be characterized by a fuel/air mixture whose combustion event is initialized only by the spark event and travels at a uniform speed and burn rate throughout the cylinder. The combustion should move uniformly from the origination of the spark event, three dimensionally outward toward the cylinder walls. On the other hand, abnormal combustion does not follow this routine and is grouped into two categories; knock and surface-ignition.

Knock is another term for abnormal detonations of the fuel/air mixture after the spark event and earned its name due to the metallic pinging sound it makes on the engine cylinders which can be heard by the human ear. These detonations normally cause much higher cylinder pressures and create a shock wave that propagates through the cylinder in an oscillatory manner. Figure 2 illustrates the effect of several intensities of knock on in-cylinder pressure of an IC engine [5]. Notice for normal combustion, a smooth uniform pressure profile should be exhibited. The cause of knock can be attributed to incorrect spark timing, compression ratio, cylinder temperature/pressure, or fuel octane rating. If the spark timing is too advanced, it will create too much of a pressure increase in the cylinder causing the remaining fuel to auto-ignite. If the compression ratio of the engine is too high for the octane rating of the fuel, detonation will occur. As discussed in the previous section, the octane rating of the fuel is a direct indicator on the knocking characteristic using a particular fuel. The higher the

octane rating of the fuel the less likely you are to have knock exhibited. In this thesis, the knocking characteristics will be examined with the spark timing and compression ratio fixed and with either the fuel octane rating varied or fuel temperature increased. Since n-Heptane has a zero octane rating, the engine is expected to demonstrate high signs of knocking.

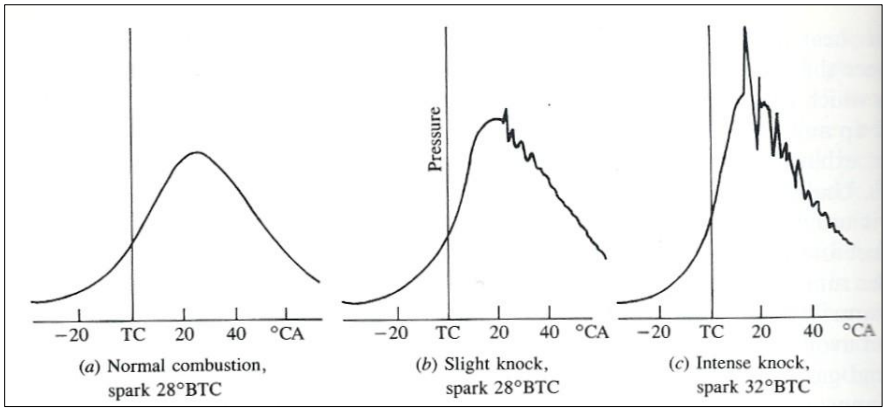

Figure 2. Engine knock intensities [5]

The second type of abnormal combustion is called surface-ignition. This event is when the mixture is ignited by something other than the spark event. This can occur before the spark event, pre-ignition, but can also occur after, post-ignition. The cause is due to “hot spots” left on the cylinder walls by glowing carbon build up or an overheated spark plug and/or exhaust valve.

Research Fuels.

The two fuels that will be used in this research are n-Heptane and iso-Octane due to their octane number rating and because they are pure simple chain hydrocarbon fuels. Iso-Octane is expected to provide similar performance as gasoline and will be used as a reference. N-Heptane is a zero octane fuel

being used to ideally isolate the effects of its low octane rating from additional chemical effects that would be present using a complex chain hydrocarbon such as JP-8. Several physical and thermodynamic properties of these two fuels can be found in Table 3[6][7][8].

Table 3. Properties of n-Heptane and i-Octane; fuel boiling temperature, heating values and latent heat of formation taken at 1 atm, density and specific heat are function of fuel temperature at 1 atm.

Fuel	Formula	MW (kg/kmol)	T_{boil} (K)	T_{crit} (K)	P_{crit} (MPa)	HHV (kJ/kg)	LHV (kJ/kg)
n-Heptane	C_7H_{16}	100.20	371.60	537.70	2.62	48,456	44,926
i-Octane	C_8H_{18}	114.22	398.40	567.50	2.40	48,275	44,791
	H_{fg} (kJ/kg)	ρ (kg/m^3)			C_p (kJ/kg*K)		
	316	$(-0.8624)T_{fuel} + 936.24$			$(0.0039)T_{fuel} + 1.0805$		
	300	$(-0.8169)T_{fuel} + 941.53$			$(0.0037)T_{fuel} + 1.1331$		

T_{boil} is the temperature at which the fuels vapor pressure equals atmospheric pressure, and therefore the liquid begins to transform into a vapor. The critical temperature and pressure, T_{crit} and P_{crit}, are the points at which there is no distinct liquid or vapor phase. The heating values, or heat of combustion, represent the amount of energy produced from a complete combustion of fuel and oxygen. The higher heating value assumes that all of the water in the combustion products has condensed to a liquid, where the lower heating value assumes the opposite [8]. The latent heat of formation, H_{fg}, is the amount of energy needed to transform the species from a liquid to a vapor and is measured at the boiling point. The density and specific heat of the two fuels are listed as

linear functions of temperature in Table 3, with a correlation to the actual values of at least 99.97%.

Engine Geometry.

There are several important geometric features of an IC engine that need to be defined. A cylinder is made up of three distinct components; the crankshaft, connecting rod and piston, which are illustrated in Figure 3. The bore, *b*, is defined as the diameter of the cylinder.

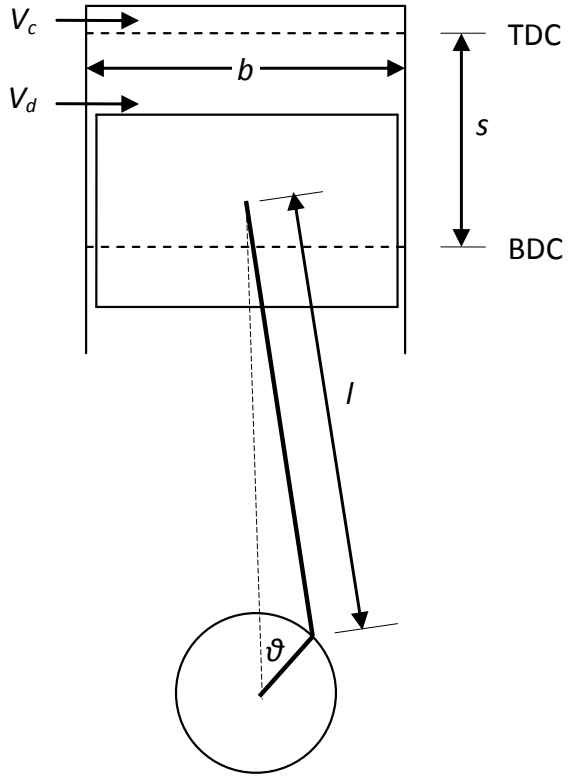

Figure 3. Engine cylinder geometry

The crank angle, θ, is defined as the change in angle between the current crankshaft position and the position of the crankshaft when the piston is at the top of the stroke. TDC, θ = 0°, is defined as the highest point that the piston

travels in the cylinder, or can be defined as the top of the stroke. Inversely, BDC, θ = 180°, is the bottom of the stroke, or lowest point in the cylinder that the piston travels. The stroke, *s*, is defined as the linear distance the piston travels between TDC and BDC. The connecting rod connects the piston to the crankshaft and has a length, *l*.

Compression ratio is an important characteristic of an internal combustion engine and is defined below in Equation 2. High compression ratios are desirable because more energy is able to be extracted from the fuel mixture. However a drawback is a greater tendency of the mixture to detonate; i.e. knock.

$$Compression\ Ratio = \frac{Maximum\ Cylinder\ Volume}{Minimum\ Cylinder\ Volume} = \frac{V_d + V_c}{V_c} \quad (2)$$

Small spark ignition engines typically have a compression ratio between six and eleven [5]. The displacement volume can be expressed in terms of bore and stroke, shown in Equation 3.

$$V_d = \frac{\pi}{4} b^2 s \quad (3)$$

Mean piston speed is the average speed of the piston per cycle and is a function of engine rotation speed and stroke as defined in Equation 4, where *N* is the engine rotation speed.

$$\overline{U} = 2sN \quad (4)$$

Internal Combustion Engine Performance Criteria.

There are three main terms used to evaluate the work done per cycle in an IC engine; power, torque and mean effective pressure. All three can be expressed in terms of each other. Many times these terms will be preceded by the term *brake* meaning final output at the engine shaft or total usable output. Brake torque, τ, is the measure of the work done per unit rotation of the crank and is commonly measured from a dynamometer. The brake power is the rate at which the work is done and can be expressed in terms of torque and engine speed as in Equation 5.

$$P_b = 2\pi N\tau \tag{5}$$

The brake mean effective pressure is the work done per unit displacement volume and is defined in Equation 6 for a four stroke cycle.

$$bmep = \frac{4\pi(\tau_b)}{V_d} = \frac{2P_b}{V_d N} \tag{6}$$

Perhaps the most important performance criterion on an IC engine is its efficiency. This can be expressed by either thermal efficiency or specific fuel consumption, and both are inversely related. For this thesis, the specific fuel consumption will be used to evaluate engine efficiency. This criterion is a measure of how efficiently the engine is using the fuel supplied and turning it into work output. The brake specific fuel consumption is a function of fuel mass flow rate and brake power as expressed in Equation 7.

$$bsfc = \frac{\dot{m}_f}{P_b} \tag{7}$$

With the performance criteria defined, we can now use it in an effective manner to evaluate engine performance. One way to do this is by creating an engine performance map, which illustrates the operating characteristics of an engine over its full load and speed range. A contour plot is used with engine speed as the x-axis, brake mean effective pressure as the y-axis with contour lines representing brake specific fuel consumption. Figure 4 shows an example from a Wankel KKM 502.

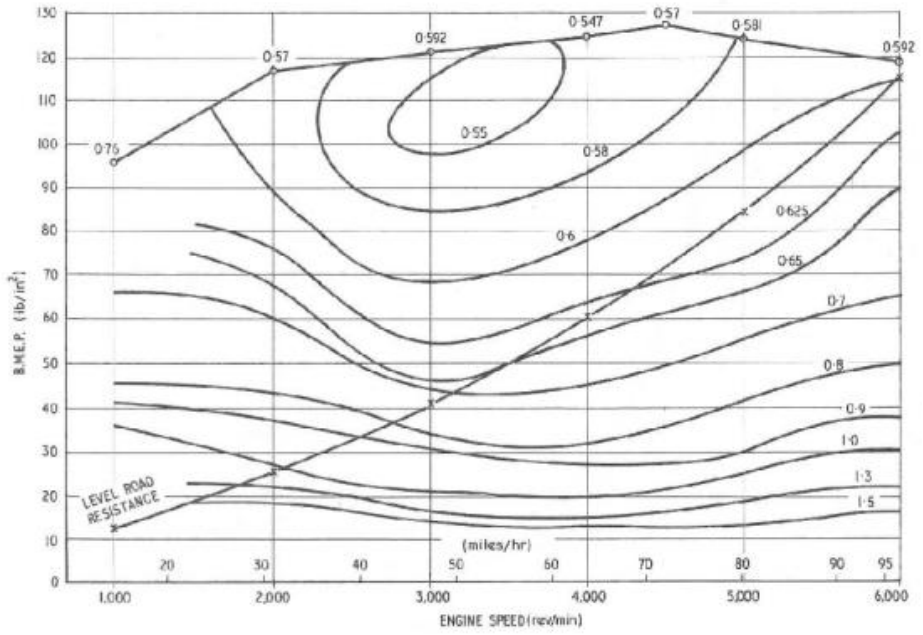

Figure 4. Wankel KKM 502 engine performance map

Notice how the minimum BSFC creates and island on the plot and the values increase as you travel radially outward. This is a typical trend among IC engines.

This performance map can be used to determine the range of loading and speed to operate the engine at to obtain the lowest BSFC.

Relevant Research

U.S. Army Vehicle Technology Directorate (VTD).

The VTD was the organization chosen by the US Army to run tests and develop procedures for operating the FUJI BF-34EI IC engine on JP-8. Since this engine is the current power plant of the Silver Fox UAS, it was chosen for the research. The VTD's mission is to explore and develop new propulsion technologies and have been promoting small propulsion efforts for several years. Two key points addressed in this research that will be discussed is one, JP-8 starting issues, and two, engine performance analysis with JP-8.

The basic laboratory experimental setup included a water brake for engine loading and both a belt pulley mechanism and direct drive coupling for connection of the engine. The belt pulley mechanism was used for a majority of the testing, but was found to be troublesome due to belt slippage and engine structural failures because of the increased stresses. The direct drive configuration consisted of a Lovejoy Jaw/Spider type aluminum coupling, which also had issues with its rapid wear and failures due to the pulsing loads of the IC engine. The LabView Signal Express served as the data acquisition software and they used a large amount of instrumentation to measure pressures (in-cylinder, inlet, crankcase, ambient and carburetor), temperatures (in-cylinder, head, front/rear bearing, inlet air/fuel, crankcase), spark, speed and torque.

The first issue that was addressed in the research was cold starting the engine with JP-8. Eight different methods were tried and only three were considered successful. The methods that did not succeed, for different reasons, were a direct JP-8 start, heated fuel to 395K, heated fuel with hot air, copper heater adapter to raise fuel temp to 670K, and heating the cylinder head with heat tape. The first method that worked consisted of starting the engine with gasoline and then transitioning to JP-8. This method was the simplest, but would still require gasoline in the field, defeating the purpose. The second method was to heat the cylinder head to at least 367K with a hot air gun, which worked but was unfavorable due to requiring a heat gun with a 120V source which could be hard to obtain in the field. The third, and preferable, successful method included using a localized air/fuel heating source. This localized source takes power from a 12V automobile battery and only requires around 2 minutes to heat to desired temperatures. However, n-Heptane or iso-Octane used in this research, cold starting was not an issue and none of these methods were needed.

The water brake was used to measure the performance of this engine with both gasoline and JP-8. An automated program was setup to slowly increase the load on the engine until it sensed that the engine exhibited a pre-determined reduction in RPM. Three runs were completed with JP-8 and gasoline. Excessive slippage of the belt was noted in the tests and resulted in a low measured power of ~1 HP with gasoline. With the direct drive configuration and JP-8, a maximum power of ~1.6 HP at 7000 RPM and maximum torque of 1.33

ft-lb at 5500 RPM was measured. Several engine modifications were made to ideally improve peak power and torque, which included carburetor modification for increased air flow, gas ports in the piston head to aid in ring sealing, and re-ringing the piston to reduce ring cylinder clearance. All of the attempted modifications failed to increase power.

Cylinder pressure was taken at a 5 kHz rate and for a peak power stroke resulted in a range of peak pressures between 326.6 - 412.5 psia. It was also noted that they experienced heavy oil blow by during engine testing.

AFRL/RZTC Small Engine Thrust Stand.

At AFRL/RZTC a lot of focus has been transferred to small engines. These engines are the power plant of many new UAS's and normally exhibit poor efficiency. With this in mind a test setup that could measure torque was needed. Additionally since the propellers used on these engines come from the R/C arena, there are not normally thrust coefficients in the specifications. Therefore, a thrust stand, using 25 lb load cells was created to measure thrust and torque on small engines at AFRL/RZTC. The engine looked at in this study was the Fuji BF34-EI.

This thrust stand takes advantage of air bearings to reduce the effects of friction on the results. The authors noted that there was considerable amount of noise in the load cell readings from the vibrations of the one cylinder engine. Using a 17x10 APC propeller, the power, torque, thrust and BSFC were able to be determined. The peak values recorded with that propeller were 1.25 hp, 0.95 ft-lb of torque, 11 lb-force of thrust and a BSFC of 0.4 lb/hr/hp all at around 6500

RPM. These points were recorded using a National Instruments Compact Rio load cell module. The data was taken at 5 kHz with samples being averaged every second. Taking advantage of the Compact Rio data acquisition hardware, some high speed torque data was also presented in this research. This data demonstrates the amount of instantaneous torque that is present in the engine during each cycle. Maximum instantaneous torque at 6300 RPM was shown to be between 6 and 8.3 ft-lb. This information will prove helpful in determining the correct vibration dampers for the dynamometer engine stand.

A disadvantage noted with the static thrust stand is that in order to determine the propeller efficiency, data must be taken at different incoming wind velocities. Additionally, the propeller loading profile will change depending on the incoming wind velocity. Since a wind tunnel was not available, a mobile platform was built to allow the thrust stand to operate at different airspeeds. The results were that as airspeed increases, net thrust decreases and propeller efficiency increases. The static propeller loading profile was used in this Thesis as the dyno operating points where spark timing was varied and stock configurations with each fuel compared. The data from this mobile thrust stand will be important in the future to know where on the engine map the load profiles land when at different wind velocities.

While the thrust stand setup here offers its own advantages, it would not be ideal for this thesis because it relies on a propeller to provide the engine loading, therefore only allowing data to be taken with one engine loading per engine speed. A variable pitch prop could be used to obtain multiple loadings but

one is not currently available. Therefore, for this research a dynamometer was used to apply the engine loading.

Liquid Fuel Injection for a Small Rotary Engine.

The University of California at Berkeley completed research to develop a fuel injection system for a small scale rotary engine. The fuel flow rates in this study were between 10 and 100 mg/sec. These fuel flow rates are about one half of what the Fuji BF-34EI is capable of, but the same concepts, with a larger valve could still be applied. In addition to the fuel metering system, the paper also addressed the need for a small evaporator to heat the fuel. The researchers used a piece of aluminum for the base of the evaporator. Fifty Watt electrical strip heaters were placed on each side of the aluminum block to provide the heat flux. The metal block had three 1/8" channels drilled into it for the fuel passage. A temperature controller that used a thermocouple connected to the aluminum block was used to provide the heat control.

Converting the Fuji's fuel metering device from the carburetor over to fuel injection was not completed, but is included as a future research topic in chapter V. However, a fuel heating system was built and used, which took advantage of concepts from this previous research.

Summary

In this chapter, basic concepts, issues and performance criteria of internal combustion engines were presented. The octane rating scale was introduced and was tied into knocking characteristics and engine compression ratio. Next,

three previous research initiatives were presented with an emphasis on the relevant information that applies to this Thesis. We saw that the US Army had conducted limited dynamometer testing on this research engine, but had hardware issues that could have adversely affected the limited amount of performance data. Also their research was not focused on engine efficiency, but instead on if JP-8 could be used in the field on this engine. AFRL's thrust stand research was presented, but it was determined the thrust stand could not provide the engine loading requirements needed for the research in this Thesis. Finally, the University of California's research was presented with the focus on the heat exchanger they fabricated. The objective of this research is to fill the void of previous work, by providing engine performance data and to complete preliminary steps to use JP-8 in this engine efficiently.

III. Methodology

Overview

The first part of this chapter will lay out the complete experimental setup, which focuses entirely on the dynamometer test stand. The components that will be discussed include the fuel delivery system, air delivery system, dynamometer and its mounting and cooling system, engine and its mounting system, data acquisition hardware, throttle controller, fuel heater, measurement sensors and starter system. Secondly, the actual experimental setup and operating conditions will be shown for each test.

Engine & Dynamometer Test Stand.

Main Components.

The test setup for this research is all in support of the Fuji engine and dynamometer. The engine, shown in Figure 5, is a single cylinder, spark ignition, four stroke gasoline engine. The manufacturer specifications can be found in Table 4.

Table 4. Fuji BF-34EI specifications

Displacement	33.5 cc
Weight	2.0 kg
Bore/Stroke	39 x 28mm
Peak Horsepower	2.0 hp @ 7000 RPM
Peak Torque	1.45 ft-lb @ 5000 RPM
Compression Ratio*	8:1
RPM	1,400 - 9000 RPM
Fuel	Automotive Gasoline

* Measured value. Not specified from manufacturer.

The dynamometer, shown in Figure 6, is a Magtrol 1WB65, which is rated at a max torque of 7.3 ft-lb and uses an eddy-current brake control. The dynamometer is coupled with a power supply, TSC401 torque/speed signal conditioner and the DSP6001 controller.

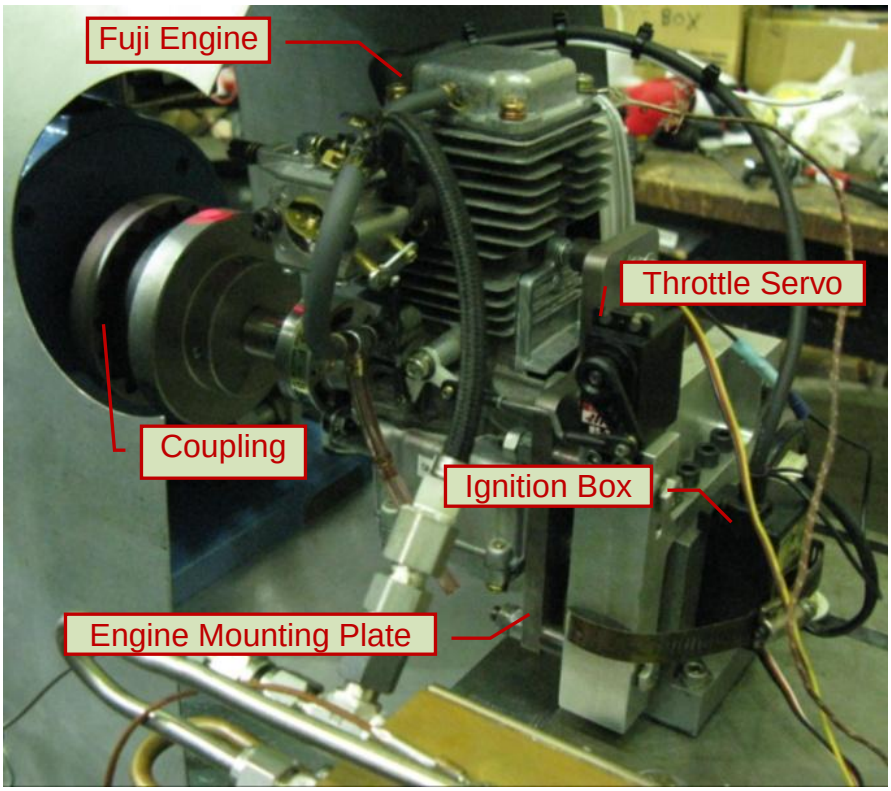

Figure 5. Fuji engine

The engine is mounted on an adjustable sliding plate that allows the engine to move fore/aft of the dyno to enable couplings to be changed. The engine plate that attaches to the rear of the engine can be shimmed up/down to allow for correct alignment. The entire engine assembly sits on a plate mounted on four vibration dampers. The vibration dampers, McMaster Carr part #64875K9, are rated for a maximum deflection of 0.10” at 210 lbs. A detailed analysis to determine these dampers can be found in Appendix D. The dimensions of each

of these mounting plates can be found in Appendix F. The engine and dyno shafts are coupled together using a Martin Quadra-Flex coupling. The coupling has a maximum RPM rating of 6000.

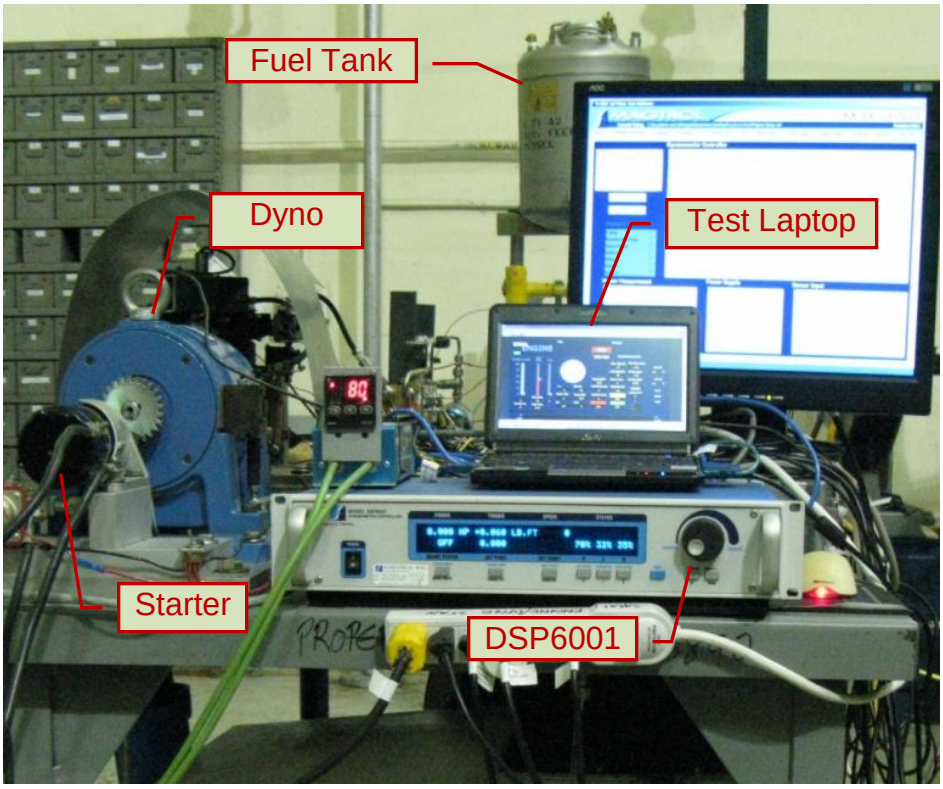

Figure 6. Dynamometer setup

The stock Fuji spark timing controller (ignition box shown in Figure 5) was used for some of the data presented in this paper. The stock timing is a function of engine speed (measured from a magnetic crankshaft position sensor) and is assumed to be optimized for the factory recommended fuel (gasoline) and carbon propeller (17x10). For data with varied spark timing, a different ignition box and controller were used. The variable ignition was provided by a C-H ignition box, part #25. Both the stock box and C-H box require 5V power. A program using a PIC18 chip was written in-house and used the stock crankshaft

sensor to determine shaft position. This program requires a 0-5V analog input signal to set the actual spark timing. This input signal is supplied by the National Instruments (NI) Fieldpoint via a slider bar on the small engine LabView program. This slider bar is calibrated with a user input for the maximum and minimum spark timing. The spark program allowed a maximum advance of 60 degrees before top dead center (BTDC) up to a minimum of 10 degrees after top dead center (ATDC). The crankshaft position sensor outputs a high to low to high digital square wave signal. The point on the square wave that the signal drops to zero was measured to be approximately 45.1 degrees BTDC. Using only one signal per cycle can cause some accuracy issues when rapidly accelerating or decelerating and if at a condition where the engine is not running smoothly. However, for the data presented here, the spark timing was changed while the throttle and engine speed were held constant, thus alleviating many of these issues. Occasionally, usually during the limits of the spark timing, the engine would begin to run erratically, and led to inaccurate timing for that data point. In the future an encoder will be added to the crankshaft to increase the resolution for the position of the crankshaft and ideally eliminate any accuracy errors.

The dyno is equipped with a shaft on both ends, therefore allowing an electric gear starter to be used. The starter runs off a 12V automobile battery and is controlled by a relay and hand switch. The starter is mounted to an aluminum mounting plate that has the capability of being slid to the left or right. This allows the user to correctly adjust the tolerance of the starter teeth to the dyno gear teeth. The dimensions for this plate as well as the base plate can be

found in Appendix F. For safety concerns, the starter switch has a main shutoff control located on the small engine LabView program.

Fuel is fed from a five gallon fuel tank that is located above the table for gravity feed. The fuel travels through a course inline paper filter and then a 10 micron filter, before entering the Max Machinery flow meter. The fuel system consists of two air actuated shutoff valves, one operated remotely and the other by the local laptop. The factory carburetor is used to meter the fuel. The carburetor is equipped with both a high speed and low speed fuel jet. It is unknown what engine speed it switches from one to another.

The throttle controller is a Hitec electric servo. A Microchip PIC-18 microcontroller was programmed to control the input/output throttle box. Figure 7 shows the input throttle percentage versus the angle of the throttle butterfly valve. The raw throttle data that is recorded is the input percentage, not the

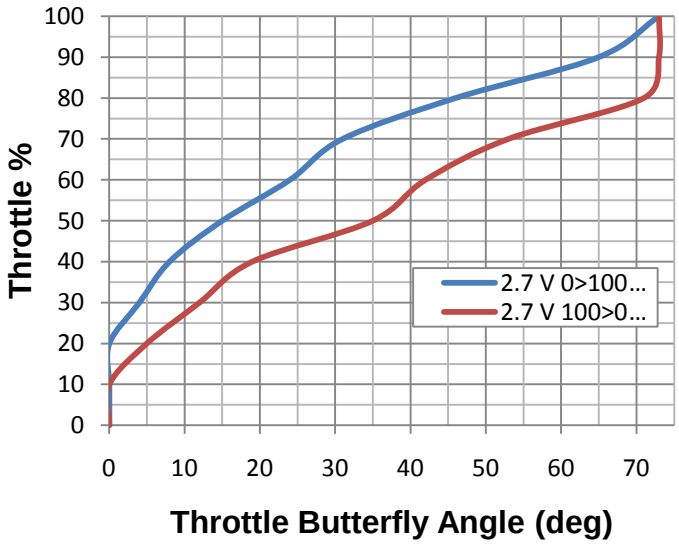

Figure 7. Throttle input percentage vs. butterfly angle

actual throttle position, and therefore the actual position cannot be determined with any certainty. This fact does not affect the results of any one of the individual experiments, but it does not allow multiple tests to be compared. After the engine is mounted to the test stand, the throttle arm movement can be calibrated in the LabView small engine program, by specifying a max voltage that is output at 100 percent throttle input.

There are several cooling mechanisms on the setup. To cool the dynamometer, a closed circuit water system is used with a 20 micron filter. Compressed air (shop air) cools the engine and is controlled by an electronic actuator. A flat tipped nozzle is used on the air line to spread the air flow and cool by convection. Additionally, when high-speed cylinder pressure data is taken with the PCB sensor, compressed air must also be used to cool the dynamic pressure transducer.

A laptop runs the Small Engine LabView program due to having a solid state hard drive to withstand the vibrations on the test table from the IC engine. The Small Engine program was written in house and provides the input hub to control the testing (see Figure 8). National Instruments FieldPoint was used as the data acquisition (DAQ) hardware in this setup. The Fieldpoint has eight different modules to accept all of the data; one CTR-502, RLY-425, AI-118, AO-210 and two TC-120 modules. The CTR-502 is a counter module that is used to record the pulses from the optical engine speed sensor and fuel flow meter. The RLY-425 controls all of the electrical relays including the main fuel, cooling air, starter, ignition and heater. The AI-118 accepts the torque analog output from

the dynamometer controller. The AO-210 provides the analog output to the throttle control servo and variable spark timing boxes. The two TC-120 modules house the temperature inputs from all of the thermocouples.

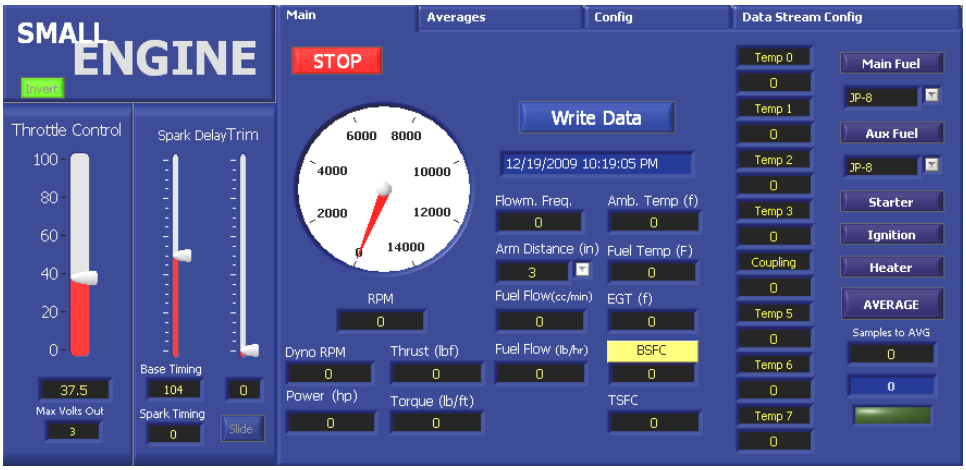

Figure 8. Small engine LabView program

The AI-118 module is only capable of operating at 10 kS/s. To obtain the high speed cylinder pressure data, hardware capable of at least 40 kS/s was desired. To obtain this, a separate National Instruments PCI slot analog input card, model #PCI-6040E, was purchased. This card has a single channel input rating of 500 kS/s and a multi-channel rating of 250 kS/s. A BNC terminal block, model #BNC-2100, was used in conjunction with this card.

Sensors.

Two different pressure sensors were used in this research, a PCB brand and Optrand Brand. Both sensors take advantage of a spark plug mount to obtain pressure from the cylinder head. The PCB pressure sensor, model #112B11, was used in conjunction with a spark plug mount, model #65A. This sensor is a charge output type that requires an in-line charge converter, and has

a resonant frequency of greater than or equal to 200 kHz. The Optrand sensor is an AutoPSI-TC, model # D822D6-SP, which is a temperature compensated variant. This sensor is a fully self-contained unit that uses optical fibers to transmit the signal. The resonant frequency on this sensor is 120 kHz. In order to obtain a true cylinder pressure, both of these sensors require a reference pressure, normally obtained from a pressure sensor placed in the intake manifold. But, this reference pressure sensor was not installed; therefore the resulting pressure presented in the data is either normalized pressure (P/P_{max}) or "un-calibrated pressure", which leads to a correct magnitude, but incorrect true value.

All of the temperatures on the test setup are measured using K-type thermocouples, but they differ slightly. The cold and heated fuel temperatures are measured using a probe thermocouple. The heater block and engine block temperature both use a bolt down ring thermocouple. The ambient temperature is measured by an open ended beaded wire thermocouple. All of the thermocouples are installed on the TC-120 module in the Fieldpoint.

The Max Machinery flow meter, model #213, is capable of a volumetric flow range of 1-1800 cc/min with a measurement error of less than 0.2%. This meter uses a four piston design that transmits a pulse every shaft revolution. Every revolution corresponds to 0.89 cubic centimeters of fluid. The small engine program takes the number of pulses per second and multiplies it by this constant to obtain the volumetric flow rate. This flow rate can then be multiplied by the fuel density to obtain the mass flow rate.

The engine speed is measured by a Monarch Instrument optical sensor, model #ROS-W. This sensor has a speed rating of 1-250,000 RPM. Two small pieces of reflective tape are placed approximately 180 degrees apart on the engine side of the Quadraflex coupling. The sensor outputs a pulse every time one of the pieces of tape passes by. Two pulses per revolution were used to obtain a better resolution by accounting for the non-constant shaft rotation.

The analog output from the dynamometer controller is used to record the torque. This signal is output at 120Hz. For a majority of the data presented in this thesis, the DAQ only captured one of these data points per second. The current configuration, however, is setup to take each of the 120 data points per second and average them together creating a more accurate representation of that second in time.

Electric Fuel Heater Fabrication.

It is known [9] that when using JP-8, substantial energy must be added to the mixture in order for the fuel to completely vaporize. An analysis was completed to determine whether increased mixture temperature was needed as well for the two research fuels (Appendix C). It is shown that for n-Heptane, until the mixture temperature falls below 265K and below 277K for iso-Octane, additional heat is not required in order to keep the fuel a vapor in the mixture. It is expected that the ambient temperature of air for testing would not drop to below 280K. Therefore, a heater would not be necessary to keep the fuel in a vapor state; however additional tests were still completed to evaluate the effects of the increased mixture temperature on performance. The two methods to

achieve a higher mixture temperature to either heat the air or the fuel; the latter was chosen.

The electric heater design was based on a similar heater presented earlier in this paper. The base of the heater is a 2”x2”x8” block of pure copper. Copper was chosen simply due to its high conductivity. One drawback with using copper, is that is has a max usable temperature around 477K. Therefore, calculations were done (Appendix C) to determine the approximate fuel temperature at the exit of the heat exchanger. The concluding results were that the maximum copper block temperature needed to heat our fuel to our desired values will be less than copper’s max usable temperature. Four fuel passage ways were machined into the copper with threaded fittings at each exit point. Swagelok fittings and 180 degree bent copper tubing was used to route the fuel back through each passage. The heater was then bolted to a stand to remove it from the table top.

Two Watlow 750 Watt, 120V strip heaters were attached to both sides of the copper block. A temperature controller, Watlow part # E5CSVQ1TFAC100240, was used to regulate the electrical output. The user is able to input a set block temperature and the controller used the temperature input from a thermocouple placed on the copper block with feedback control to regulate the voltage. A probe thermocouple is also placed in the fuel stream at the exit of the heater to obtain the actual fluid temperature. A solid state relay was used, part # G3NA220BDC524, to avoid routing the 120V a/c current through the controller.

Limitations

The main limitation in this research turned out to be the engine to dynamometer coupling. Many design attempts were made, with most ending in failure. The first coupling used was a Lovejoy spider type coupling with aluminum hubs and composite core. This coupling failed due to excessive vibrations causing damage to the engine crankshaft and dynamometer bearings. A small driveshaft coupling system was designed next, but due to recommendations from the US army, a Martin Quadraflex coupling was chosen instead. Two sizes of this coupling were evaluated; size 5 and 6. These couplings carry a maximum torque specification of 20 ft-lb and 37.5 ft-lb respectfully, which are 20 to 37 times the maximum averaged torque of the research engine. The size 5 Quadraflex coupling carries a maximum speed rating of 7600 RPM, which would cover the speed range needed for this research. The size 5 coupling was evaluated but resulted in a rubber element failure during higher loading of the engine. The size 6 Quadraflex coupling has not exhibited any failures, but only carries a speed rating of 6000 RPM, thus limiting our testing. A combination of the two was also evaluated, using only the size 5 coupling for test points between 6000 and 7600 RPM. This proved unsuccessful as well, with an identical rubber element failure even with low engine loading.

Lastly, a Lovejoy torsional LF series coupling was recommended by Lovejoy engineers to withstand the vibrations of the single cylinder engine. This coupling carries a maximum torque rating of 16.7 ft-lb and maximum speed rating

of 10,000 RPM. Two attempts were made with this coupling, both proving unsuccessful. The first attempt failed after one of the bolts came loose from the coupling, which was attributed to incorrect installation. The second attempt, after correct installation also ended with a failure of the rubber element between the two hubs.

Therefore, during this research only the size 6 Martin Quadraflex coupling was able to withstand the vibrations due to the single cylinder engine, but unfortunately limited the test data to below 6000 RPM. For future work, perhaps one of the larger size Lovejoy torsional LF series couplings would provide the stiffness required. Also, if a mechanism was added to the test stand to dampen the vibrations of the engine, one of the previously used couplings may work.

The second limitation in the research was the fuel flow meter. During the heated fuel testing, the max machinery flow meter's readings became unreliable at temperature above 344K for n-Heptane. Theoretically the fuel should still be in a fully liquid state at this temperature and ambient pressure, but the fuel readings acted as if a vapor lock situation was starting to occur. The set of heated fuel tests were completed last in the research and time was not allotted to determine the cause.

Uncertainty Analysis

The two measured values used in the results with error are torque and fuel flow. BSFC is a calculated value comprised of both of these values. Therefore an uncertainty analysis was completed on torque and BSFC[10]. The fuel flow

measurement has a constant error of no greater than 0.2%, where as the load cell used in the dynamometer for the torque measurement has a 0.5% error at full load (7.7 ft-lbs). The resulting error for torque and BSFC for a certain measured torque value can be seen in Table 5.

Table 5. Uncertainty analysis for torque and BSFC

Torque	Torque Uncertainty	BSFC Uncertainty
0.1	36.88%	36.88%
0.2	18.44%	18.45%
0.3	12.29%	12.30%
0.4	9.22%	9.23%
0.5	7.38%	7.39%
0.6	6.15%	6.17%
0.7	5.27%	5.29%
0.8	4.61%	4.64%
0.9	4.10%	4.13%
1	3.69%	3.72%
1.1	3.35%	3.39%
1.2	3.07%	3.11%
1.3	2.84%	2.88%
1.4	2.63%	2.68%

Experimental Setup and Conditions

Engine Performance Map.

As mentioned earlier, the coupling limits RPM to less than 6000. Although not ideal, this still allowed data to be taken for a partial engine map. An engine map is a common way to present the operating characteristics of an IC engine over its full load and speed range [5] and will be defined as BMEP versus engine speed, with contours of BSFC. To create this map, torque versus speed and fuel flow data must be known at different loadings of the engine. The dyno with its brake produced the load. The engine throttle was increased in 10 percent

increments and the dyno controller was used to load the engine to different RPM set-points for approximately eight seconds per data point. The data was taken at 200 RPM increments from 5900 RPM down to where the engine would stop running at that particular throttle setting. All data was taken at a rate of 1 Hz. The hysteresis with the throttle servo (Figure 7) is not a factor in creating the engine map, because the goal is to get data at different loading points. Any throttle movement, creating a difference from the previous setting, is all that is needed. The DSP6001 was used to manually select each of the RPM set-points, which ultimately resulted in a slight drift in the RPM. The engine maps were created using a stock factory delivered configuration (including spark timing) for the two research fuels.

After the data was taken, several post processing events were accomplished. The raw data included throttle, RPM, torque, volumetric fuel flow rate and various temperatures. The data was sorted and grouped into subset files with the same throttle setting. Next the data for each RPM setting, ideally eight data points, is calculated for a mean and standard deviation and the data point is deleted if its difference from the mean is greater than 1.75 standard deviations[11]. The remaining data points for that particular throttle setting and particular RPM setting are then averaged to get one data point per RPM setting. The now filtered data is put into matrix form, in order to create a contour plot. Matlab was used to interpolate between the points if there were any gaps in the data. The Matlab program can be found in Appendix A.

Knocking Characterization.

It is known from chapter II that knocking can be caused by a few different factors. In this test, the goal was to characterize any knocking that would be apparent by only changing the octane rating of the fuel. The stock setup was used including the stock ignition box. To see if knock was evident, high speed cylinder pressure data was taken at the different test points. The high speed data was taken at 40 kHz for 0.5 seconds. Normally knock is apparent at higher loadings, so data was taken at several points with high throttle/low speed using both fuels. The complete test matrix can be found in Table 6.

Table 6. Knock characterization test conditions

Test #	1→2	3→6
Throttle (%)	85	80-90
Engine Speed (RPM)	5000/4000	5000/4000/3500/ 3000/2700/2500
Ambient Temp (K)	294	293-294
Fuel Temp (K)	290	290
Fuel Type	i-Octane	n-Heptane

Variable Spark Timing.

One thing that must be evaluated to optimize the performance of this engine is spark timing. It is known that n-Heptane will combust faster than iso-Octane [12], therefore the spark timing should need to be retarded to obtain the most efficient cycle. To evaluate the effect of spark timing on BSFC and maximum torque, engine loading points were chosen that corresponded to a typical 17x10 propeller. To set the engine up for each of these points, spark timing was set to stock and the engine was held at a constant speed by the dyno. Then the throttle was adjusted until the desired torque value was obtained. At

this operating point, the spark timing was adjusted starting with 60 degrees BTDC, every 5 degrees until -10 degrees BTDC was reached. For several of the operating points, when the timing was set around the adjustment limits, the engine ran rough or quit completely. These data points were discarded from the analysis. The test conditions during this experiment can be found in Table 7.

Table 7. Varied spark timing conditions

Condition	
Engine Speed (RPM)	2700, 3000, 3500, 4500, 5000, 5500, 5700
Ambient Temp (K)	291-296
Fuel Type	n-Heptane
Fuel Temp (K)	281-286

Heated Fuel.

A series of tests were run to see how a higher air/fuel mixture temperature, via heating the fuel, would affect the performance of this engine. The first experiment consisted using a constant heat flux into the fuel to increase the mixture temperature. These test conditions can be found in Table 8.

Table 8. Heated n-Heptane test #1 conditions

Condition	
Engine Speed (RPM)	4000
Throttle	80%
Ambient Temp (K)	289
Fuel Type	n-Heptane
Fuel Temp (K)	Varied - 289>372

With the throttle and speed held constant, the heater was turned on with the fuel temperature constantly increasing approximately 0.31 Kelvin per second to a

max temperature of 372K. The fuel flow measurement however became unreliable at around 338K. It was determined that by only heating the fuel, this would in turn cause the density of the fuel to decrease which leads to a smaller mass flow rate and therefore a leaner mixture. To separate the effects of the heated fuel from the effects of a change in stoichiometry, a second test was needed.

The second experiment consisted of again slowly heating the n-Heptane fuel and comparing it to varying the ambient temperature fuel flow rate by the carburetor high speed needle. Due to the difficulty of obtaining a small accurate step size with the human eye, the step size was limited to 1/8 of a turn at a time over a range of 1/2 of a turn. The same positions were used at each fuel temperature and are illustrated in Figure 9.

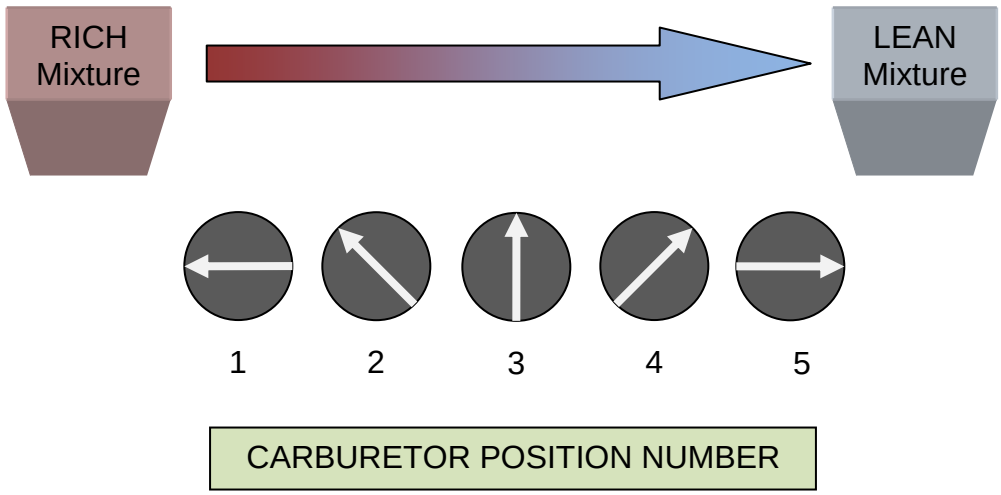

Figure 9. Carburetor position overview

The test conditions for the second test can be found in Table 9. This test was also unsuccessful with separating the effects of fuel temperature from the equivalence ratios, therefore leading to the third and final experiment.

Table 9. Heated fuel test #2 conditions

Condition	
Engine Speed (RPM)	4000
Throttle	80%
Ambient Temp (K)	283
Fuel Type	n-Heptane
Fuel Temp (K)	Varied - 283>334

The third test was performed to accommodate for the changing equivalence ratio of the mixture, and also to take measurements at a constant fuel temperature. Additionally, it was thought that due to high rate of heat flux in the first experiment that this could lead to in-accurate fuel flow rate measurements. In this test, again the dynamometer was used to hold the engine at a constant speed and the throttle was fixed. Complete conditions found in Table 10.

Table 10. Heated fuel test #3 conditions

Condition		
Fuel Type	n-Heptane	i-Octane
Engine Speed (RPM)	4000	4000
Throttle	100%	100%
Ambient Temp (K)	281-285	284-285
Fuel Temp (K)	Ambient/300/311 322/333	Ambient/300/311

Five different fuel temperatures were chosen and the carburetor's high speed needle valve was used (Figure 9) to change the equivalence ratio of the mixture. Since the heater was over designed, it proved difficult to heat the fuel to the desired temperature without it overshooting. To accommodate for this, the set temperature was set much lower than the desired temperature and a compressed air source was used to provide cooling in the case of overshoot. This method worked well and the measurements were taken when the fuel temperature had stabilized. It should be noted that between the beginning and end of measurements per temperature point, the fuel temperature was shown to drop up to 3.5 Kelvin. At least eight data points were taken per needle position.

IV. Analysis and Results

Cylinder Pressure and Knock

The first series of tests performed used the PCB pressure transducer. The high speed data was taken at 40 kHz for 0.5 seconds. With this transducer, the profile of the pressure curve in the data is accurate, however the magnitude and true pressure value may not be. This is due to not having a reference pressure and the spark plug mount had a slight crack in it causing pressure loss. Therefore, all of the pressure curves were normalized by dividing the pressure by the peak pressure of the profile. Expectations were that knock would not be seen with iso-Octane, but would be exhibited with n-Heptane [5]. Two methods used to evaluate the knocking characteristic were visually and statistically.

To visually address the knock, the recorded pressure curves were compared with Figure 2. The iso-Octane performed as expected, and did not exhibit any signs of knocking in the load ranges evaluated. When n-Heptane was used however, signs of slight knocking were evident at the high load data points, which were less than 3000 RPM at 80% throttle and less than 3300 RPM at 90% throttle. Figure 10 shows an example of n-Heptane slightly knocking with 90% throttle at 3000 RPM. As seen in the figure after the peak cylinder pressure is reached, the pressure curve begins to oscillate slightly.

To statistically evaluate the knock, a standard deviation of the pressure curve was calculated. A range of pressure beyond the peak (10-40) was chosen so that a linear fit could be used to provide estimated “no knock” pressures.

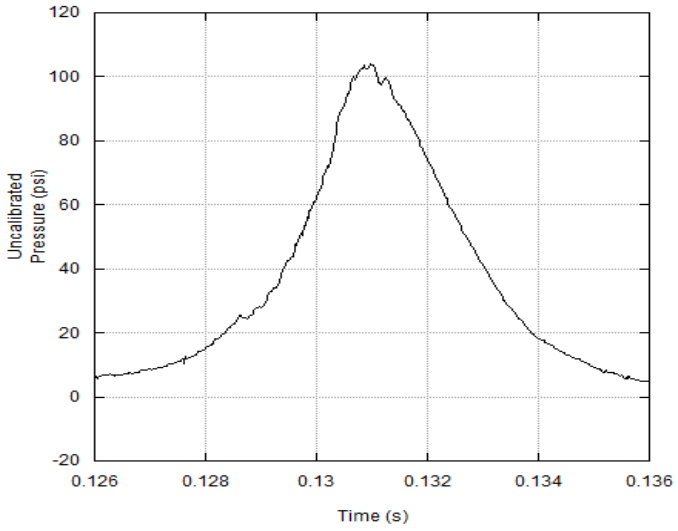

Figure 10. n-Heptane knock profile at 90% throttle, 3000 RPM, 30° BTDC timing

This method produced accurate results for the range shown, but ideally a curve fit technique should be used to evaluate the whole profile and not just one section. To calculate the standard deviation between the actual and theoretical pressure, equation 8 was used,

$$\sigma = \left(\frac{\sum_{i=1}^{N} (P_{meas} - P_{trend})^2}{N} \right)^{1/2} \tag{8}$$

where *N* is the total number of pressure points. For each high speed data file (raw data shown in Appendix E), a standard deviation was calculated for each power cycle pressure curve in the data set. Next the mean, minimum and maximum deviation for that data set is calculated. The minimum and maximum deviation was used to represent high and low error of the mean. The resulting

mean standard deviation with error is plotted in Figure 11 with corresponding throttle position and engine speed shown in Table 11.

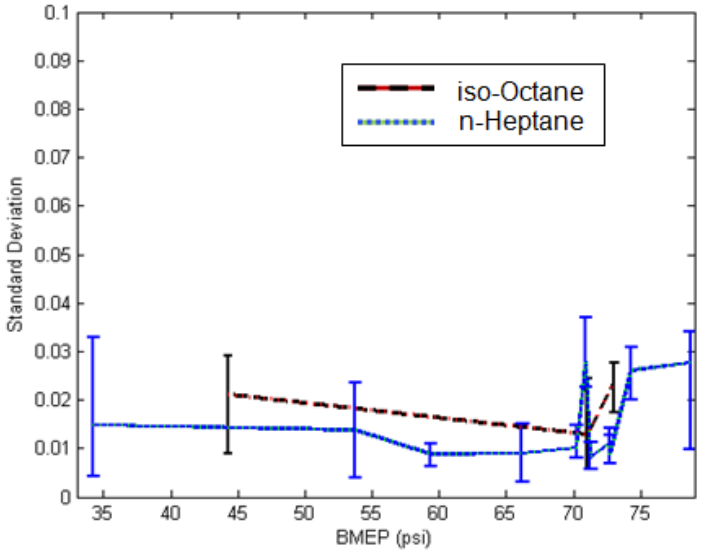

Figure 11. Standard deviation for pressures of iso-Octane and n-Heptane at multiple engine loadings using stock timing

Table 11. Engine speed, throttle position and BMEP for data in Figure 11

	RPM	Throttle	BMEP
Octane	5000	40	44.26
	5000	85	72.99
	4000	85	71.04
Heptane	5000	85	74.30
	5000	85	70.90
	4000	85	78.68
	3670	85	53.69
	3500	85	34.19
	3000	80	70.20
	2700	80	72.68
	2500	80	71.25
	2900	80	72.72
	3300	90	59.32

As with the visual analysis, the trend of deviation versus BMEP shows no significant increase. Analyzing the trend further, it can be argued that when the error is taken into account, the deviation across the BMEP becomes constant. To address the severity of the knock by the standard deviation value proved to be a challenge. Since there is no documented correlation between the standard deviation knock severity, only a comparison of the two fuels could be made. When compared, n-Heptane shows no higher deviation than iso-Octane. Therefore, the only conclusion that can be made is that both fuels have the same knocking characteristics in this engine at the engine loads evaluated.

The severity of the knock that was shown with n-Heptane was much less than what was expected. The mild knock severity is thought to be due to both the high cylinder surface area-to-volume ratio and the low compression ratio of the engine. The result of a high area-to-volume ratio is that more heat can be dissipated, thus leaving less “hot spots” on the cylinder walls that could cause surface ignition. In addition, this engine’s compression ratio, approximately 8, is near the lower end of the range for small spark-ignition engines [5]. A lower compression ratio results in lower cylinder temperatures and pressures and thus reduces the probability of pre-ignition/knock. However, even though this mild severity was demonstrated, different ambient conditions could provide different results.

In addition to high engine loading, knock characteristics were analyzed during the heated fuel tests. Three temperatures were evaluated with n-Heptane, 289K (ambient), 311K and 344K, all at 100% throttle and 4000 RPM.

This set of data was captured using the Optrand pressure sensor. The high speed data was taken at 40 kHz for 0.5 seconds. The pressure sensor did however fail at the end of this testing. The magnitudes of the pressure profiles are assumed to be inaccurate due to the overheated pressure sensor, but the profiles are assumed to be true. Similarly with earlier data, the pressures were normalized by dividing by the peak value. Two data sets were taken for ambient and 311K fuel temperature, however once the pressure transducer failed, only 3 power cycles were able to be captured at the 344K fuel temperature (Raw data can be found in Appendix E). The same statistical approach was used for this data to obtain an average standard deviation at each temperature and can be seen in Figure 12.

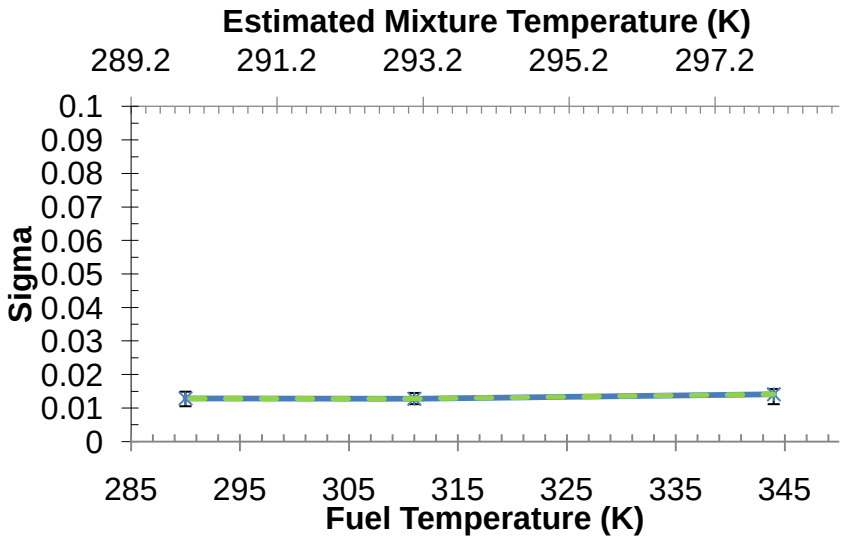

Figure 12. Knock variance vs. fuel temperature for n-Heptane at 4000 RPM with 100% throttle, 42° BTDC timing and 289K air temperature

The expectation for the standard deviation versus fuel temperature trend is an increase in deviation as fuel temperature increases. Comparing our results however, the standard deviation stayed constant through the three temperatures. The upper x-axis of Figure 12 is the estimated mixture temperature, which is based off an air temperature of 289K. From the plot, it is clear that heating the fuel by 50 Kelvin only increases the mixture temperature by about 10 Kelvin. This fact could explain why no increase in knock was exhibited with higher fuel temperatures. On the other hand, if the air temperature was increased by 50 Kelvin, the knock characteristics with n-Heptane could be much worse.

Engine Performance Map

One of the research objectives was to compare the BSFC for the two fuels in a stock, factory delivered configuration. The engine map for iso-Octane and n-Heptane were used to complete this objective and can be seen in Figure 13 and Figure 14, respectively. Comparing the contour lines over the entire engine map indicate n-Heptane has on average a 4.1% lower BSFC than iso-Octane. Alternatively, to perhaps obtain a more useful result, the BSFC was compared along a 17x10 propeller engine loading (shown in Figure 13). The resulting BSFC with both fuels was plotted against engine speed and is shown in Figure 15. N-Heptane is shown to exhibit on average 12.91% lower BSFC along this specific loading line when compared to iso-Octane. Generally when comparing a low ON fuel with a high ON fuel, a decrease in brake specific fuel consumption should be evident [12], and it appears to be verified in this engine by these results.

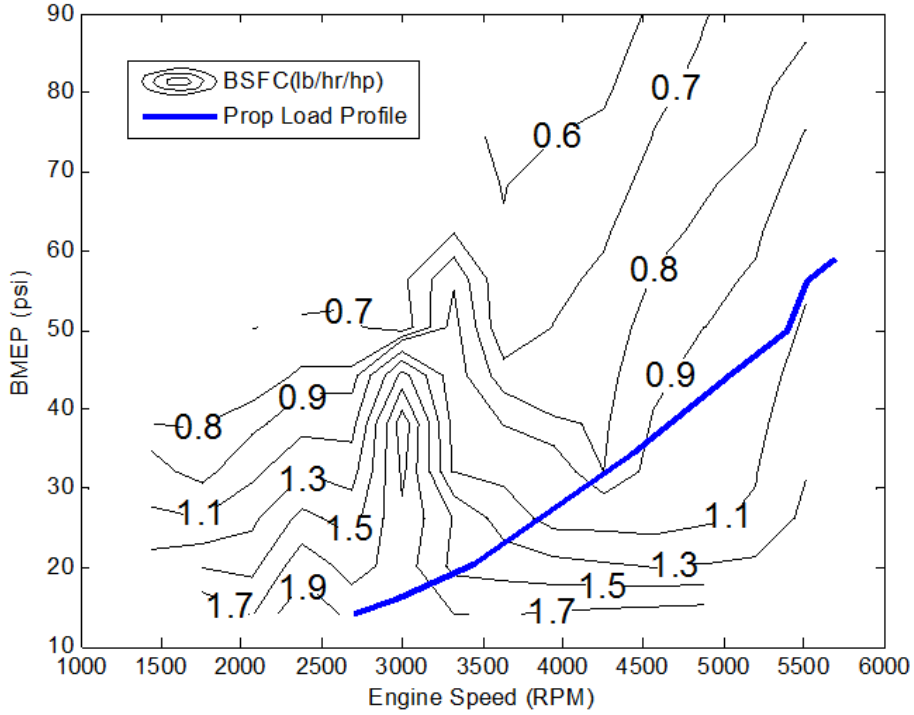

Figure 13. Fuji BF-34EI engine map with iso-Octane using stock timing

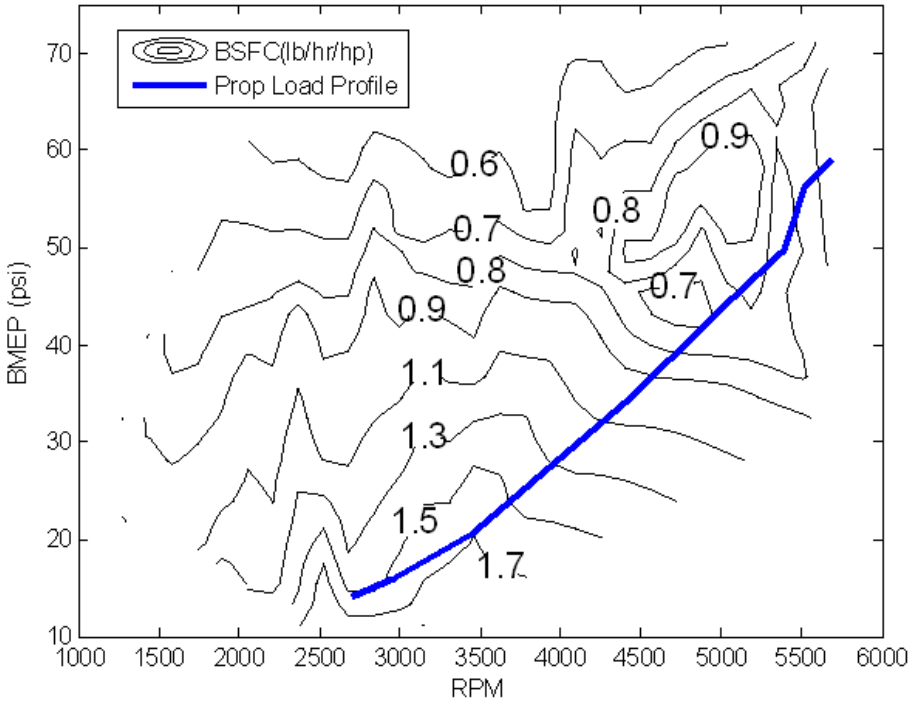

Figure 14. Fuji BF-34EI engine map with n-Heptane using stock timing

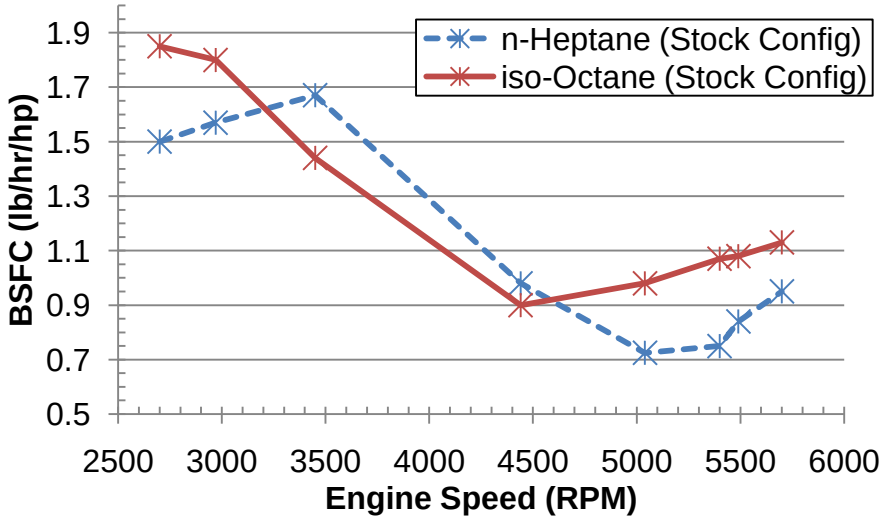

Figure 15. BSFC vs. engine speed for n-Heptane and iso-Octane using a factory configured engine (stock timing, carburetor needle position) with a typical 17x10 propeller load

Since the torque is constant along a particular load line, the BSFC's shown in Figure 15 must be driven by fuel flow. To make a comparison of the two engine maps simpler, a percent difference contour plot was created and can be seen in Figure 16. The contour lines on this plot relate to the percent decrease in BSFC from iso-Octane to n-Heptane. Therefore a positive percentage favors n-Heptane (black scan line area) and a negative one favors iso-Octane (green checkered area). This figure is particularly helpful in showing that there are distinct loading areas that are desirable depending on the type of fuel being used. Ultimately, even though on average n-Heptane exhibits less specific fuel consumption, in order to truly assess the positive (or negative) impact of using n-Heptane the real world operating conditions are needed.

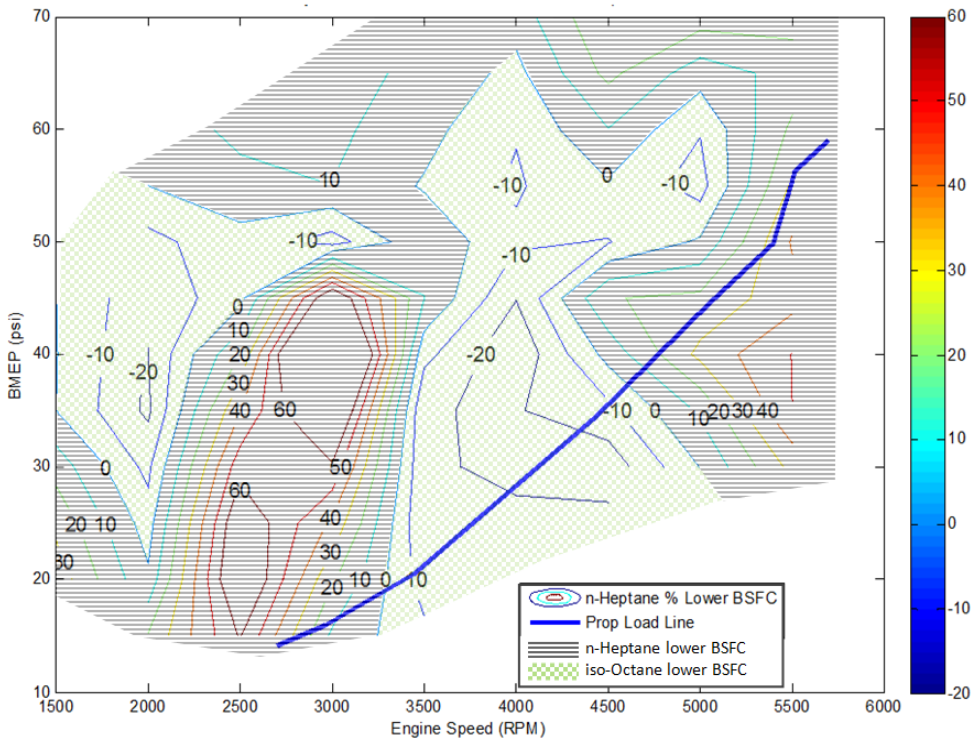

Figure 16. Percent difference contour plot between n-Heptane and iso-Octane engine maps

For example, even if on average n-Heptane has 14.1% lower BSFC over the 17x10 prop loading, the scenario could be that 90% of the time the UAV is operating in the favorable iso-Octane region, therefore making the use of the average value inaccurate.

Spark Timing Optimization

The first objective before optimizing on spark timing was to see if it was even needed. To address this concern, the peaks of the cylinder pressure profiles were analyzed. Figure 17 shows a comparison of a selected pressure profile of n-Heptane and iso-Octane for the Fuji engine. For this plot, the ignition

signal was not recorded, but it is indicated on the n-Heptane curve at 2 milliseconds.

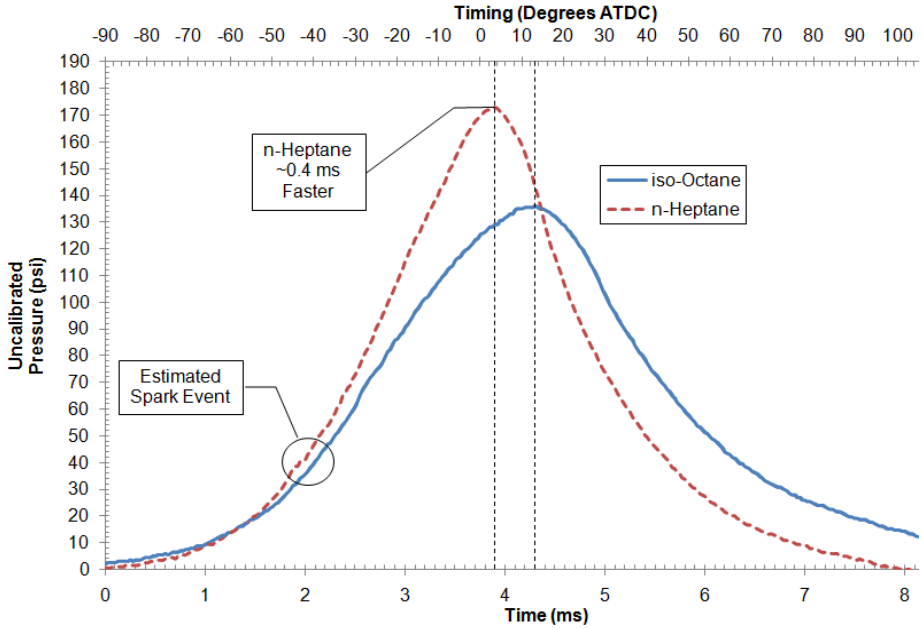

Figure 17. Fuji cylinder pressure profile for iso-Octane & n-Heptane at 85% throttle, 4000 RPM, 42° BTDC timing and 295K ambient temperature

Ideally, independent of what fuel is used, the pressure profile should be similar during the compression phase of the engine cycle up to ignition. The plot shows a close correlation in the curves before the ignition event. After the ignition of the n-Heptane mixture, the peak pressure occurred at about 0.4 milliseconds sooner than the iso-Octane mixture. This result agrees with documented ignition times [9] and with experimental results showing a 5-10 cm/s increase in laminar flame speed with n-Heptane over iso-Octane [13]. In Figure 17, the maximum cylinder pressure for n-Heptane was consistently higher for this data point, which should correlate to overall higher power. However, when the data is compared at the 85% throttle/4000 RPM operating point, the iso-Octane

mixture outputs 0.87 Hp compared to 0.8 Hp from n-Heptane. The cause for this occurrence is hypothesized to be due to spark timing. In theory, the ideal peak cylinder pressure for any fuel should occur around 16 degrees ATDC [5]. Converting the 0.4ms difference in peak values to degrees at 4000 RPM, you obtain 9.6 degrees. Assuming that the iso-Octane peak pressure occurs at or near the ideal point of 16 degrees ATDC, leaves the n-Heptane peak at 6.4 degrees ATDC. This result alone would indicate than in order to obtain the maximum work from the combustion cycle for n-Heptane, the spark timing needs to be optimized to allow the peak of the pressure curve to be at 16 degrees ATDC.

The Optrand pressure sensor was used to take another look at the cylinder pressures with n-Heptane. For this data, a reference pressure was not used, but the magnitudes are correct. Also, the spark signal and crankshaft signal were recorded to be able to accurately place the pressure profiles on a degree axis. The three n-Heptane pressure curves versus crankshaft position can be seen in Figure 18 and versus time in Figure 19. These figures show several important things; the magnitude of pressure, location of the peaks and timing of the spark. The stock timing box is variable and a function of engine speed. The spark timing demonstrated on these pressure profiles match up well with the stock timing curve (can be seen in Figure 25); which validate the results. The 4000 and 4500 RPM curves both have similar magnitudes, but the 3500 RPM curve is considerably lower. To help explain this, the recorded fuel flow rates were looked at. Theoretically, if the throttle and carburetor needle valves

are held at a fixed location, the amount of fuel per cycle used should be the same regardless of engine speed.

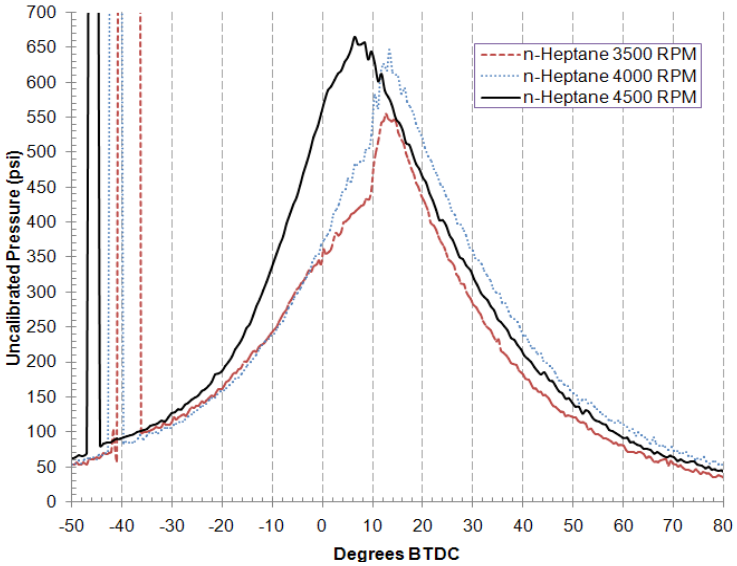

Figure 18. Cylinder pressure vs. crankshaft position for n-Heptane at 3500, 4000 and 4500 RPM with stock timing, 100% throttle and 293K ambient temperature

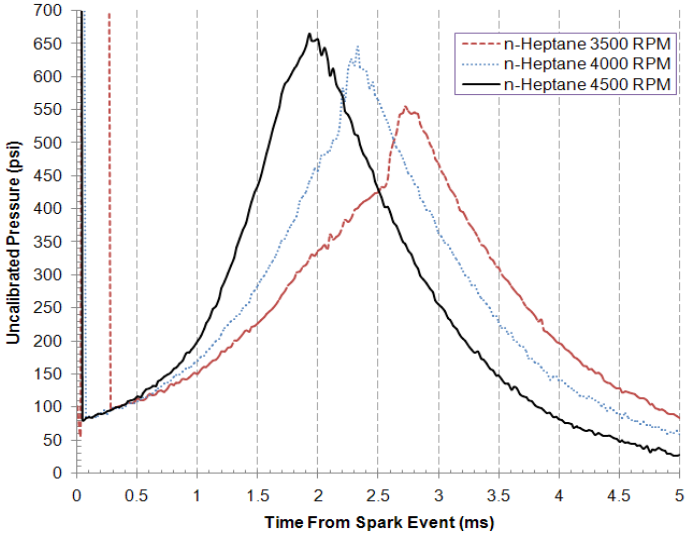

Figure 19. Cylinder pressure vs. relative time (0 ms at spark event) for n-Heptane at 3500, 4000 and 4500 RPM with stock timing, 100% throttle and 293K ambient temperature

Table 12 shows that for 4000 and 4500 RPM, the average volume of fuel per cycle is about the same, but this is not the case for 3500 RPM.

Table 12. Average volume of n-Heptane per cycle

Avg Engine Speed (RPM)	4504.29	4020.00	3506.67
Avg Torque (ft-lb)	1.29	1.22	0.60
Avg Fuel Flow Rate (cc/min)	7.96	7.00	4.48
Volume of Fuel per Cycle (mm3)	3.54	3.48	2.56

If less fuel was being brought into the cylinder each cycle, this would lead to less energy being produced and in turn less cylinder pressures, which would account for the pressure profile of 3500 RPM in Figure 18. This demonstrates the need for a small scale fuel injector, as it is clear this carburetor is not the most accurate at metering the fuel. Lastly, the location of the peak pressure profile needed to be examined to determine if spark timing should be adjusted for max performance. It should be noted, for all of the pressure data presented in Figure 18 and Figure 19, a representative profile was chosen for each condition. The location of the peak pressure and magnitudes of the pressures can change slightly from one cycle to another due to the nature of IC engines (as seen in the raw data in Appendix E). In Figure 18, the peak pressure lies at 6.44, 13.44 and 14.57 for 4500, 4000 and 3500 RPM, respectfully. One reason for the difference in location with respect to TDC is the fact that the timing is changing versus engine speed. The measured timing for the three curves 4500, 4000 and 3500 RPM is 45, 42 and 41 degrees, respectfully. It is clear that the stock timing is not

ideal for n-Heptane. Alternatively, when these same pressure profiles are plotted versus time (Figure 19), an interesting trend is noticed. The time it takes the combustion event to reach its maximum pressure decreases as engine speed increases. This trend will be important later during the spark timing discussion.

The analysis of the n-Heptane pressure profiles showed the need to optimize the timing to obtain our maximum performance. When several BMEP versus rpm points were evaluated corresponding to the typical load profile (shown in Figure 13), it is shown that varied spark timing only has a small affect on BSFC. High speed data was taken for each spark timing step which included the crankshaft signal, timing box output signal, spark signal and cylinder pressure. An example of one cycle of the raw data can be seen in Figure 20.

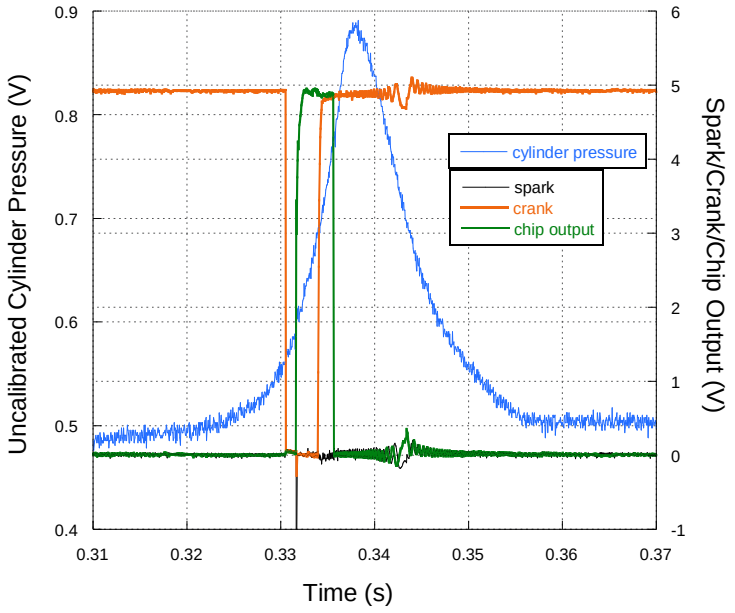

Figure 20. High speed data example using n-Heptane at 2700 RPM, 35° BTDC timing, 16% throttle and 296K ambient temperature

Each one of these files were analyzed and one of the items looked at was the actual spark timing versus the input spark timing. The crankshaft sensor's high to low signal is known to occur at 45.1 degrees BTDC, therefore the delta between the crankshaft high to low signal and spark signal was taken and converted to degrees. Figure 21 shows the true error between the set value and actual value for each engine speed. Excluding the endpoints of 3000 RPM, the error is within +/- 5 degrees. Due to the non-constant nature of the IC engine and only knowing the crankshaft position at one point in the cycle, there was a small amount of error in the timing from cycle to cycle.

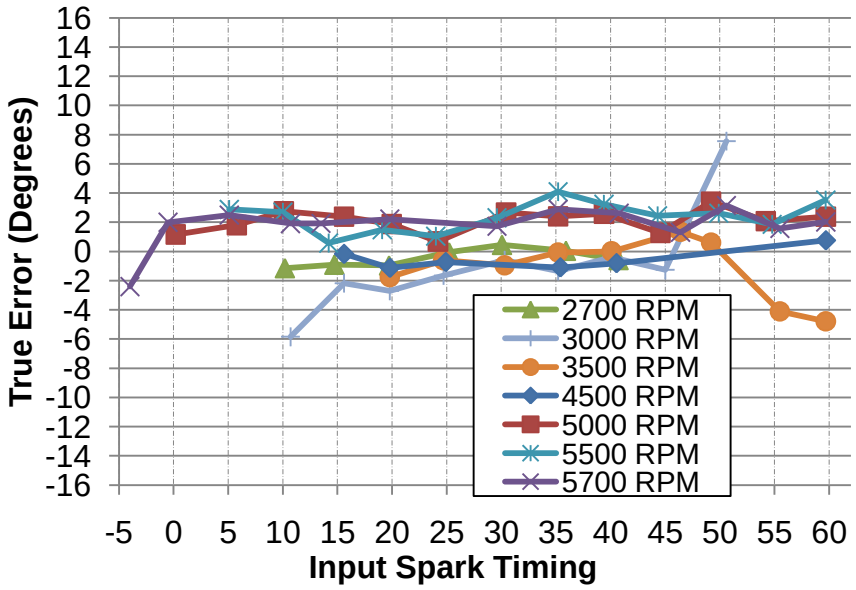

Figure 21. Input vs. actual spark timing

Only one cycle was analyzed per data point however, which would explain the inconsistent error versus timing. To obtain a more accurate error estimate for each engine speed, in order to plot the actual timing, the average of each of the errors were taken. A bar graph of these average errors can be found in Figure

22. The DAQ records the spark timing which you have inputted, therefore the average error was needed to obtain actual spark timing.

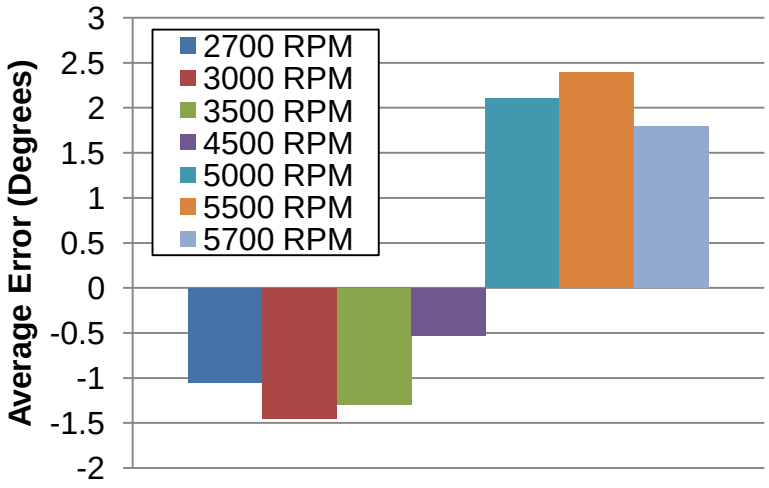

Figure 22. Average spark timing error

There are three main items that will be looked at to determine the optimum spark timing; torque, fuel flow and BSFC. Depending on the situation, one may want to set the timing to obtain the maximum torque or vice versa, the minimum fuel flow. The raw data consisted of eight to ten data points per timing value. The data was plotted and any obvious outliers in the data were discarded. The remaining data points were averaged based on timing. Additionally, as discussed earlier, the timing values were adjusted according to the average error for that particular engine speed. Next, the averaged values of torque, fuel flow and BSFC were plotted against the actual timing. It is known [5] that the trend of torque versus spark advance should be parabolic; therefore a parabolic trend line was fitted to the averaged torque data. The trend seen with the fuel flow rate is that it stays constant versus spark timing, which should be expected since the throttle and carburetor were held fixed at each engine speed and theoretically would allow

the engine to intake the same amount of fuel each cycle. The averaged data plots for each of the load points and the raw data can be found in Appendix E. All of this data is summarized in Figure 23 for minimum BSFC and Figure 24 for maximum torque.

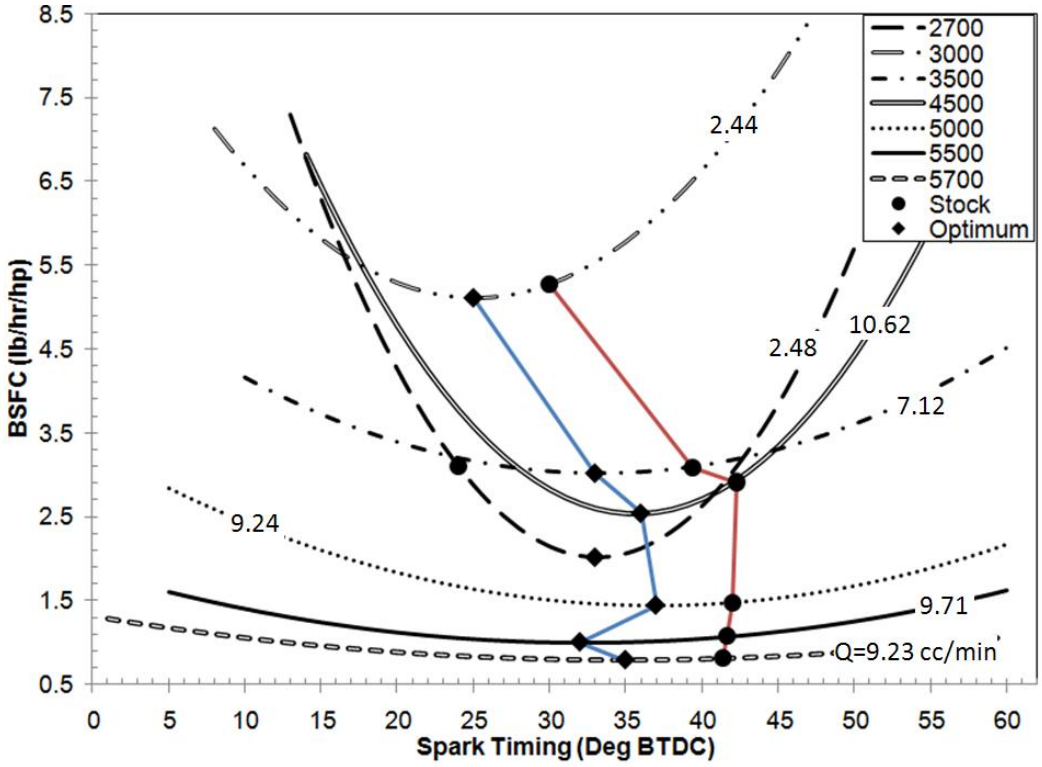

Figure 23. Summary of BSFC vs. ignition timing for n-Heptane for a 17x10 prop engine loading

The curves represent the parabolic trend lines fitted to the averaged data (in Appendix E). Since the fuel flow rate was constant over the timing, the average value for each engine speed is overlaid onto the trend line. Next, the optimum timing location and stock timing locations were overlaid onto the trend lines for each engine speed. Lastly, (ignoring the 2700 RPM curve) a line was drawn connecting the optimum and stock points.

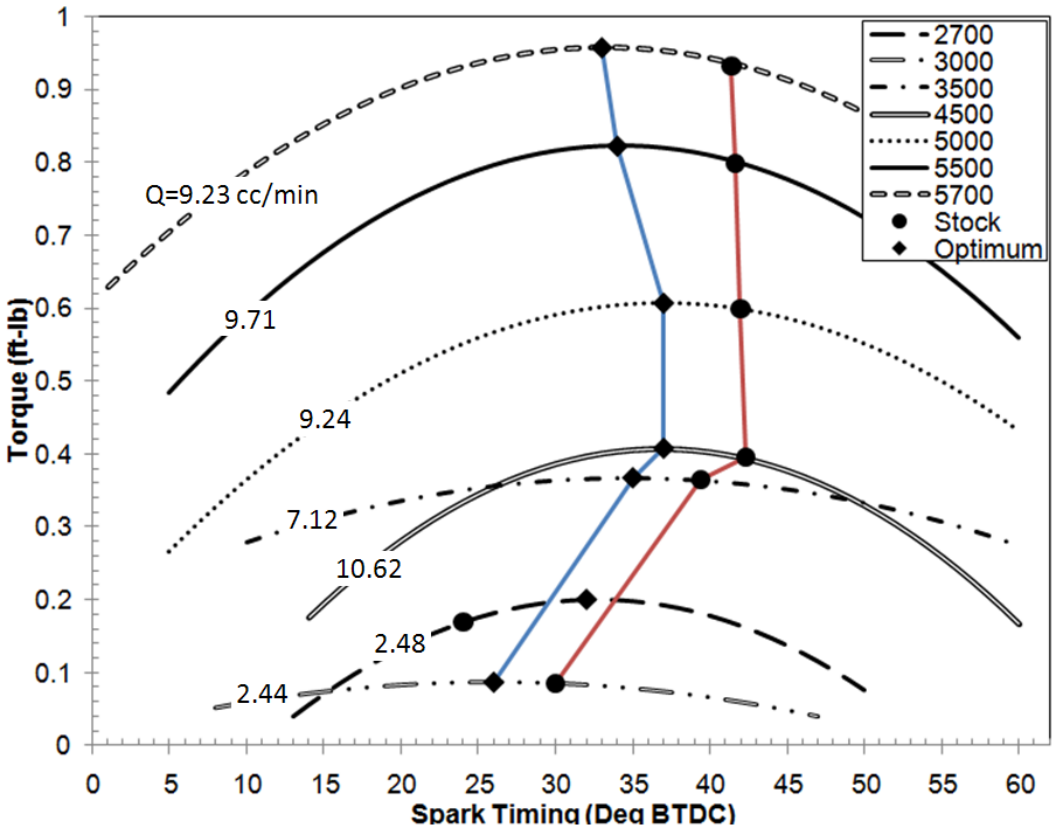

Figure 24. Summary of torque vs. ignition timing for n-Heptane for a 17x10 prop engine loading

Depending on engine loading it appears that BSFC and torque can be greatly affected by the spark timing. Comparing the optimum and stock points show that for n-Heptane, the timing needs to be shifted five to seven degrees. Next, the optimum timing points for n-Heptane are looked at more closely.

Since the fuel flow rates being near constant through the range of timing, the resulting optimum timing for a minimum BSFC and maximum torque is very similar. For each engine speed tested, the optimum spark timing for max torque and minimum BSFC were tabulated and plotted (Figure 25). In addition, the stock ignition box spark timing sequence was plotted.

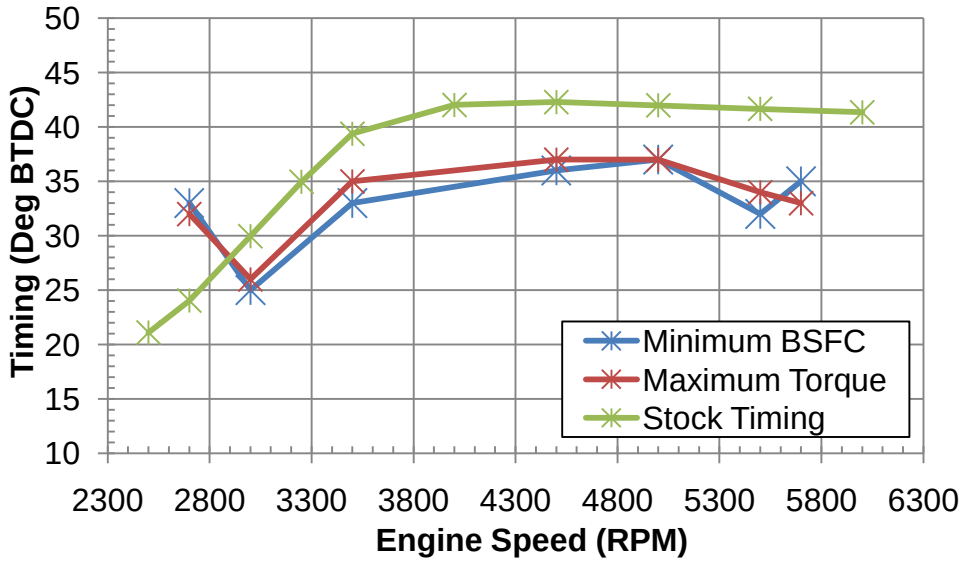

Figure 25. Optimum spark advance (BTDC) for maximum torque and minimum BSFC vs. stock with n-Heptane

The stock timing is assumed to be optimized for gasoline; therefore one expectation was for n-Heptane to require less spark advance. A second expectation was that the optimum timing (regardless of fuel type) at stoichiometric conditions should follow a trend of greater advance as engine speed increases. The first expectation was verified with the exception of the 2700 RPM data point. Out of each of the engine speeds tested, the 2700 RPM point actually had the highest correlation from its trend line, which suggests it being the most accurate in the set. The test temperatures at each optimum timing point are tabulated in Table 13. The average ambient and fuel temperatures for each data set are within 6 Kelvin, but head temperatures vary up to 27 Kelvin. The goal of looking at the test temperature was to correlate a lower mixture or cylinder temperature to the 2700 RPM point, which would result

in the mixture burning slower and thus requiring more spark advance, but there seems to be no real correlation between test temperatures and optimum timing.

Table 13. Test temperatures at the optimum spark timing for n-Heptane

	Average Temperatures at the Optimum Timing		
RPM	Head Temp (K)	Fuel Temp (K)	Ambient Temp (K)
2700	353.52	286.30	295.75
3000	355.22	284.11	294.11
3500	376.08	282.44	292.75
4500	347.22	281.33	291.33
5000	382.36	287.44	292.87
5500	370.32	284.67	292.49
5700	380.00	283.00	292.33

The carburetor is equipped with both a low speed and high speed jet. Although the engine speed that it transitions is not known, if 2700 RPM happened to be using the low speed fuel jet, it could have been set to a different air/fuel ratio therefore altering the time it would take for the mixture to fully combust.

The second expectation did not seem to be as clearly met. The optimum spark timing advance increased until 3500 RPM and then leveled off at around 35 degrees BTDC. If the crankshaft position is translated back to the time domain, the constant degrees would translate to a decrease in time between the spark event and peak pressure as the engine speed increased. This trend has been seen before in Figure 19. One cause of this trend may be that the equivalence ratio is not constant across the engine speeds. It is known [8] that laminar flame speeds decrease as the air to fuel mixture drifts from stoichiometric conditions. Unfortunately, since the air flow was not measured and the

volumetric efficiency is not known, the equivalence ratio cannot be calculated or estimated to any degree of accuracy. Another reason for this trend could be that at higher engine speeds, the flow into the cylinder is becoming more turbulent, which leads to better mixing of the air and fuel and in turn to greater flame speeds, therefore eliminating the need to advance the spark.

To analyze the performance effects of optimizing the spark timing by itself, both the minimum BSFC and maximum torque was tabulated. Table 14 shows the percent decrease in BSFC between the stock timing and optimum timing. Table 15 outlines the desired torque and the percent increase from the actual torque at stock timing and optimized torque.

Table 14. BSFC comparison between stock and optimized spark timing with n-Heptane at a typical 17x10 propeller engine loading

RPM	BSFC w/Stock Timing (lb/hr/hp)	BSFC w/Optimized Timing (lb/hr/hp)	% Decrease
2700	3.103	2.012	35.16%
3000	5.274	5.111	3.09%
3500	3.084	3.016	2.21%
4500	2.911	2.537	12.83%
5000	1.477	1.441	2.39%
5500	1.077	1.002	7.01%
5700	0.812	0.789	2.85%
		Average	**9.36%**

As seen in the both tables, depending on the engine speed and loading, the benefit can vary from slight to considerable. The 2700 and 4500 RPM points benefitted the most. On average, for the loading and speed points that were assessed, the BSFC was decreased by 9.36% and torque increased by 4.45%.

Table 15. Torque comparison between stock and optimized spark timing with n-Heptane at a typical propeller engine loading

RPM	Desired Torque for Prop Load (ft-lb)	Actual Torque at Stock Timing (ft-lb)	Torque at Optimized Timing (ft-lb)	% Increase
2700	0.1920	0.1693	0.2004	18.40%
3000	0.2160	0.0851	0.0867	1.89%
3500	0.2780	0.3646	0.3673	0.74%
4500	0.4680	0.3955	0.4077	3.08%
5000	0.6010	0.5987	0.6068	1.37%
5500	0.7400	0.7982	0.8221	3.00%
5700	0.8010	0.9323	0.9572	2.68%
Average				**4.45%**

This isolated result highlights the fact that a factory configured engine is able to be used with n-Heptane without a real need to optimize the spark timing. However the result presented here is for one load profile and could be considerable different at a different engine loading and/or ambient conditions. I believe the benefit of optimizing on the spark timing can only be accurately assessed if a wider range of engine operating conditions are looked at and if it is coupled with the optimization of equivalence ratio and mixture temperature at the same time.

Heated Fuel Analysis

For the first test using a heated n-Heptane mixture, the results of BSFC can be seen in Figure 26 and Figure 27 for torque and fuel flow. The results were plotted against fuel temperature. Analyzing Figure 26, the results seem very positive, with BSFC decreasing dramatically as the fuel temperature is increased.

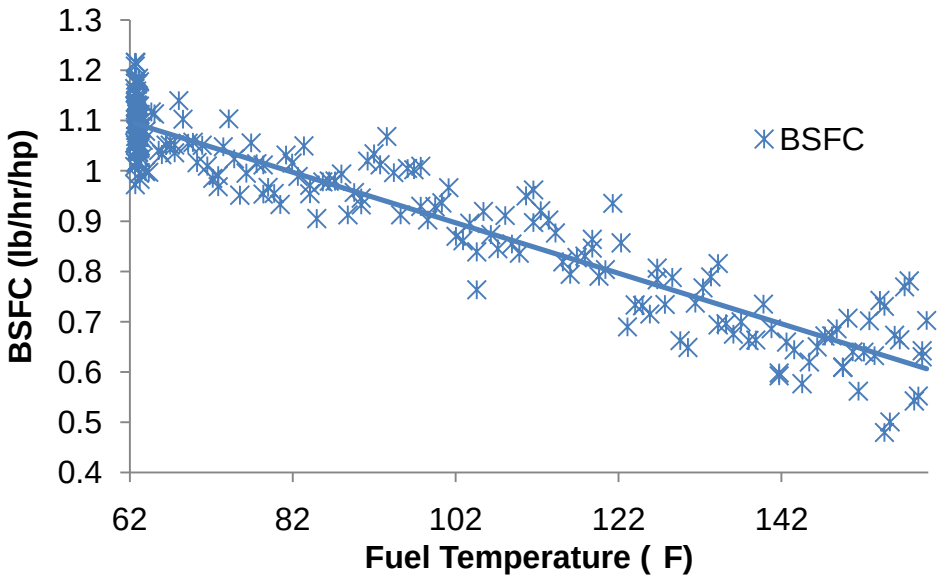

Figure 26. BSFC vs. fuel temperature for heated n-Heptane test #1 at 4000 RPM, 85% throttle and 42° BTDC timing

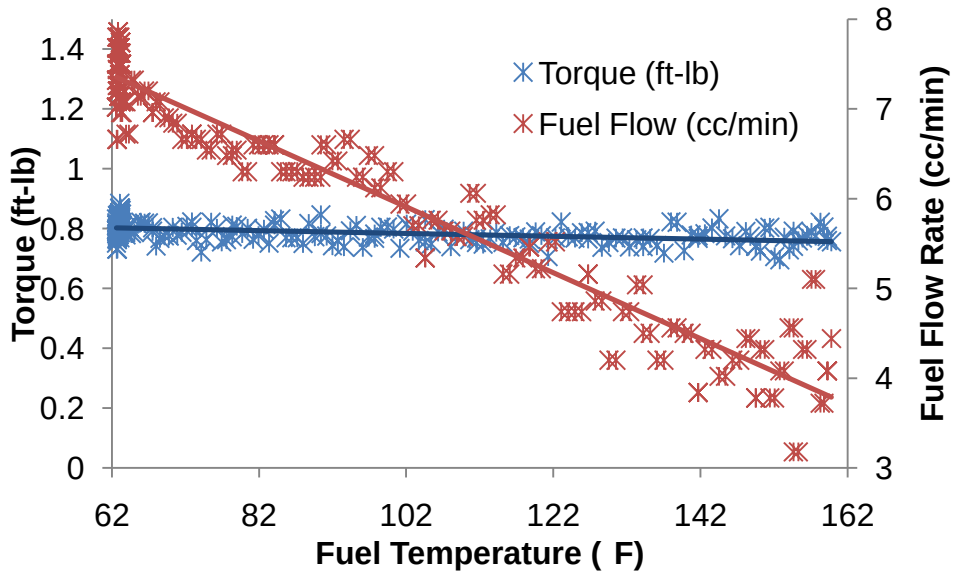

Figure 27. Torque and fuel flow rate for heated n-Heptane test #1 at 4000 RPM, 85% throttle and 42° BTDC timing

However, when the raw torque and fuel flow data are plotted, it can be seen that torque does not appear to be dependent on fuel temperature, but the fuel flow rate is decreasing with fuel temperature. Therefore it appears that BSFC is being dominated by the fuel flow rate. The experiment was run at a constant throttle, engine speed and carburetor needle position, but as fuel is heated, its density decreases which in turn leads to a leaner mixture. Therefore, the decreased specific fuel consumption seems to be more a function of equivalence ratio than fuel temperature. To separate the effects of equivalence ratio from the effects of fuel temperature, a second experiment was completed.

In this experiment, two variables were changed. First, using n-Heptane at ambient room temperature, the carburetor's high speed needle was changed while engine speed and throttle were held fixed. Next, once again the heater was turned on and the fuel constantly rose in temperature. The resulting BSFC and torque from each of these scenarios can now be plotted versus fuel flow and compared (Figure 29 and Figure 28). Using heat to lean the mixture appears to increase BSFC and decrease torque. However at the lowest fuel flow rates, the heated mixture appears to produce as much torque and lower BSFC than the ambient temperature mixture. Ideally with heating the fuel, it should cause the ignition times to decrease, therefore incorrect spark timing for the heated mixture could be a cause for the decrease performance at higher fuel flow rates. Even thought the first two experiments did not isolate the effects of fuel temperature on performance, it is clear from the results that equivalence ratio has a substantial effect on BSFC and torque.

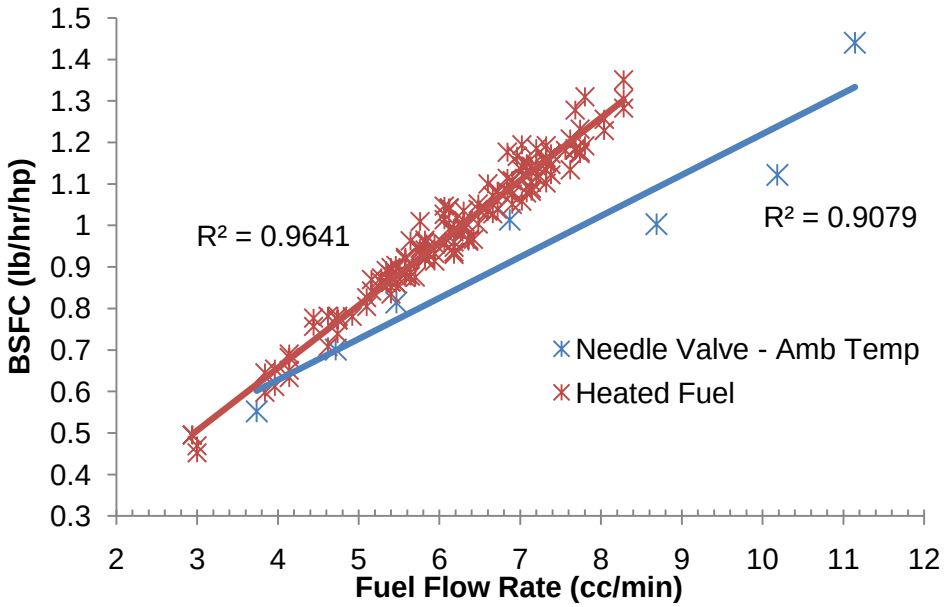

Figure 29. Equivalence ratio affect on BSFC vs. volumetric fuel flow rate with n-Heptane at 4000 RPM, 42° BTDC timing, 100% throttle

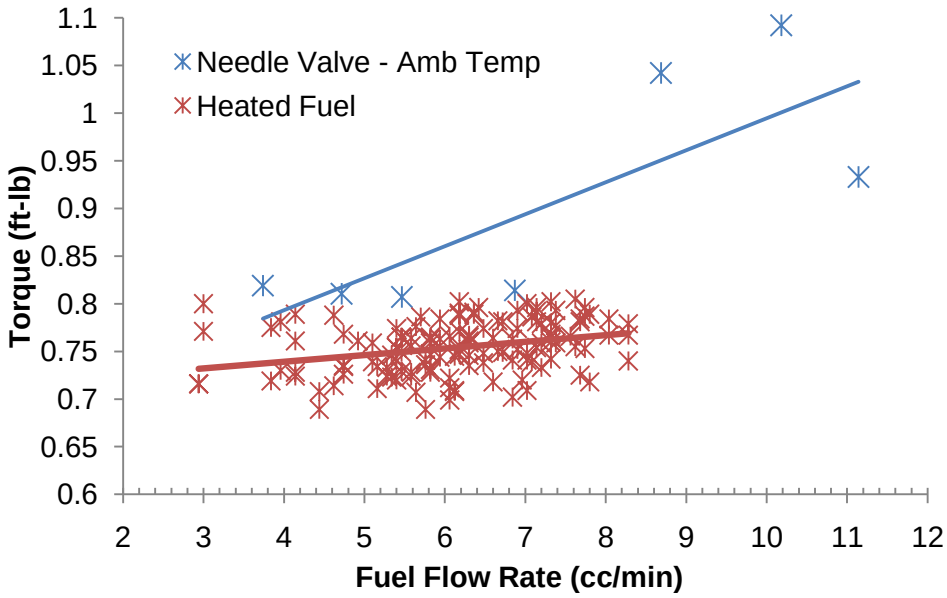

Figure 28. Equivalence ratio affect on torque vs. volumetric fuel flow rate with n-Heptane at 4000 RPM, 42° BTDC timing, 100% throttle

The last heated fuel experiment took another step to increase accuracy and separate the affect of a heated mixture from equivalence ratio. This test was completed with both n-Heptane and iso-Octane for reference. For n-Heptane, the leanest mixture (carburetor needle position 5 in Figure 9) caused the engine to run rough, which led to scattered data. These fuel flow rates are denoted on the resulting figures. Similarly for iso-Octane, position 4 had scattered data, but the engine would not run at all using position 5. Additionally for iso-Octane, only ambient temperature, 300 and 311K data was taken before the engine slipped its rear crankshaft seal and ended the experiment. In the heated fuel analysis (Appendix C), at an ambient temperature of 280 K, both a stoichiometric n-Heptane and iso-Octane mixture should not need heat addition to fully vaporize in the air. Using the highest fuel temperatures (311K for iso-Octane and 344K for n-Heptane) the estimated stoichiometric mixture temperature at 280K ambient temperature is 284K for iso-Octane and 289K for n-Heptane. Both of these mixture temperatures are above the liquid vapor lines, therefore much benefit is not expected from the vaporization standpoint. One other benefit would be the extra energy you could obtain from a heated mixture. This however, if assuming a 10K increase (best case), would only attribute to 20 kJ/kg when multiplied by the specific heat of the fuel. This value is only 0.045% of the heat of combustion. These theoretical calculations were verified by the experiment. The BSFC was plotted against the volumetric fuel flow rate for each temperature and fuel and can be seen in Figure 30 and Figure 32. Additionally, torque was plotted against volumetric fuel flow rate and is shown in Figure 31 and Figure 33.

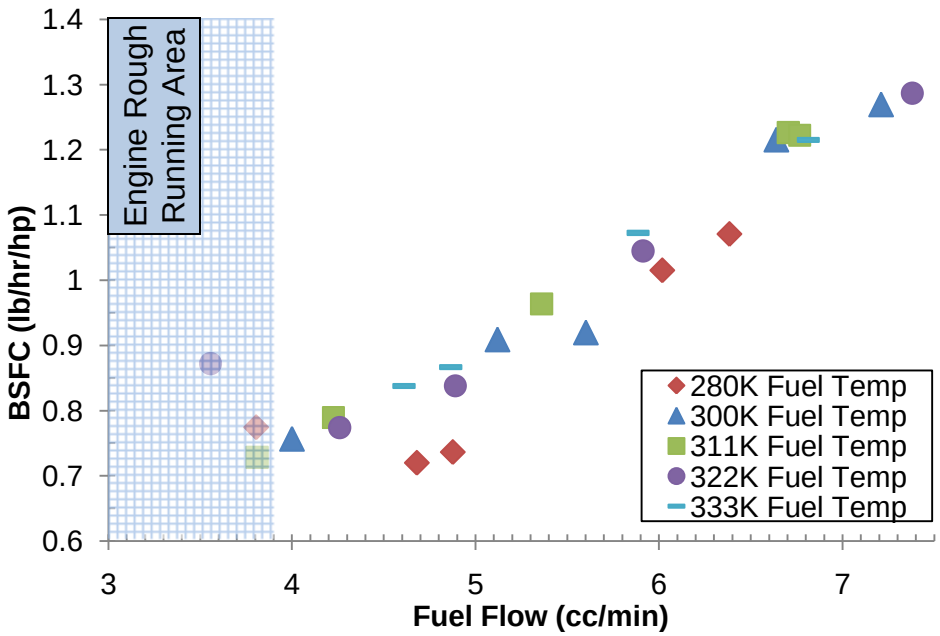

Figure 30. Heated fuel affect on BSFC vs. volumetric fuel flow for n-Heptane at 4000 RPM, 42° BTDC timing, WOT

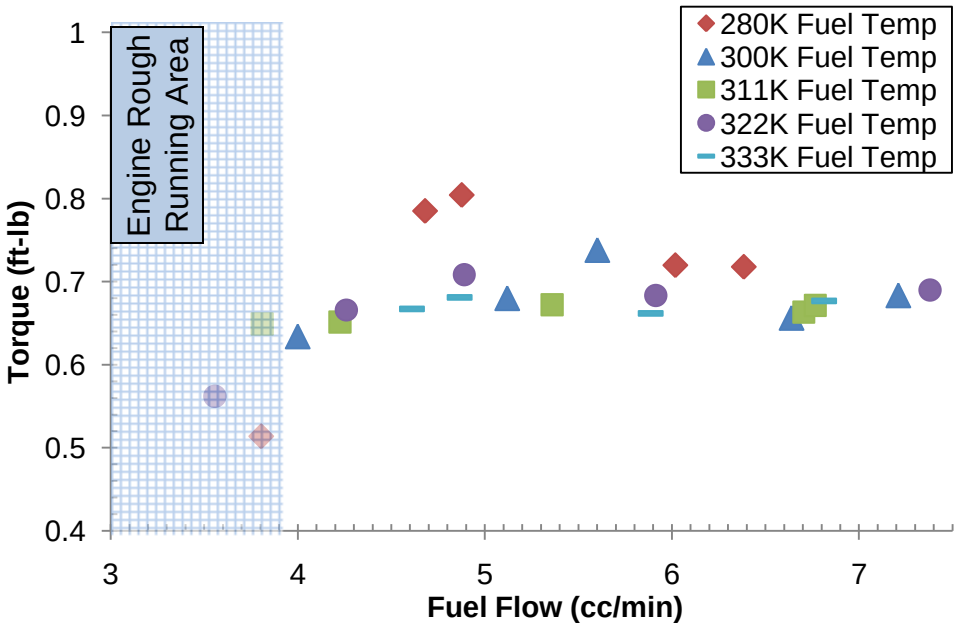

Figure 31. Heated fuel affect on Torque vs. volumetric fuel flow for n-Heptane at 4000 RPM, 42° BTDC timing, WOT

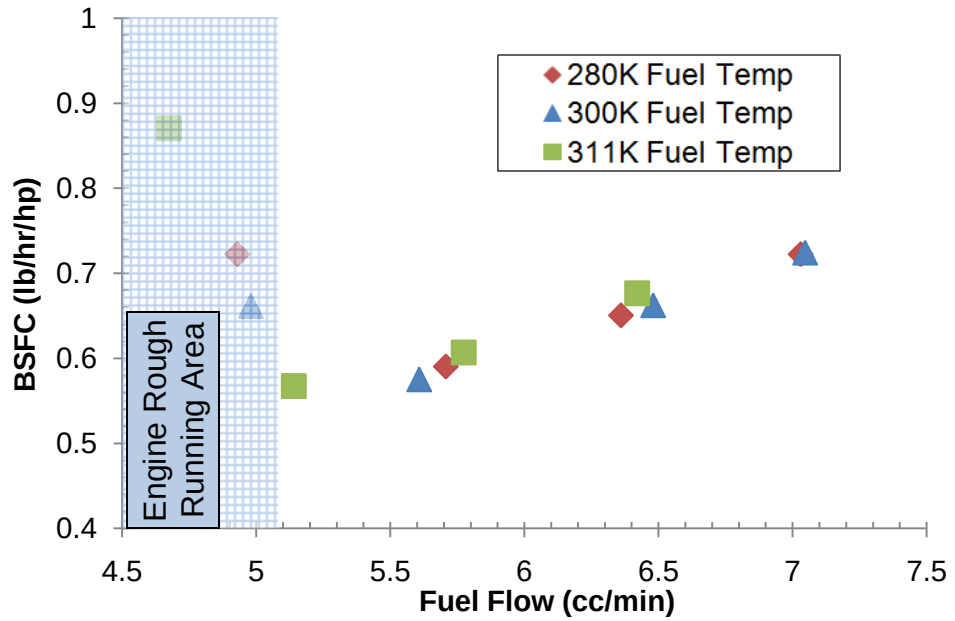

Figure 32. Heated fuel affect on BSFC vs. volumetric fuel flow for iso-Octane at 4000 RPM, 42° BTDC timing, 100% throttle

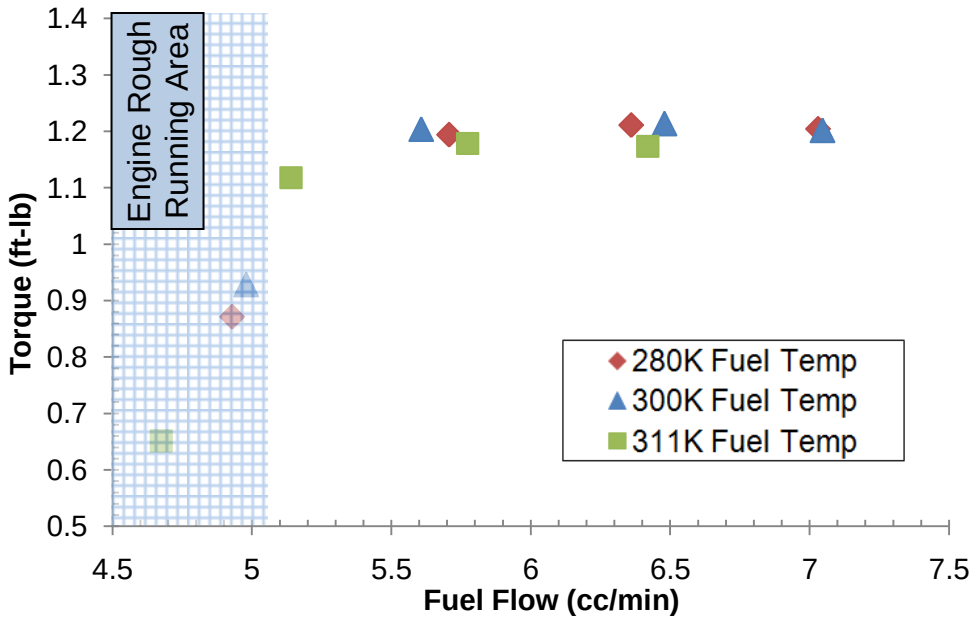

Figure 33. Heated fuel affect on Torque vs. volumetric fuel flow for iso-Octane at 4000 RPM, 42° BTDC timing, 100% throttle

For n-Heptane, its minimum BSFC and maximum torque appear to occur at ambient fuel temperatures, but it is argued that the measurement error leads to it overlapping the other data. There was no benefit seen in the data for iso-Octane. The increased fuel temperature and ultimately the mixture temperature appear to have little to no effect on the performance of this engine. Alternatively the equivalence ratio seems to have the greatest effect. The raw data can be found in Appendix F.

Specifically comparing the iso-Octane and n-Heptane performance, the iso-Octane for this operating point has a greater torque output and leads to a lower BSFC. This could have been predicted as this result matches well with BSFC difference map in Figure 16.

V. Conclusions and Recommendations

Conclusions of Research

The FUJI BF34-EI, a stock gasoline spark ignition engine, successfully ran a zero ON fuel (n-Heptane) with decreased BSFC compared to a high ON fuel (iso-Octane); specifically an average of 4.1% lower in a stock configuration over its entire engine loading and an average of 12.61% lower over a 17x10 propeller load profile. If only spark timing was varied using n-Heptane over the propeller load, an average decrease of 9.4% for BSFC and increase of 4.45% for torque was exhibited. These particular results were at ambient conditions and it is expected that BSFC can be reduced greater by optimizing equivalence ratio with spark timing. The effect of slightly heating both fuels to increase mixture temperature was shown to have negligible effects on the BSFC and torque of this engine. If the mixture temperature (via the air) is above the liquid-vapor temperature, the fuel temperature must be heated much higher to see an increase in energy, due to the magnitude of the fuels heat of combustion.

The knocking characteristic of this engine using n-Heptane was shown to be very slight to non-existent when compared to iso-Octane. Ultimately, the results show that a factory, as delivered, engine will run n-Heptane with negligible effects of knock and with increased performance (min BSFC) at specific engine loading points when compared to iso-Octane. The results of this Thesis can be directly related to JP-8, which provide steps toward NATO and the OSD's single fuel approach with this engine. A future objective is to maximize

performance by optimizing spark timing and equivalence ratio to reduce the BSFC to less than 0.5 lb/hr/hp across a specific propeller load profile.

Recommendations for Future Research

Below is a list of recommend future research and objectives. Using JP-8 and maximizing efficiency with it in these small engines are critical for the future of UAS's.

1. Complete an efficiency and power optimization on three variables; spark timing, equivalence ratio and fuel mixture temperature, for a given number of engine loading points. Suggest choosing a grid of operating points on the performance map.
2. Optimizing the Fuji engine with JP-8. Use #1 as a starting point.
3. Due to limited UAS payload, the volumetric efficiency of this engine needs to be mapped in order to effectively vary equivalence ratio via a fuel injector without needing an air flow sensor.
4. Setup new hardware in support of tests in #1 to #3
    a. Setup a higher accurate throttle controller which includes a measurement of actual throttle butterfly valve position.
    b. Use the Lee Company micro dispensing valve to setup a fuel injector for this engine.
    c. Setup an air flow sensor to be able to obtain actual fuel/air ratio.
    d. Add encoder to the crankshaft to allow for a high accuracy spark timing setting.

Bibliography

1 Korres, D.M. and Karonis, E. Lois. Use of Alternative Fuels on a Diesel Engine. In *1st International Energy Conversion Engineering Conference* (Portsmouth 2003), American Institute of Aeronautics and Astronautics.

2 Wu, P.C. and Hottel, H.C. *Fossil Fuel Combustion, A Source Book*. John Wiley and Sons, New York, 1991.

3 Defense, U.S. Office of Secretary of. *Unmanned Systems Roadmap 2007-2032*. 2007.

4 Totten, George E., Westbrook, Steven R., and Shah, Rajesh J. *Fuels and Lubricants Handbook: Technology, Properties, Performance, and Testing*. ASTM International, Glen Burnie, 2003.

5 Heywood, John B. *Internal Combustion Engine Fundamentals*. McGraw-Hill, Inc, New York, 1988.

6 E.W. Lemmon, M.O. McLinden, D.G. Friend. Thermophysical Properties of Fluid Systems. In *NIST Chemistry WebBook, NIST Standard Reference Database Number 69*. National Institute of Standards and Technology, Gaithersburg, 2009. http://webbook.nist.gov, (Retrieved 9 July 2009).

7 Reynolds, William C. *Thermodynamic Properties in SI; Graphs, Tables and Computational Equations for 40 Substances*. Department of Mechanical Engineering at Stanford University, Stanford, 1979.

8 Turns, Stephen R. *An Introduction to Combustion: Concepts and Applications*. McGraw-Hill, 2000.

9 Tucker, Kelly C. *A Flash Vaporization System for Detonation of Hydrocarbon Fuels in a Pulse Detonation Engine*. PhD Dissertation, Air Force Institute of Technology, Wright Patterson AFB, 2005.

10 Moffat, R.J. Describing the Uncertainties in Experimental Results. In *Experimental Thermal and Fluid Science*. 1988.

11 Bradford, N.C. *Experimental Measurements: Precision, Error and Truth*. John Wiley & Sons Ltd. , New York, 1985.

12 Shen, Yi-Tao, Wang, Jian-Zhong, Shuai, Shi-Jin, and Wang, Jian-Xin. Effects of Octane Number on Gasoline Engine Performance. In *Neiranji Gongcheng/Chinese Internal Combustion Engine Engineering* (Beijing 2008), Chinese Society for Internal Combustion Engines, 52-56.

13 Kumar, K., Freeh, J.E., Sung, C.J., and Huang, Y. Laminar Flame Speeds of Preheated iso-Octane/O2/N2 and n-Heptane/O2/N2 Mixtures. *Journal of Propulsion and Power*, 23, 2 (Mar-Apr 2007), 428-436.

Appendix A: Matlab Code

Engine Performance Map

```
% Written by Capt. Cary Wilson - Fall 2009 - AFIT

% This program will import raw data from LabView and perform several tasks:
%       [A] - Delete all Rows of data that have RPM<1000, Torque<=0,
%       m_dot<=0 and throttle setting<20
%       [B] - Sort Data by Throttle (ascending) first, then by RPM
%       (ascending) second
%       [C] - Create seperate data files for each throttle setting and
%       delete any that have less than 10 data points
%       [D] - Look at data with matching RPM and first filter any points
%       that lie outside of the specified standard deviations and second average
the
%       remaining data points together to create one data point per RPM.
%       [E] - Produce several plots

% NOTE: Raw Data file must have no titles and columns should be sorted as
% follows:

%[Throttle(%)][RPM][Torque(Ft-Lb)][Power(hp][Fuel Mass Flow(lb/hr)][BSFC]..
%..[BMEP(psi)][Ambient Temp(F)][EGT(F)][Fuel Temp(F)][T1(F)][T2(F)]

%For Octane > From CC/min to lb/hr , Multiply by 0.092542562  (At 74 deg
%F) and 0.088932713 (@ 140 deg F)----------  To calculate BMEP Multiply
%Torque by 73.764523893229736
%
%For Heptane > From CC/min to lb/hr , Multiply by 0.08626997  (@140 deg F),
%and 0.090135114 (@74 deg F)

%

clear all; close all; clc;
load data.txt

% ---------- Part [A]
p=0;
for s=1:1:length(data)
   if p==0
      if data(s,2)<1000
      p=s;
            elseif data(s,3)<=0
```

```
            p=s;
                    elseif data(s,5)<=0
                    p=s;
                        elseif data(s,1)<5
                        p=s;
        end
    else
        if data(s,2)<1000
        p=[p;s];
            elseif data(s,3)<=0
            p=[p;s];
                    elseif data(s,5)<=0
                    p=[p;s];
                        elseif data(s,1)<5
                        p=[p;s];
        end
    end
end
if p==0;
else
    data(p,:)=[];
end
% -------------- Part [B]
data = sortrows(data,[1 2]);

% -------------- Part [C]

k=1;i=0;
for s=1:1:length(data)
    a=data(k,1);
    b=data(s,1);
    if b>a
        q=s-1;
        if (q-k)>9
            if i==0
                A={data(k:q,:)};
                k=s;
                i=1;
            else
                A=[A;{data(k:q,:)}];
                k=s;
            end
        elseif (q-k)<=10
            k=s;
        end
```

```
    end
    if s==length(data)
        if (s-k)>9
            A=[A;{data(k:s,:)}];
        else
        end
    end
end

% ---------- Part [D]
scale=1.75;    %How many times the std deviation
z=1;
for u=1:1:length(A)
k=1;
[rows,col]=size(A{u,1});
    if z==1
        for s=1:1:rows
        a=A{u,1}(k,2);
        b=A{u,1}(s,2);
        if b>(a+60)     %Add 60 rpm to the value to cover the grouping of -0+60
            q=s-1;
            if q-k<=4   %Ignores data that has less than 4 data points

            else
            if k==1
                if k==q
                    tot=A{1,1}(k,:);
                else
                    count=A{1,1}(k:q,:);     %Create a new variable containing all rows
with
                    %the same RPM
                    [n,p] = size(count);
                    tot_mean=mean(count);
                    tot_std=std(count);
                    MeanMat = repmat(tot_mean,n,1);  %Create a matrix repeating the
mean
                    %standard deviation values
                    SigmaMat = repmat(tot_std,n,1);
                    outliers = abs(count - MeanMat) > scale*SigmaMat;  %If any one of
the rows
                    %in 'count' are greater than 3 std deviations a "1"
                    %will appear in the column
                    count(any(outliers,2),:) = [];  % Any row containing a "1" will be
deleted
                    tot=mean(count);
```

```
            end
        else
            if k==q
                tot=[tot;A{1,1}(k,:)];
            else
                count=A{1,1}(k:q,:);
                [n,p] = size(count);
                tot_mean=mean(count);
                tot_std=std(count);
                MeanMat = repmat(tot_mean,n,1);
                SigmaMat = repmat(tot_std,n,1);
                outliers = abs(count - MeanMat) > scale*SigmaMat;
                count(any(outliers,2),:) = [];
                tot=[tot;mean(count)];
            end
        end
        k=s;
        end
    end
    if s==rows
        if k==s
            tot=[tot;A{1,1}(k,:)];
        else
            count=A{1,1}(k:s,:);
            [n,p] = size(count);
            tot_mean=mean(count);
            tot_std=std(count);
            MeanMat = repmat(tot_mean,n,1);
            SigmaMat = repmat(tot_std,n,1);
            outliers = abs(count - MeanMat) > scale*SigmaMat;
            count(any(outliers,2),:) = [];
            tot=[tot;mean(count)];
        end
    end
    end
else
    for s=1:1:rows
        a=A{u,1}(k,2);
        b=A{u,1}(s,2);
        if b>(a+60)
            q=s-1;
            if q-k<=4

            else
                if k==q
```

```
                tot=[tot;A{u,1}(k,:)];
            else
                count=A{u,1}(k:q,:);
                [n,p] = size(count);
                tot_mean=mean(count);
                tot_std=std(count);
                MeanMat = repmat(tot_mean,n,1);
                SigmaMat = repmat(tot_std,n,1);
                outliers = abs(count - MeanMat) > scale*SigmaMat;
                count(any(outliers,2),:) = [];
                tot=[tot;mean(count)];
            end
        end
        k=s;
    end
    if s==rows
        if k==s
            tot=[tot;A{u,1}(k,:)];
        else
            count=A{u,1}(k:s,:);
            [n,p] = size(count);
            tot_mean=mean(count);
            tot_std=std(count);
            MeanMat = repmat(tot_mean,n,1);
            SigmaMat = repmat(tot_std,n,1);
            outliers = abs(count - MeanMat) > scale*SigmaMat;
            count(any(outliers,2),:) = [];
            tot=[tot;mean(count)];
        end
    end
  end
end
z=z+1;
end


%Further Filtering of data combined
            scale=2.3;
            tot_a=tot;
            [n,p] = size(tot);
            tot_mean=mean(tot);
            tot_std=std(tot);
            MeanMat = repmat(tot_mean,n,1);
            [x,y]=size(MeanMat);
            MeanMat=[tot(:,1:2) MeanMat(:,3:y)];
```

```
            SigmaMat = repmat(tot_std,n,1);
            outliers = abs(tot - MeanMat) > scale*SigmaMat;
            tot(any(outliers,2),:) = [];        %tot variable is final cut of data with all
throttle settings

        %       scatter(tot_a(:,5),tot_a(:,4))
        %       hold on
        %       scatter(tot(:,5),tot(:,4),'.r')
        %       figure
        %       scatter(tot_a(:,2),tot_a(:,5))
        %       hold on
        %       scatter(tot(:,2),tot(:,5),'.r')

% ---------------- Part [E]

%Determine how many throttle settings there are and create seperate file
%per throttle setting
k=1;  throttle=1;
for s=1:1:length(tot)
   a=tot(k,1);
   b=tot(s,1);
   if b>a
      q=s-1;
      eval(['ts' num2str(throttle) '= tot(k:q,:);']);
      throttle=throttle+1;
      k=s;
   elseif s==length(tot)
      eval(['ts' num2str(throttle) '=tot(k:s,:);']);
   end
end

%Goto plot syntax depending on number of throttle setting files
if throttle == 11

plotvariable='plot(ts1(:,x),ts1(:,y),''.b'',ts2(:,x),ts2(:,y),''og'',ts3(:,x),ts3(:,y),''sr'',ts4(:,
x),ts4(:,y),''*k'',ts5(:,x),ts5(:,y),''xc'',ts6(:,x),ts6(:,y),''+m'',ts7(:,x),ts7(:,y),''db'',ts8(:,x
),ts8(:,y),''^g'',ts9(:,x),ts9(:,y),''hr'',ts10(:,x),ts10(:,y),''pk'',ts11(:,x),ts11(:,y),''<c'')';

trendvariable='plot(tse1(:,1),tse1(:,2),''b'',tse2(:,1),tse2(:,2),''g'',tse3(:,1),tse3(:,2),''
r'',tse4(:,1),tse4(:,2),''k'',tse5(:,1),tse5(:,2),''c'',tse6(:,1),tse6(:,2),''m'',tse7(:,1),tse7(
:,2),''b'',tse8(:,1),tse8(:,2),''g'',tse9(:,1),tse9(:,2),''r'',tse10(:,1),tse10(:,2),''k'',tse11(:,
1),tse11(:,2),''c'',''Linewidth'',2)';
   legendvariable='legend([num2str(round(ts1(1,1)))
''%''],[num2str(round(ts2(1,1))) ''%''],[num2str(round(ts3(1,1)))
''%''],[num2str(round(ts4(1,1))) ''%''],[num2str(round(ts5(1,1)))
```

```
"%"],[num2str(round(ts6(1,1))) "%"],[num2str(round(ts7(1,1)))
"%"],[num2str(round(ts8(1,1))) "%"],[num2str(round(ts9(1,1)))
"%"],[num2str(round(ts10(1,1))) "%"],[num2str(round(ts11(1,1))) "%"])';
elseif throttle == 10

plotvariable='plot(ts1(:,x),ts1(:,y),".b",ts2(:,x),ts2(:,y),"og",ts3(:,x),ts3(:,y),"se",ts4(:
,x),ts4(:,y),"*k",ts5(:,x),ts5(:,y),"xc",ts6(:,x),ts6(:,y),"+m",ts7(:,x),ts7(:,y),"db",ts8(:,
x),ts8(:,y),"^g",ts9(:,x),ts9(:,y),"hr",ts10(:,x),ts10(:,y),"pk")';

trendvariable='plot(tse1(:,1),tse1(:,2),"b",tse2(:,1),tse2(:,2),"g",tse3(:,1),tse3(:,2),"
e",tse4(:,1),tse4(:,2),"k",tse5(:,1),tse5(:,2),"c",tse6(:,1),tse6(:,2),"m",tse7(:,1),tse7
(:,2),"b",tse8(:,1),tse8(:,2),"g",tse9(:,1),tse9(:,2),"r",tse10(:,1),tse10(:,2),"k","Linew
idth",2)';
   legendvariable='legend([num2str(round(ts1(1,1)))
"%"],[num2str(round(ts2(1,1))) "%"],[num2str(round(ts3(1,1)))
"%"],[num2str(round(ts4(1,1))) "%"],[num2str(round(ts5(1,1)))
"%"],[num2str(round(ts6(1,1))) "%"],[num2str(round(ts7(1,1)))
"%"],[num2str(round(ts8(1,1))) "%"],[num2str(round(ts9(1,1)))
"%"],[num2str(round(ts10(1,1))) "%"])';
elseif throttle == 9

plotvariable='plot(ts1(:,x),ts1(:,y),".b",ts2(:,x),ts2(:,y),"og",ts3(:,x),ts3(:,y),"sr",ts4(:,
x),ts4(:,y),"*k",ts5(:,x),ts5(:,y),"xc",ts6(:,x),ts6(:,y),"+m",ts7(:,x),ts7(:,y),"db",ts8(:,x
),ts8(:,y),"^g",ts9(:,x),ts9(:,y),"hr")';

trendvariable='plot(tse1(:,1),tse1(:,2),"b",tse2(:,1),tse2(:,2),"g",tse3(:,1),tse3(:,2),"
r",tse4(:,1),tse4(:,2),"k",tse5(:,1),tse5(:,2),"c",tse6(:,1),tse6(:,2),"m",tse7(:,1),tse7(
:,2),"b",tse8(:,1),tse8(:,2),"g",tse9(:,1),tse9(:,2),"r","Linewidth",2)';
   legendvariable='legend([num2str(round(ts1(1,1)))
"%"],[num2str(round(ts2(1,1))) "%"],[num2str(round(ts3(1,1)))
"%"],[num2str(round(ts4(1,1))) "%"],[num2str(round(ts5(1,1)))
"%"],[num2str(round(ts6(1,1))) "%"],[num2str(round(ts7(1,1)))
"%"],[num2str(round(ts8(1,1))) "%"],[num2str(round(ts9(1,1))) "%"])';
elseif throttle == 8

plotvariable='plot(ts1(:,x),ts1(:,y),".b",ts2(:,x),ts2(:,y),"og",ts3(:,x),ts3(:,y),"sr",ts4(:,
x),ts4(:,y),"*k",ts5(:,x),ts5(:,y),"xc",ts6(:,x),ts6(:,y),"+m",ts7(:,x),ts7(:,y),"db",ts8(:,x
),ts8(:,y),"^g")';

trendvariable='plot(tse1(:,1),tse1(:,2),"b",tse2(:,1),tse2(:,2),"g",tse3(:,1),tse3(:,2),"
r",tse4(:,1),tse4(:,2),"k",tse5(:,1),tse5(:,2),"c",tse6(:,1),tse6(:,2),"m",tse7(:,1),tse7(
:,2),"b",tse8(:,1),tse8(:,2),"g","Linewidth",2)';
   legendvariable='legend([num2str(round(ts1(1,1)))
"%"],[num2str(round(ts2(1,1))) "%"],[num2str(round(ts3(1,1)))
"%"],[num2str(round(ts4(1,1))) "%"],[num2str(round(ts5(1,1)))
```

```
''%''],[num2str(round(ts6(1,1))) ''%''],[num2str(round(ts7(1,1)))
''%''],[num2str(round(ts8(1,1))) ''%'']);
elseif throttle == 7

plotvariable='plot(ts1(:,x),ts1(:,y),''.b'',ts2(:,x),ts2(:,y),''og'',ts3(:,x),ts3(:,y),''sr'',ts4(:,
x),ts4(:,y),''*k'',ts5(:,x),ts5(:,y),''xc'',ts6(:,x),ts6(:,y),''+m'',ts7(:,x),ts7(:,y),''db'')';

trendvariable='plot(tse1(:,1),tse1(:,2),''b'',tse2(:,1),tse2(:,2),''g'',tse3(:,1),tse3(:,2),''
r'',tse4(:,1),tse4(:,2),''k'',tse5(:,1),tse5(:,2),''c'',tse6(:,1),tse6(:,2),''m'',tse7(:,1),tse7(
:,2),''b'',''Linewidth'',2)';
   legendvariable='legend([num2str(round(ts1(1,1)))
''%''],[num2str(round(ts2(1,1))) ''%''],[num2str(round(ts3(1,1)))
''%''],[num2str(round(ts4(1,1))) ''%''],[num2str(round(ts5(1,1)))
''%''],[num2str(round(ts6(1,1))) ''%''],[num2str(round(ts7(1,1))) ''%'']);
elseif throttle == 6

plotvariable='plot(ts1(:,x),ts1(:,y),''.b'',ts2(:,x),ts2(:,y),''og'',ts3(:,x),ts3(:,y),''sr'',ts4(:,
x),ts4(:,y),''*k'',ts5(:,x),ts5(:,y),''xc'',ts6(:,x),ts6(:,y),''+m'')';

trendvariable='plot(tse1(:,1),ts1(:,2),''b'',tse2(:,1),tse2(:,2),''g'',tse3(:,1),tse3(:,2),''r''
,tse4(:,1),tse4(:,2),''k'',tse5(:,1),tse5(:,2),''c'',tse6(:,1),tse6(:,2),''m'',''Linewidth'',2)';
   legendvariable='legend([num2str(round(ts1(1,1)))
''%''],[num2str(round(ts2(1,1))) ''%''],[num2str(round(ts3(1,1)))
''%''],[num2str(round(ts4(1,1))) ''%''],[num2str(round(ts5(1,1)))
''%''],[num2str(round(ts6(1,1))) ''%'']);
elseif throttle == 5

plotvariable='plot(ts1(:,x),ts1(:,y),''.b'',ts2(:,x),ts2(:,y),''og'',ts3(:,x),ts3(:,y),''sr'',ts4(:,
x),ts4(:,y),''*k'',ts5(:,x),ts5(:,y),''xc'')';

trendvariable='plot(tse1(:,1),tse1(:,2),''b'',tse2(:,1),tse2(:,2),''g'',tse3(:,1),tse3(:,2),''
r'',tse4(:,1),tse4(:,2),''k'',tse5(:,1),tse5(:,2),''c'',''Linewidth'',2)';
   legendvariable='legend([num2str(round(ts1(1,1)))
''%''],[num2str(round(ts2(1,1))) ''%''],[num2str(round(ts3(1,1)))
''%''],[num2str(round(ts4(1,1))) ''%''],[num2str(round(ts5(1,1))) ''%'']);
elseif throttle == 4

plotvariable='plot(ts1(:,x),ts1(:,y),''.b'',ts2(:,x),ts2(:,y),''og'',ts3(:,x),ts3(:,y),''sr'',ts4(:,
x),ts4(:,y),''*k'')';

trendvariable='plot(tse1(:,1),tse1(:,2),''b'',tse2(:,1),tse2(:,2),''g'',tse3(:,1),tse3(:,2),''
r'',tse4(:,1),tse4(:,2),''k'',''Linewidth'',2)';
   legendvariable='legend([num2str(round(ts1(1,1)))
''%''],[num2str(round(ts2(1,1))) ''%''],[num2str(round(ts3(1,1)))
''%''],[num2str(round(ts4(1,1))) ''%'']);
```

```
elseif throttle == 3
   plotvariable='plot(ts1(:,x),ts1(:,y),''.b'',ts2(:,x),ts2(:,y),''og'',ts3(:,x),ts3(:,y),''sr'')';

trendvariable='plot(tse1(:,1),tse1(:,2),''b'',tse2(:,1),tse2(:,2),''g'',tse3(:,1),tse3(:,2),''
r'',''Linewidth'',2)';
   legendvariable='legend([num2str(round(ts1(1,1)))
''%''],[num2str(round(ts2(1,1))) ''%''],[num2str(round(ts3(1,1))) ''%''])';
elseif throttle == 2
   plotvariable='plot(ts1(:,x),ts1(:,y),''.b'',ts2(:,x),ts2(:,y),''og'')';
   trendvariable='plot(tse1(:,1),tse1(:,2),''b'',tse2(:,1),tse2(:,2),''g'',''Linewidth'',2)';
   legendvariable='legend([num2str(round(ts1(1,1)))
''%''],[num2str(round(ts2(1,1))) ''%''])';
elseif throttle == 1
   plotvariable='plot(ts1(:,x),ts1(:,y),''.b'')';
   trendvariable='plot(tse1(:,1),tse1(:,2),''b'',''Linewidth'',2)';
   legendvariable='legend([num2str(round(ts1(1,1))) ''%''])';
else
end

%Create Plots
%Engine Map
      figure
      steps=30;
      x=tot(:,2);y=tot(:,7);z=tot(:,6);  %x=RPM, y=BMEP, z=BSFC
      xi=[min(x):((max(x)-min(x))/steps):max(x)]';
      yi=[min(y):((max(y)-min(y))/steps):max(y)]';     %Set grid size
      [XI,YI]=meshgrid(xi,yi);    %Create x,y grid
      ZI = griddata(x,y,z,XI,YI);     %Interpolate z values to new grid
      %create Filled in color Map
      colormap jet
      v=[.3:.1:.8 .9:.2:2];
      [C,h] = contourf(XI,YI,ZI,v);
      clabel(C,h,'manual','fontsize',14,'rotation',0);
      colorbar
      axis([1000 6000 10 90])
      caxis([0.3 2]);
      xlabel('RPM')
      ylabel('BMEP (psi)')
      title('Fuji Engine Map')
      %create black and white single line map
      figure
      [C,h] = contour(XI,YI,ZI,v,'k');
      clabel(C,h,'manual','fontsize',14,'rotation',0);
      axis([1000 6000 10 90])
      xlabel('RPM')
```

```
        ylabel('BMEP (psi)')
        title('Fuji Engine Map')
        %Add 17x10 Prop - BMEP vs RPM to map
        prop=[2700 2970 3450 4440 5040 5400 5490      5520 5700;14.16278859
15.93313716 20.50653764 34.52179718 44.33247886 49.86481815
54.58574768 56.28233173 59.08538364]';
        plot(prop(:,1),prop(:,2),'-b','linewidth',2.5)
        legend('BSFC(lb/hr/hp)')
```

High Speed PCB Pressure Reducer (Engine Loading Knock)

```
%Program written by Capt. Cary Wilson on 28Feb2010

%This program will take the raw PCB pressure data file

close all;clear all;clc;
format long
filename = uigetfile('*.*','Multiselect','on')';        %Allow user to select all of the
pressure raw data files and stores them as filename
for u=1:length(filename)
    fid = fopen(cell2mat(filename(u,1)));                %Opens each file 1 by 1
    C = textscan(fid,'%n %n %n %n %n %n %n %n %n','HeaderLines',1);
%Stores each column of raw data in variable C
    fclose(fid);                                                %Closes the file
    if u==1
        data={[C{1,1} C{1,2}]};              %Stores the time and voltage in the
variable data
    else
        data=[data;{[C{1,1} C{1,2}]}];
    end
end
title_r = ('Engine RPM''s');             %title for dialogue box
defaultans=
{'5000','5000','4000','5000','5000','4000','3670','3500','3000','2700','2500','2900','3
300','3000'};        %Default inputs to next dialogue box
answer = inputdlg(filename,title_r,1,defaultans);        %Asks user to input engine
speeds for each file name
speed = str2num(cell2mat(answer));                    %stores these speeds as the
variable speed

timetoadd=(((speed./60).^-1)./2)./(40000.^-1);      %Creates a variable that will
allow the program to skip to each power cycle
```

```
for tot=1:length(data)                                  %For loop to cycle through
each data file saved in "filename"
   speed_t = speed(tot,1);
   timetoadd_t = timetoadd(tot,1);
   data_t=data{tot,1};
   time=data_t(:,1)/2;                          %corrects the high speed data time to
half what was recorded
   pressure=(data_t(:,2)-min(data_t(:,2))).*1000;          %transform from V to
psi
   data_t=[time pressure];

      p=-1;
      for s=1:length(data_t)                    %Loop to delete any pressure spikes
(from spark interference)
         if data_t(s,2) > 300 && p < 0          %chose 300 psi
            p=s;
         elseif data_t(s,2) > 300 && p >0
            p=[p;s];
         end
      end

      if p==-1;                  %If there were no spikes, continue
      else
         data_t(p,:)=[];          %If there are, delete those rows
      end

      step=(speed_t/60)*360*(40000^-1);         %Create the degrees step size
      degrees=[10:step:40]';      %X axis from peak pressure to 30 degrees past


      j=1;k=1;
      for s=31:length(data_t)
         if s+30>length(data_t)           %End the loop if it is at the end of the raw
data
            break
         end
         if s > k
            if (mean(data_t(s:(s+30),2)) - mean(data_t((s-30):s,2)))  > 10
%Take average of 30 points before and after the curent point.  Difference will
show if the pressure is rising to isolate the curve
               k=fix(s+timetoadd_t);               %once a pressure curve is found,
the next starting point to search will be the current point plus the timetoadd
               if k>length(data_t)          %Sets k equal to the final point if it was
currently larger
                  k=length(data_t);
```

```
            end
                tot_press_profile=data_t(s:k,2)./max(data_t(s:k,2));
                [peak,loc]=max(data_t(s:k,2));      %Within the subset of begining
of pressure curve to "timetoadd" past, the peak is found with its location
                tdc=loc+s;          %loc is row in the subset, to get row in total data
file it must be added to the current position
                low_limit=fix((degrees(1,1)/step)+tdc);
                high_limit=fix((degrees(length(degrees),1)/step)+tdc);
            if high_limit < length(data_t)
                Press=data_t(low_limit:high_limit,2);    %Grabs the Pressure
between points defined in "degrees"
                ploop=Press./max(Press);    %normalizing pressure so Maximum
= 1
                %ptrend_coeff = polyfit(degrees,ploop,2);    %calculated poly
trendline coefficients from ploop  2ND ORDER POLYNOMIAL

%ptrend=degrees.*ptrend_coeff(1,1)^2+degrees.*ptrend_coeff(1,2)+ptrend_coeff
(1,3);   %Calculate theoretical pressure values 2ND ORDER POLY
                ptrend_coeff = polyfit(degrees,ploop,1);    %calculated poly
trendline coefficients from ploop  LINEAR
                ptrend=degrees.*ptrend_coeff(1,1)+ptrend_coeff(1,2);
%Calculate theoretical pressure values  LINEAR
                true_error= (ploop - ptrend).^2;    %square of the errors
                deviation=sqrt(mean(true_error));          %Variance between true
and theoretical pressure values
            else
            break
            end
            if j==1
                Press_Profile={tot_press_profile};
                Pressures=ploop;
                Trends=ptrend;
                Devs=deviation;
                j=j+1;
            else
                Press_Profile=[Press_Profile; {tot_press_profile}];
                Pressures=[Pressures ploop];        %Creates variable with all of
the normalize pressures
                Trends=[Trends ptrend];     %Creates variable with all of the trend
lines
                Devs=[Devs deviation];              %Records all of the devaiation
values
            end
        end
    else
```

```
        end
    end

  if tot == 1
    Final_Sep_Dev={[Devs']};              %Create an array with the deviations for
each pressure curve for each data file
    Final_Dev=[mean(Devs) mean(Devs)-min(Devs) max(Devs)-mean(Devs)];
%Similiar array with avarage deviation/minimum and maximum deviation for
each data file
  else
    Final_Sep_Dev=[Final_Sep_Dev {[Devs']}];
    Final_Dev=[Final_Dev;mean(Devs) mean(Devs)-min(Devs) max(Devs)-
mean(Devs)];
  end
  figure
for i=1:length(Press_Profile)
  x=time(1:length(Press_Profile{i,1}(:,1)))*1000;
  y=Press_Profile{i,1}(:,1);
  plot(x,y)
  hold on
end
title('Normalized Pressure Profiles')
xlabel('Time from Initial Pressure Rise (ms)')
ylabel('Pressure/P_m_a_x')
axis([0 6 0 1.1])
picture_name=['Pressure Plot' num2str(tot)];
screen2jpeg(picture_name)
end

%title_t = ('Throttle');
%defaultans_t= {'40','85','85','85','85','85','85','85','80','80','80','80','90','90'};
%answer_t = inputdlg(filename,title_t,1,defaultans_t);          %Allow user to input
throttle setting for each file
%throttle = str2num(cell2mat(answer_t));

figure
plot(degrees,Pressures)
hold on
plot(degrees,Trends)

load bmep.txt
temp_oct=[bmep(1:3,1) Final_Dev(1:3,:) speed(1:3,1)];
temp_oct = sortrows(temp_oct,1);
temp_hep=[bmep(4:14,1) Final_Dev(4:14,:) speed(4:14,1)];
temp_hep = sortrows(temp_hep,1);
```

```
%Plot Average Deviations for Both fuels versus BMEP
figure
errorbar(temp_oct(:,1),temp_oct(:,2),temp_oct(:,3),temp_oct(:,4),'--
k','linewidth',1.5)
hold on
errorbar(temp_hep(:,1),temp_hep(:,2),temp_hep(:,3),temp_hep(:,4),'b','linewidth',
1.5)
hold on
plot(temp_oct(:,1),temp_oct(:,2),':r','linewidth',2);
hold on
plot(temp_hep(:,1),temp_hep(:,2),':g','linewidth',2);
axis([33 79 0 .1])

ylabel('Standard Deviation')
xlabel('BMEP (psi)')
title('Octane Pressure Deviation')
screen2bmp('Overall Deviations')
```

High Speed Optrand Pressure Reducer (Heated Fuel Knock)

```
 %Program written by Capt. Cary Wilson on 18Mar2010
%This program will take the raw Optrand pressure data file

close all;clear all;clc;
format long
filename = uigetfile('*.*','Multiselect','on')';        %Allow user to select all of the
pressure raw data files and stores them as filename
for u=1:length(filename)
    fid = fopen(cell2mat(filename(u,1)));                %Opens each file 1 by 1
    C = textscan(fid,'%n %n %n %n %n %n %n %n %n','HeaderLines',1);
%Stores each column of raw data in variable C
    fclose(fid);                                                %Closes the file
    if u==1
        data={[C{1,1} C{1,2} C{1,3}]};                %Stores the time, voltage and spark
signal in the variable data
    else
        data=[data;{[C{1,1} C{1,2} C{1,3}]}];
    end
end
title_r = ('Engine RPM''s');              %title for dialogue box
defaultans= {'4000','4000','4000','4000','4000'};        %Default inputs to next
dialogue box
answer = inputdlg(filename,title_r,1,defaultans);        %Asks user to input engine
speeds for each file name
```

```
speed = str2num(cell2mat(answer));                  %stores these speeds as the
variable speed

timetoadd=(((speed./60).^-1)./3)./(40000.^-1);      %Creates a variable that will
allow the program to skip to each power cycle

for tot=1:length(data)                              %For loop to cycle through
each data file saved in "filename"
   speed_t = speed(tot,1);
   timetoadd_t = timetoadd(tot,1);
   data_t=data{tot,1};
   time=data_t(:,1)/2;                              %corrects the high speed data time to
half what was recorded
   pressure=data_t(:,2)/.00302;                     %transform from V to psi
   spark=data_t(:,3);
   data_t=[time pressure spark];

   j=1;k=1;
   for s=1:length(data_t)
      if j==1
         ctr=k;
         if abs(data_t(s,3)) > 4
            k=s;
            j=j+1;
            ctr=k+timetoadd_t;
         end
      elseif j==2
         if abs(ctr-s) > timetoadd_t
         if abs(data_t(s,3)) > 4   && (mean(data_t((s+5):(s+30),2)) -
mean(data_t((s-30):(s-5),2)))  > 10  %First pulling point at which the
            %spark goes above 4 V, then I average the 30 pressure points
            %before this and after this time and compare to disgard non
            %power cycles.
            k=s;
            newdata=data_t(s:s+150,2);    %Pull pressures from the spark to 150
points past
            newdata_n=data_t(s+10:s+200,2)./max(data_t(s+10:s+200,2));
            ctr=k+timetoadd_t;
            j=j+1;
         end
         end
      else
         if s+30 >length(data_t)
         break
         elseif abs(ctr-s) > timetoadd_t
```

```
            if abs(data_t(s,3)) > 4   && (mean(data_t((s+5):(s+30),2)) -
mean(data_t((s-30):(s-5),2)))  > 10
                k=s;
                newdata=[newdata data_t(s:s+150,2)];
                newdata_n=[newdata_n
data_t(s+10:s+200,2)./max(data_t(s+10:s+200,2))];
                ctr=k+timetoadd_t;
            end
         end
      end
   end
   figure
   plot(time(1:length(newdata_n))*1000,newdata_n)
   title('Normalized Pressure Profiles')
   xlabel('Time from Initial Pressure Rise (ms)')
   ylabel('Pressure/P_m_a_x')
   picture_name=['Pressure Plot' num2str(tot)];
   screen2jpeg(picture_name)


   step=(speed_t/60)*360*(40000^-1);          %Create the degrees step size
   degrees=[10:step:40]';       %X axis from peak pressure to 30 degrees past


   j=1;k=1;
   [l,w]=size(newdata_n);
   for i=1:w
      [peak,loc]=max(newdata_n(:,i));      %Within the subset of begining of
pressure curve to "timetoadd" past, the peak is found with its location
      tdc=loc;         %loc is row in the subset, to get row in total data file it must
be added to the current position
      low_limit=fix((degrees(1,1)/step)+tdc);
      high_limit=fix((degrees(length(degrees),1)/step)+tdc);
      Press=newdata_n(low_limit:high_limit,i);    %Grabs the Pressure between
points defined in "degrees"
      ploop=Press;    %normalizing pressure so Maximum = 1
      %ptrend_coeff = polyfit(degrees,ploop,2);    %calculated poly trendline
coefficients from ploop  2ND ORDER POLYNOMIAL

%ptrend=degrees.*ptrend_coeff(1,1)^2+degrees.*ptrend_coeff(1,2)+ptrend_coeff
(1,3);   %Calculate theoretical pressure values 2ND ORDER POLY
      ptrend_coeff = polyfit(degrees,ploop,1);    %calculated poly trendline
coefficients from ploop  LINEAR
      ptrend=degrees.*ptrend_coeff(1,1)+ptrend_coeff(1,2);   %Calculate
theoretical pressure values  LINEAR
```

```
        true_error= (ploop - ptrend).^2;    %square of the errors
        deviation=sqrt(mean(true_error));          %Variance between true and
theoretical pressure values
        if j==1
            Pressures=ploop;
            Trends=ptrend;
            Devs=deviation;
            j=j+1;
        else
            Pressures=[Pressures ploop];        %Creates variable with all of the
normalize pressures
            Trends=[Trends ptrend];     %Creates variable with all of the trend lines
            Devs=[Devs deviation];              %Records all of the devaiation values
        end
    end

    if tot == 1
        Final_Sep_Dev={[Devs']};              %Create an array with the deviations for
each pressure curve for each data file
        Final_Dev=[mean(Devs) mean(Devs)-min(Devs) max(Devs)-mean(Devs)];
%Similiar array with avarage deviation/minimum and maximum deviation for
each data file
    else
        Final_Sep_Dev=[Final_Sep_Dev {[Devs']}];
        Final_Dev=[Final_Dev;mean(Devs) mean(Devs)-min(Devs) max(Devs)-
mean(Devs)];
    end
end

ftemp=[290 290 311 311 344]';
temp_oct=[ftemp Final_Dev];
temp_oct = sortrows(temp_oct,1);
%Plot Average Deviations for Both fuels versus BMEP
figure
errorbar(temp_oct(:,1),temp_oct(:,2),temp_oct(:,3),temp_oct(:,4),'--
k','linewidth',1.5)
hold on
plot(temp_oct(:,1),temp_oct(:,2),':r','linewidth',2);
axis([285 350 0 .1])
ylabel('Standard Deviation')
xlabel('Fuel Temp(K)')
title('Heated n-Heptane Pressure Deviation')
screen2bmp('Overall Deviations')
```

Appendix B. Spark Timing Program and Schematic

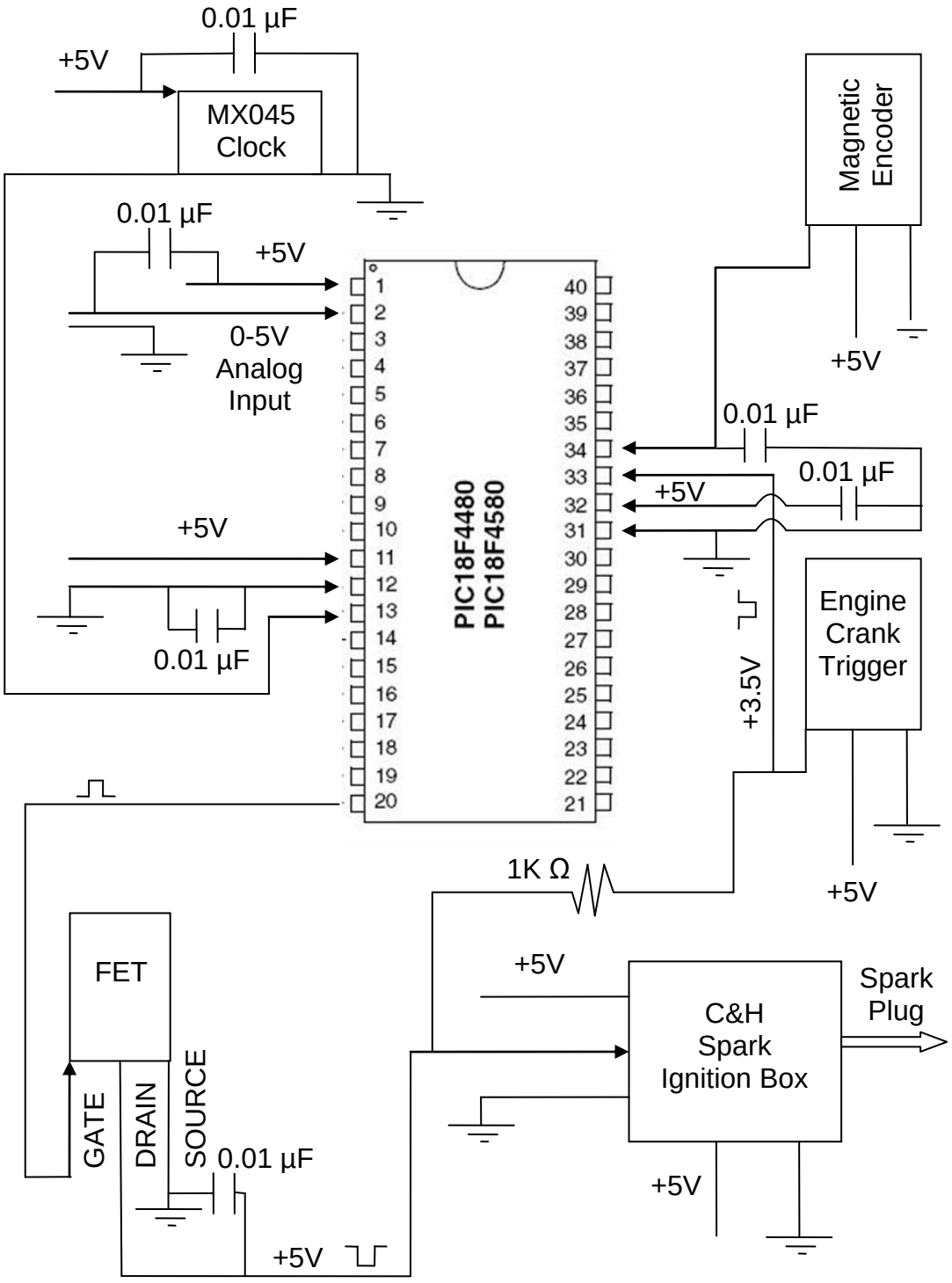

```
#include <18F452.h>
#device adc=10
#use delay(clock=40000000)
#fuses HS, NOBROWNOUT, STVREN, NOWDT, NOLVP

//This program implements variable spark timing for the fuji engine. It requires
// an input of 25 pulses per revolution and a crankshaft pulse 45.1 degrees BTDC
// to calculate correct spark angle and time. It is currently set up to wait for
// the 22nd pulse of the 25 tooth gear before it calculates the new time/angle.
// It calculates and updates the time/angle before it gets to the
// min_spark_angle where it then uses the new time to fire the spark.

#define OUTPIN_SPARK_1 PIN_D1  //pin #20.
//#define SPARK_ENABLE_PIN PIN_D7  //pin #30

//CONSTANT VARIABLES
#define rev_length_buffer 45000  //this MUST BE LARGER THAN
rotation_length_max!!!
#define rev_length_max 20000  //150 rpm; low speed limit
#define rev_length_min 500  //6000rpm rev limiter WARNING: overspinning this
engine (even a little) does damage quickly

#define spark_angle_channel 0  //desired number of degrees past
time1245/time36 pulse to fire injectors.

#define pulse_22_angle 88.3 //22nd pulse (after crankshaft pulse) from 25 tooth
gear comes at 88.3 degrees BTDC.

#define spark_angle_min -60.0   //Spark angle in degrees ATDC at 0V. So spark
will be 88.3 - 60 = 28.3 degrees after the pulse.
#define spark_angle_max 10.0  //Spark angle in degrees ATDC at 5V.

#define spark_duration 100  // 2ms / 20us = 100

int16 time1, jj, time_pulse_17, time_pulse_22;

int16 stoptime_1, sparktime_1;
int16 stoptime_1_new, sparktime_1_new;
int8  sparktime_1_ready, rev_updated;

int16 rev_length;

float spark_angle_slope, spark_angle_intercept;

signed int16 spark_delay;
```

```
#int_TIMER2
TIMER2_isr()
{
  time1++;
  if (time1 >= rev_length_buffer){  //reset time if engine is not spinning so that
buffer does not overflow.
     time1 = 0;
     rev_length = rev_length_buffer;
  }

 //  if (input(SPARK_ENABLE_PIN) == TRUE){
     if ((rev_length >= rev_length_min) && (rev_length <= rev_length_max)){
        if (time1 == sparktime_1) output_low(OUTPIN_SPARK_1);
        else if (time1 == stoptime_1) output_high(OUTPIN_SPARK_1);
     }
 //  }
  else{
     output_high(OUTPIN_SPARK_1);
  }

  if (sparktime_1_ready == TRUE){  //recieve new spark times if they are ready
     sparktime_1 = sparktime_1_new;
     stoptime_1 = stoptime_1_new;
     sparktime_1_ready = FALSE;
  }

} //End of Timer Interrupt ****************************************************

//Pin RB0 (#33)
//crankshaft timing pulse*****************************************************
#int_EXT
EXT_isr()
{
//crankshaft pulse sets 25 tooth gear count to zero
  jj = 0;
}
//End of crankshaft timing pulse interrupt************************************

//Pin RB1 (#34)
//25 tooth gear timing pulse**************************************************
#int_EXT1
EXT1_isr()
{
  jj++; //increment 25 tooth gear count for each tooth
```

```
   //measure time between 17th and 22nd pulse (5 pulses) on 25 tooth gear and
multiply by 5 to get rev_length
   if (jj == 17) time_pulse_17 = time1;
   if (jj == 22){
      time_pulse_22 = time1;
      rev_length = (time_pulse_22 - time_pulse_17) * 5;
      time1 = 0;
      set_timer2(0);
      rev_updated = TRUE;
   }
}
//End of 25 tooth gear timing pulse interrupt**********************************

void main()
{
   setup_adc_ports(A_ANALOG);
   setup_adc(ADC_CLOCK_DIV_64);
   setup_psp(PSP_DISABLED);
   setup_spi(FALSE);
   setup_wdt(WDT_OFF);
   setup_timer_0(RTCC_INTERNAL);
   setup_timer_1(T1_DISABLED);
   setup_timer_2(T2_DIV_BY_1,199,1);  //Time is now 20 microseconds -
>(200*4/40000000)*1=0.00002
   setup_timer_3(T3_DISABLED);
   setup_ccp1(CCP_OFF);
   setup_ccp2(CCP_OFF);
   disable_interrupts(INT_TIMER2);  //Block interrupts momentarily
   disable_interrupts(INT_EXT);
   disable_interrupts(INT_EXT1);
   ext_int_edge(H_TO_L);  //Look for negative edges on interrupt 0
   ext_int_edge(1,H_TO_L);  //Look for negative edges on interrupt 1

   //Initialize variables*****************************************************
   time1 = 0;
   jj = 0;

   rev_length = rev_length_max;  //Default to a high cycle time

   //adding pulse_22_angle calculates the actual angle after 22nd pulse for min
and max spark angle
   spark_angle_slope = ((spark_angle_max + pulse_22_angle) -
(spark_angle_min + pulse_22_angle)) / 360.0 / 1023.0;
   spark_angle_intercept = (spark_angle_min + pulse_22_angle) / 360.0;
```

```
  set_adc_channel(spark_angle_channel);
  delay_us(100);
  spark_delay = (spark_angle_slope * read_adc() + spark_angle_intercept) *
rev_length;
  if (spark_delay <=0) spark_delay = 1;

  sparktime_1 = spark_delay;
  stoptime_1 = sparktime_1 + spark_duration;
  sparktime_1_new = sparktime_1;
  stoptime_1_new = stoptime_1;
  output_high(OUTPIN_SPARK_1);
  sparktime_1_ready = FALSE;
  rev_updated == FALSE;

  //End initialize variables************************************************

  enable_interrupts(INT_TIMER2);  //Enable timing
  enable_interrupts(INT_EXT);  //Begin watching crankshaft timing pulse
  enable_interrupts(INT_EXT1);  //Begin watching 25 tooth gear timing pulse
  enable_interrupts(GLOBAL);  //Enable Global interrupt

  while (1){

    while ((jj != 22) && (rev_updated == FALSE)) {}  //wait until 25 tooth gear
22nd pulse and updated rev_length to calc new time
    spark_delay = (spark_angle_slope * read_adc() + spark_angle_intercept) *
rev_length;
    sparktime_1_new = spark_delay;
    stoptime_1_new = sparktime_1_new + spark_duration;
    sparktime_1_ready = TRUE;
    rev_updated == FALSE;
  }
}
```

Appendix C: Fuel Vaporization Analysis

The following analysis assumes the fuel has atomized into the air at the point of entry in the venturi in the carburetor. The first part of the analysis is to find the minimum resulting mixture temperature needed to keep the fuel in a vapor state while entering the cylinder. Using Dalton's Law of Partial Pressure, the partial pressures for both iso-Octane and n-Heptane mixed with air at an atmospheric pressure of 14.3 psi were calculated, and can be found in Table 16. These pressures were then used along with vapor saturation table lookups from the National Institute of Standards and Technology Chemistry WebBook to determine the required temperature needed to achieve a 100% vapor state[6].

Table 16. Partial pressure and 100% vapor temperature for 2 fuels

Fuel	Partial Pressure (kPa)	Temperature (K)
iso-Octane	1.63	277
n-Heptane	1.85	265

Figure 34 and Figure 35 show the liquid vapor equilibrium for a homogenous air and iso-Octane/n-Heptane mixture. These plots are based on an intake pressure of 14.3 psi. The lowest air temperature expected in the test cell is 280K. Therefore no additional heat should be needed for either fuel to keep the mixture in a vapor state. However, a fuel heater was still built to examine the effects of heating the fuel on BSFC and torque.

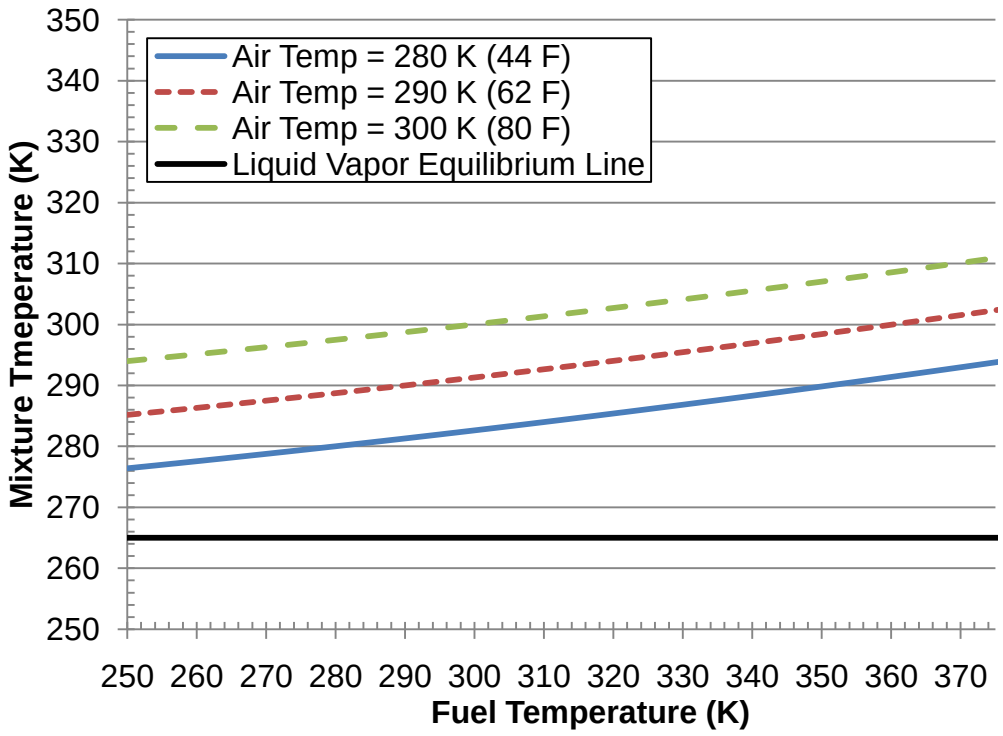

Figure 34. Stoichiometric n-Heptane and air mixture liquid vapor equilibrium at 14.3 psi for three temperatures

To heat the fuel to the desired temperatures, a heat exchanger must be used. Two options were determined; one using a electrical heater and two trying a cross flow heat exchanger using the exhaust from the engine. When researching option two, the average exhaust gas temperature of this engine was between 477K and 600K depending on the engine speed. Preliminary calculations show that this option could work, and it would also be beneficial in a real world application. Nevertheless, it also possessed two main disadvantages; the fuel flow would be running through the engine exhaust and it would not address the cold start issues associated with JP-8. Therefore, option one was

chosen, and would be comprised of a metal block with electrical strip heaters attached.

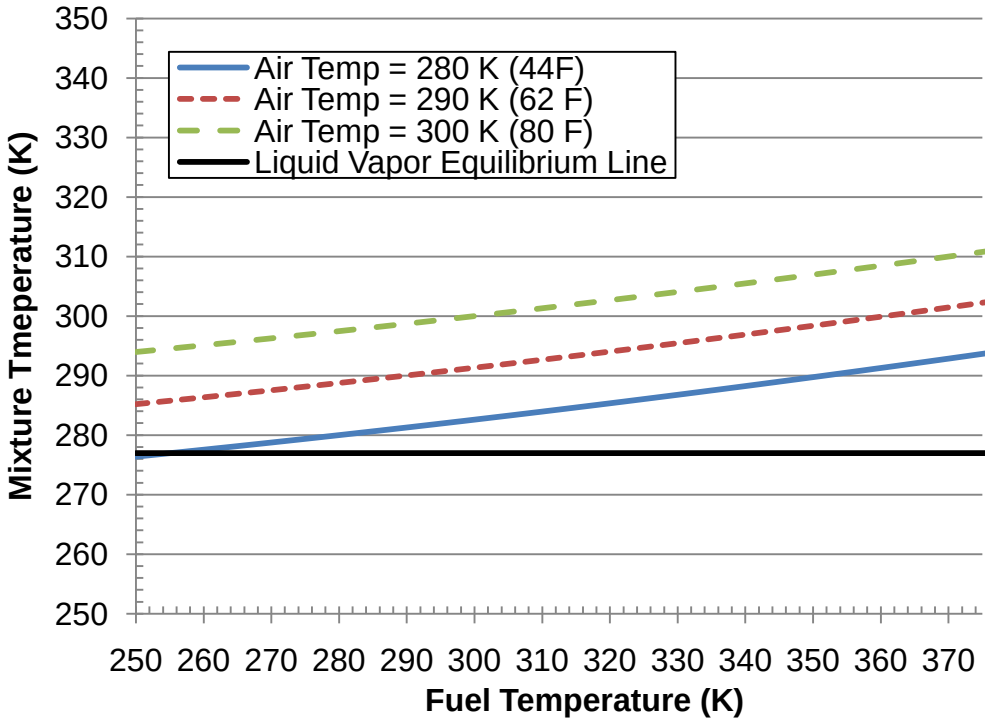

Figure 35. Stoichiometric iso-Octane and air mixture liquid vapor equilibrium at 14.3 psi for three temperatures

To estimate the total power needed from the strip heaters, the first law of thermodynamics was used. Assuming no heat loss (all energy from the strip heater is transferred to fuel), and the fluid stays in liquid form, neglecting latent heat from boiling effects, the energy equation is used (Eq. 9).

$$q = \dot{m} C_p \Delta T \tag{9}$$

A max fuel flow rate of 14 cc/min and a temperature change of 80K were used in the calculation. This resulted in approximately 30 Watts of total energy needed. An error in calculating the fuel flow rate was made in the initial calculations,

therefore yielding resulting energy requirement of 1500 Watts. While this amount of energy is several orders of magnitude larger than what is needed for n-Heptane, it does provide the expansion needed in the future for heating JP-8.

A heat transfer analysis was done to estimate the temperature of the fuel exiting the heater. The block temperature is considered to be constant, and for simplification, outer surface convection resistance and tube wall conduction resistance is considered negligible. Also, negligible kinetic and potential energy effects are assumed. The estimation was done using a quarter section of the heater (Figure 36).

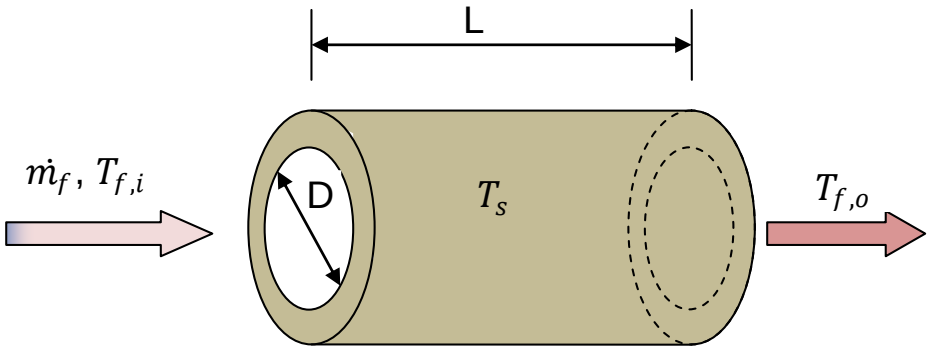

Figure 36. Heater exchanger tube section

The first step was to determine if the fuel flow would be laminar or turbulent based on the Reynolds number; Equation 10.

$$Re_D = \frac{4\dot{m}}{\pi D \mu} \tag{10}$$

Using the worst case scenario, max fuel temperature of ~ 477K, n-Heptane, and a 16 cc/min flow rate, the Reynolds Number was calculated to be approximately 500. Laminar flow is normally considered with Reynolds Numbers less than

2300, thus our flow will theoretically always be laminar. The convection coefficient was then determined by using tabulated values of the Nusselt number for laminar flow in a circular tube; Equation 11.

$$Nu_D = \frac{hD}{k} = 3.66 \tag{11}$$

With the convection coefficient known, an estimated exit temperature for the fuel can now be calculated. Using the overall tube energy balance, Equation 12 and convection rate equation (based off log mean temperature difference), Equation 13, our exit temperature can be solved for; Equation 14.

$$q_{conv} = \dot{m} c_p (T_{f,o} - T_{f,i}) \tag{12}$$

$$q_{conv} = \bar{h} A_s \Delta T_{lm} \tag{13}$$

$$T_{f,o} = T_s + \left(T_{f,i} - T_s\right) e^{\left(\frac{-\bar{h}\pi DL}{\dot{m} c_p}\right)} \tag{14}$$

The results of the heat transfer rates can be found in Table 17.

Table 17. Summary of heater transfer rates

Fuel Flow	8 cc/min	12 cc/min	16 cc/min
Heater Wall Set point (C)	Fuel Out (Kelvin)	Fuel Out (Kelvin)	Fuel Out (Kelvin)
27	300	300	300
37	310	310	309
47	320	319	318
57	330	329	328
67	340	339	337
77	350	349	347
87	360	358	356
97	370	368	365
107	380	378	375

117	390	388	384
127	400	397	393
137	410	407	403
147	420	417	412
157	429	427	422
167	439	436	431
177	449	446	440
187	459	456	450
197	469	466	459

This table lists the estimated fuel temperature based on the heater block temperature and volumetric fuel flow rate. Notice that even at higher set point temperatures and fuel flow rates, the estimated exit fuel temperature is very close to the set point. This can be attributed to two key points. One being that fuel travels through the heater block four times, therefore maximizing the heat transfer. To iterate this point, a specific case is examined; inlet fuel temperature 289K, 16 cc/min flow rate, and heater wall set point of 400 degrees Kelvin. The results of this calculation can be seen in Table 18.

Table 18. Heat transfer example calculation

Fuel OUT - 1 Pass (Kelvin)	ΔT	Fuel OUT - 2 Pass (Kelvin)	ΔT	Fuel OUT - 3 Pass (Kelvin)	ΔT	Fuel OUT - 4 Pass (Kelvin)	ΔT
347.21	58.65	374.99	27.78	388.15	13.16	394.38	6.23

This calculation shows that only about half of the original required heat addition was accounted for on the first pass through the heat exchanger. But by the time the fuel exits after three more passes through the heater, the temperature is very close to the desired value. The second reason for the seemingly optimistic

calculations in Table 17 is the fact that they are theoretical calculations that assume ideal conditions that normally are not seen in experimental settings.

Appendix D: Piston Peak Force and Torque Calculations

One of the challenges in designing a setup using a single piston engine is the excessive amounts of vibration produced from the engine. To reduce these vibrations from the rest of the test table, calculations were done to estimate the total force that would be exerted on the vibration dampers. Forces from the engine come from the acceleration and deceleration of the piston during each revolution. Using the engine's max rated torque or calculating the mean effective pressure on the piston cannot be used because these values are averages. Therefore I need to know the max instantaneous force exerted from the piston. From Newton's first law, to find the force of the piston, the acceleration and mass must be known. The weight of the piston was measured to be 2.2 oz. and if divided by the earth's gravitational force, 32.2 ft/s^2, a mass of 0.004254 slugs is obtained. To find the acceleration of the piston, the equation of a position with respect to crank angle, equation 15, was derived twice to produce equation 16 [5].

$$s(\theta) = r\cos\theta + \sqrt{(l^2 - r^2\sin^2\theta)} \tag{15}$$

$$a(\theta) = -r\cos\theta - \frac{r^2(\cos^2\theta - \sin^2\theta)}{\sqrt{(l^2 - r^2\sin^2\theta)}} - \frac{r^4(\cos^2\theta\sin^2\theta)}{\left(\sqrt{(l^2 - r^2\sin^2\theta)}\right)^3} \tag{16}$$

The result however is in the angle domain, and therefore must be translated to the time domain in order to be useful. Since the angular velocity is constant, we can assume that the crank angle equals the angular velocity multiplied by time. Specifically, the result from equation 16, which is in distance per radians

squared, needs to be multiplied by the angular velocity squared to obtain a distance per second squared value. The translational force can now be calculated and multiplied by the crankshaft radius to obtain the peak rotational torque. As verification, four high speed torque data points were taken from the engine at 50 kHz. Table 19 outlines the estimated vs. measured values at different engine speeds.

Table 19. Theoretical vs. actual piston instantaneous torque

Engine Speed (rpm)	Estimated Max Piston Acceleration (ft/s^2)	Estimated Piston Force (lbf)	Estimated Max Torque (ft-lbf)	Measured Peak Torque (ft-lbf)	Percent Error (%)
4400	14657	62.4	3.27	3.03	-7.92%
4800	17443	74.2	3.9	4.7	17.02%
5900	26353	112.1	5.89	6.56	10.21%
6300	30048	127.8	6.71	7.55	11.13%

From the measured torque data, there was a considerable difference in the peak instantaneous torque from one cycle to the next. The peak value listed in Table 19 is the average of the peaks during 0.5 seconds of data. The result from this study shows that the actual peak torque for this engine can be estimated to within +/-17%. To have a worst case scenario for maximum peak torque, the estimated piston force at 6000 RPM (max rating of Quadraflex coupling) of 115.96 lbs was multiplied by the error factor resulting in 134.55 lbs. Since the engine mounting plate sits on four vibration dampers, this peak torque must be divided by four resulting in 33.64 lbs of force per damper. The coupling carries a parallel misalignment specification of +/- 0.01”, therefore providing a maximum deflection allowable of 0.02”. The vibration dampers that were chosen allow a

maximum deflection of 0.1” at its maximum loading of 210 lbs. After scaling this down to our maximum loading of 33.64 lbs, it is determined that the dampers will only allow 0.016” of deflection, therefore within the tolerance of the coupling.

Appendix E: Experiment Raw Data

Engine Loading Knock Characteristics

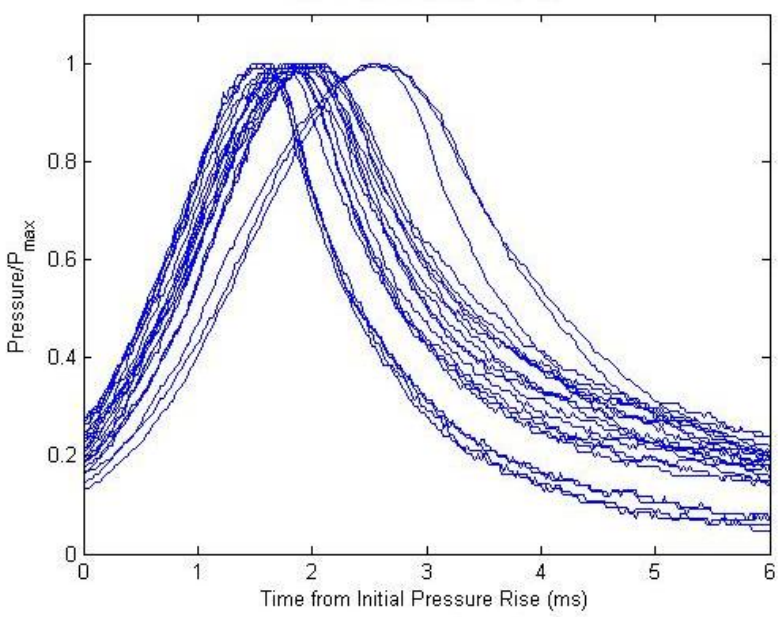

Figure 37. Normalized pressure profiles over 0.5 seconds with iso-Octane at 5000 RPM, 40% throttle and stock timing

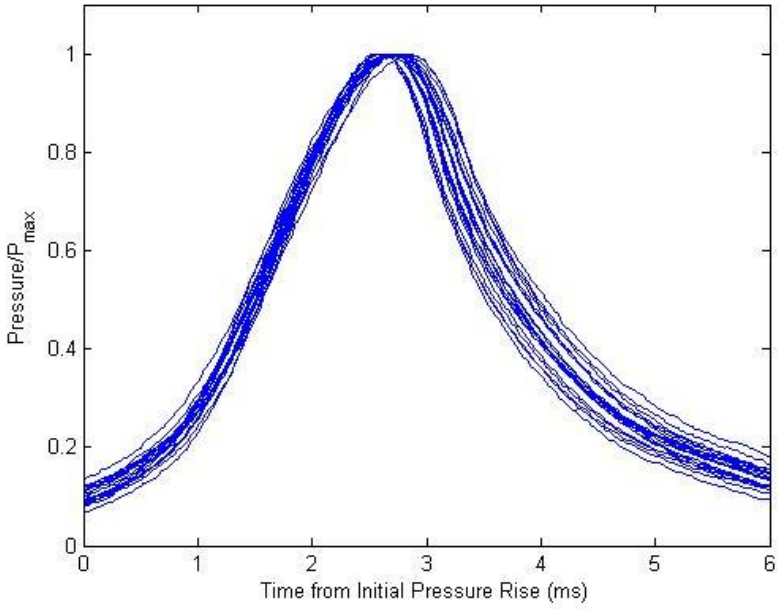

Figure 38. Normalized pressure profiles over 0.5 seconds with iso-Octane at 5000 RPM, 85% throttle and stock timing

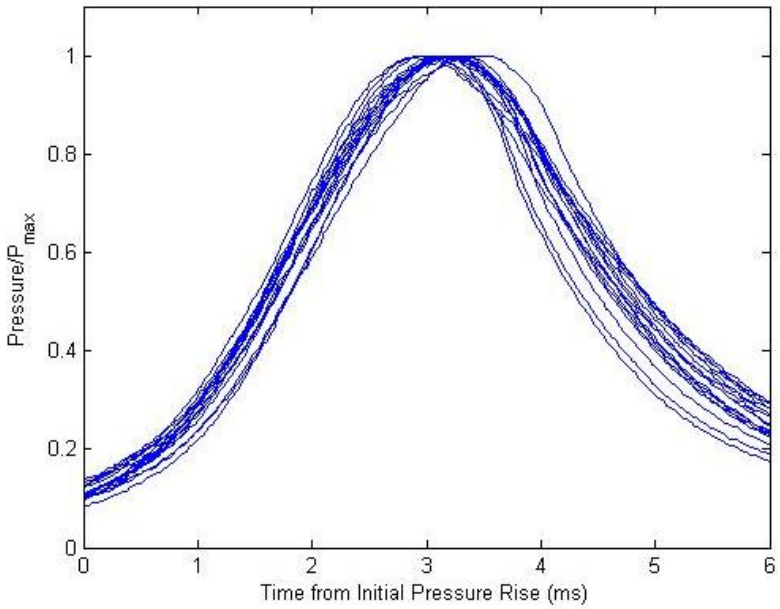

Figure 39. Normalized pressure profiles over 0.5 seconds with iso-Octane at 4000 RPM, 85% throttle and stock timing

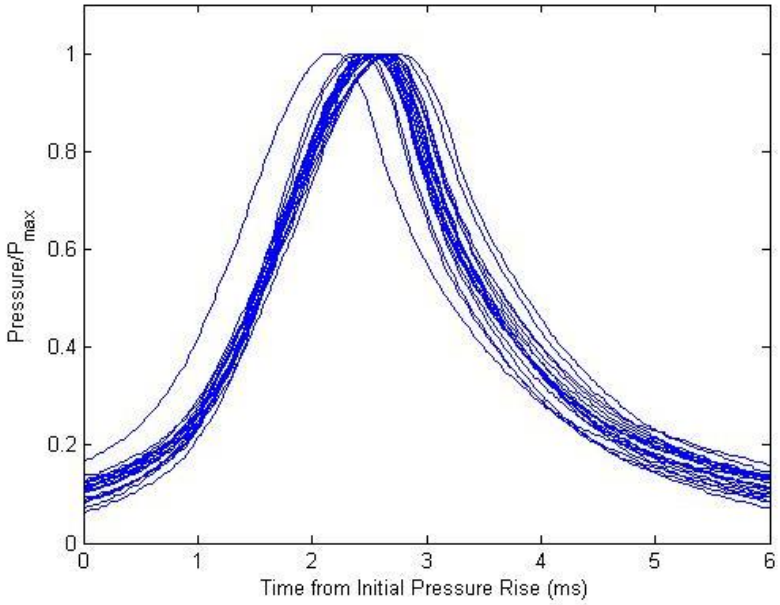

Figure 40. Normalized pressure profiles over 0.5 seconds with n-Heptane at 5000 RPM, 85% throttle and stock timing

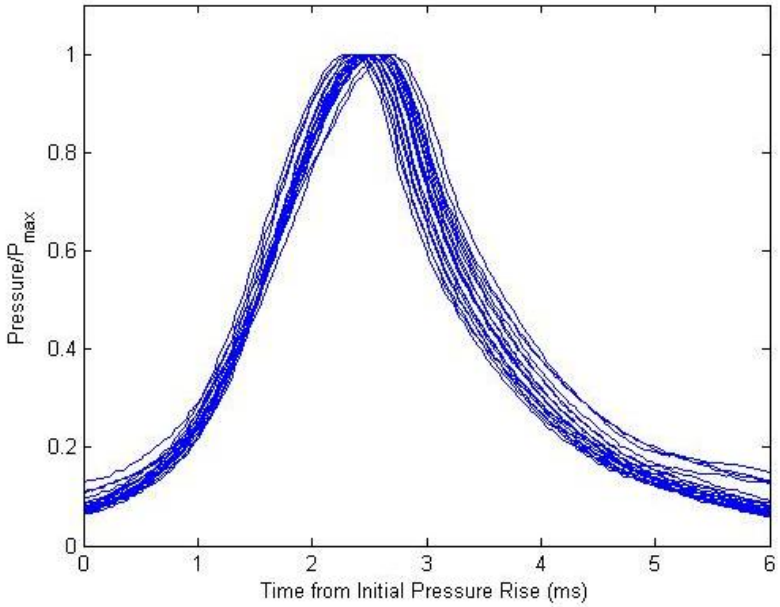

Figure 41. Normalized pressure profiles over 0.5 seconds with n-Heptane at 5000 RPM, 85% throttle and stock timing

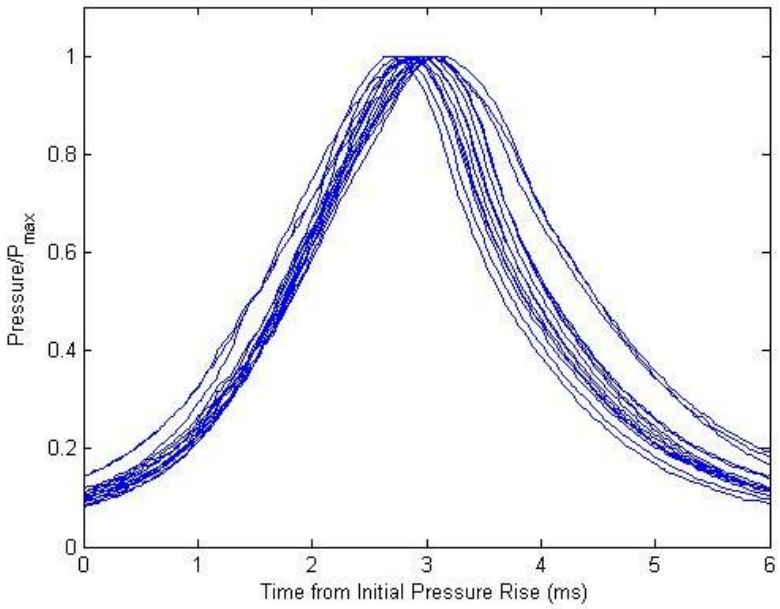

Figure 42. Normalized pressure profiles over 0.5 seconds with n-Heptane at 4000 RPM, 85% throttle and stock timing

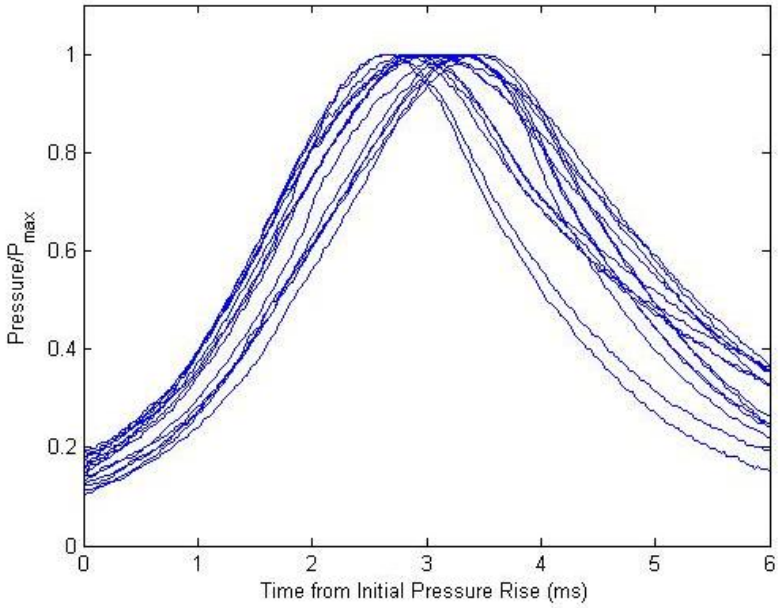

Figure 43. Normalized pressure profiles over 0.5 seconds with n-Heptane at 3670 RPM, 85% throttle and stock timing

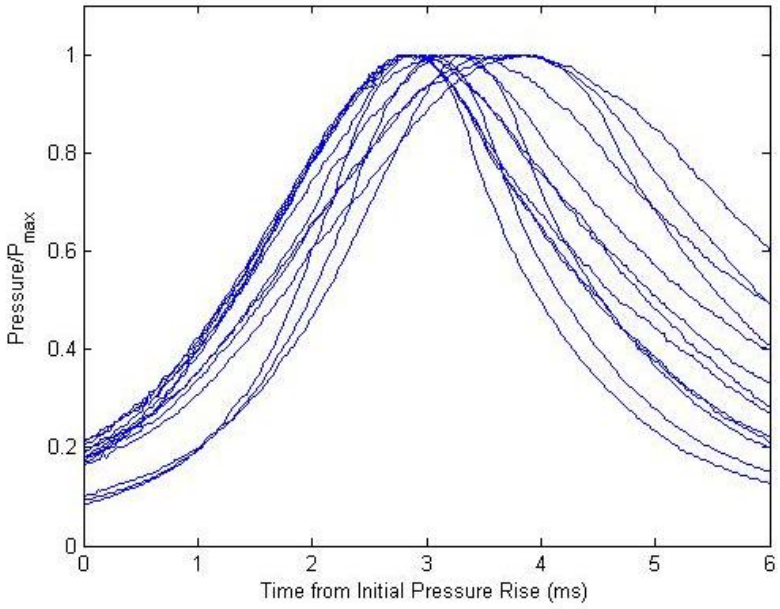

Figure 44. Normalized pressure profiles over 0.5 seconds with n-Heptane at 3500 RPM, 85% throttle and stock timing

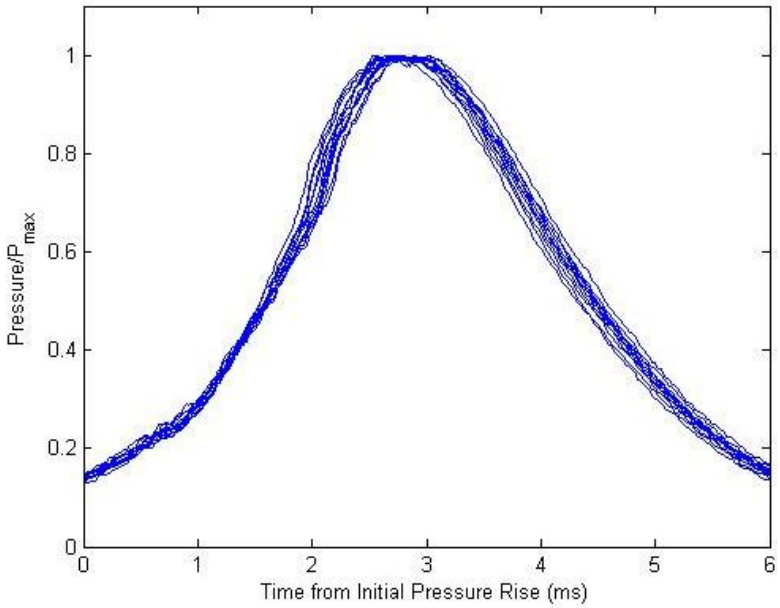

Figure 45. Normalized pressure profiles over 0.5 seconds with n-Heptane at 3000 RPM, 80% throttle and stock timing

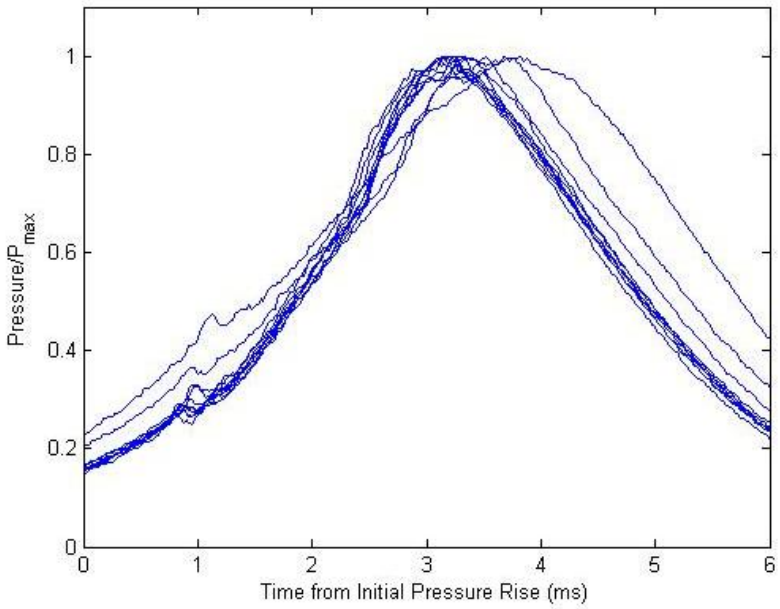

Figure 46. Normalized pressure profiles over 0.5 seconds with n-Heptane at 2700 RPM, 80% throttle and stock timing

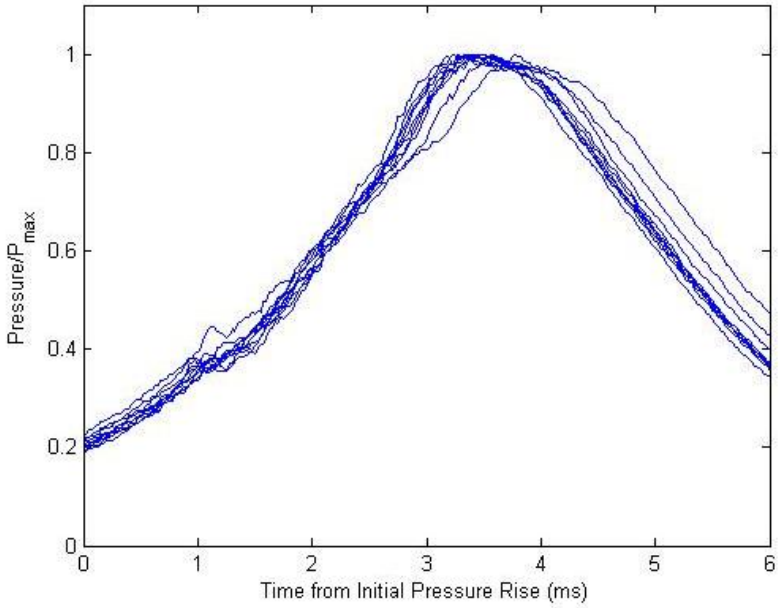

Figure 47. Normalized pressure profiles over 0.5 seconds with n-Heptane at 2500 RPM, 80% throttle and stock timing

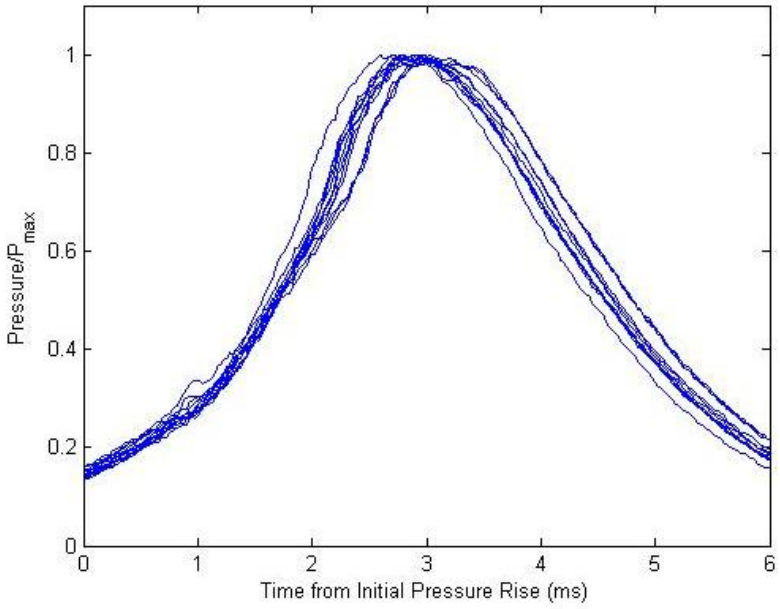

Figure 48. Normalized pressure profiles over 0.5 seconds with n-Heptane at 2900 RPM, 80% throttle and stock timing

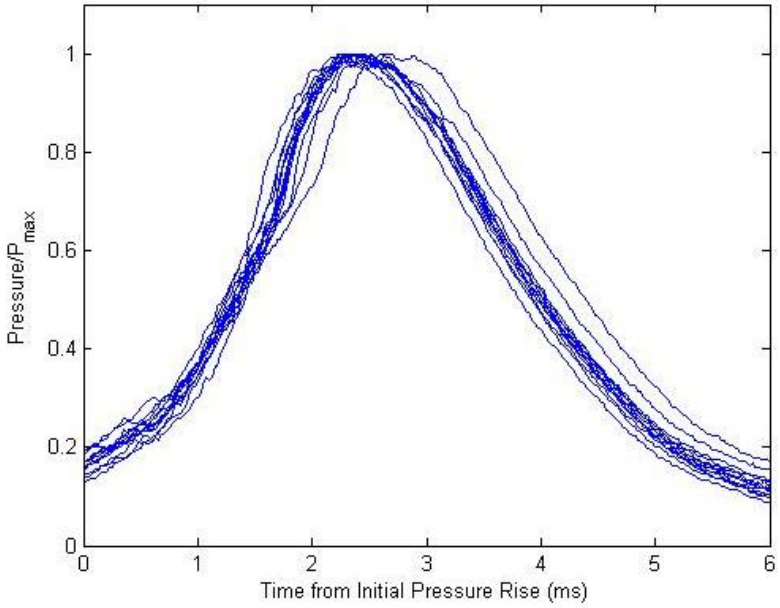

Figure 49. Normalized pressure profiles over 0.5 seconds with n-Heptane at 3300 RPM, 90% throttle and stock timing

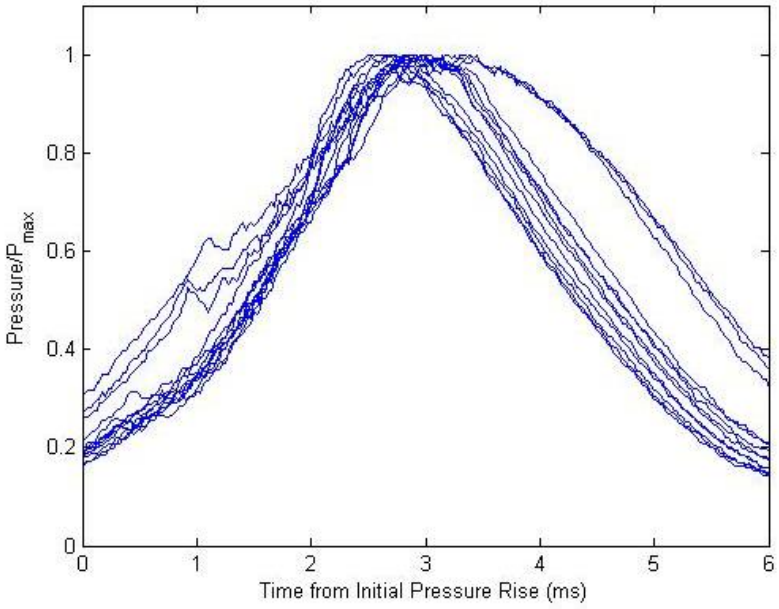

Figure 50. Normalized pressure profiles over 0.5 seconds with n-Heptane at 3000 RPM, 90% throttle and stock timing

Heated n-Heptane Knock Characteristics

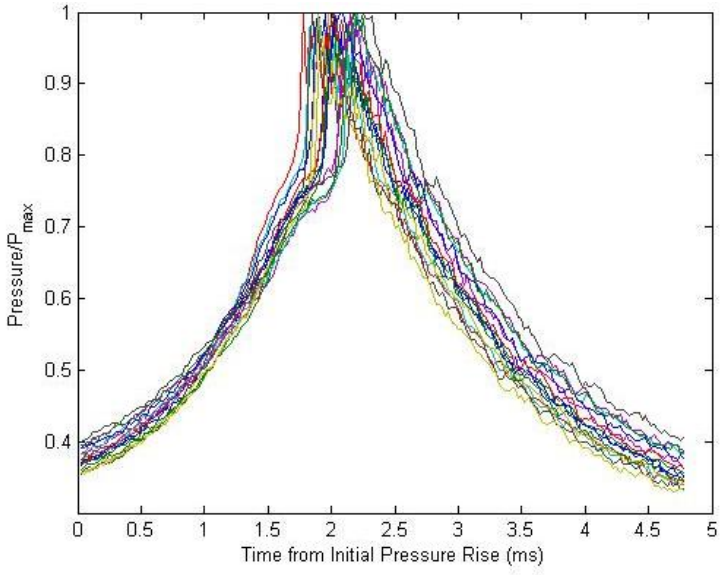

Figure 51. Normalized pressure profiles over 0.5 seconds with n-Heptane at 4000 RPM, 100% throttle, 290K fuel temp and stock timing

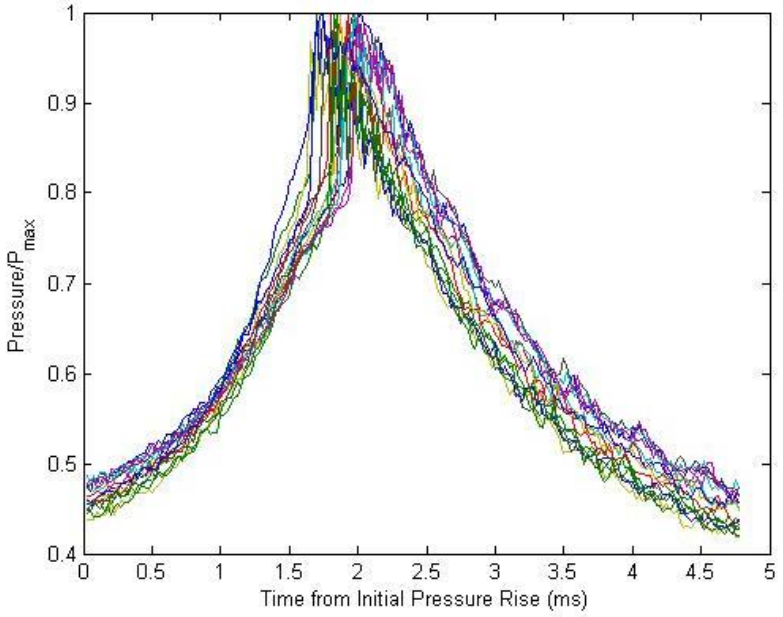

Figure 52. Normalized pressure profiles over 0.5 seconds with n-Heptane at 4000 RPM, 100% throttle, 311K fuel temp and stock timing

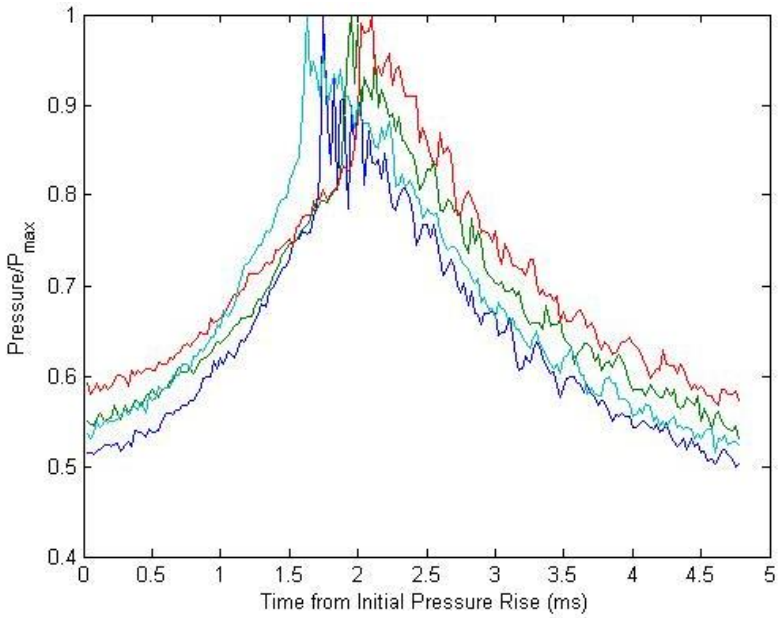

Figure 53. Normalized pressure profiles over 0.5 seconds with n-Heptane at 4000 RPM, 100% throttle, 344K fuel temp and stock timing

Variable Spark Timing

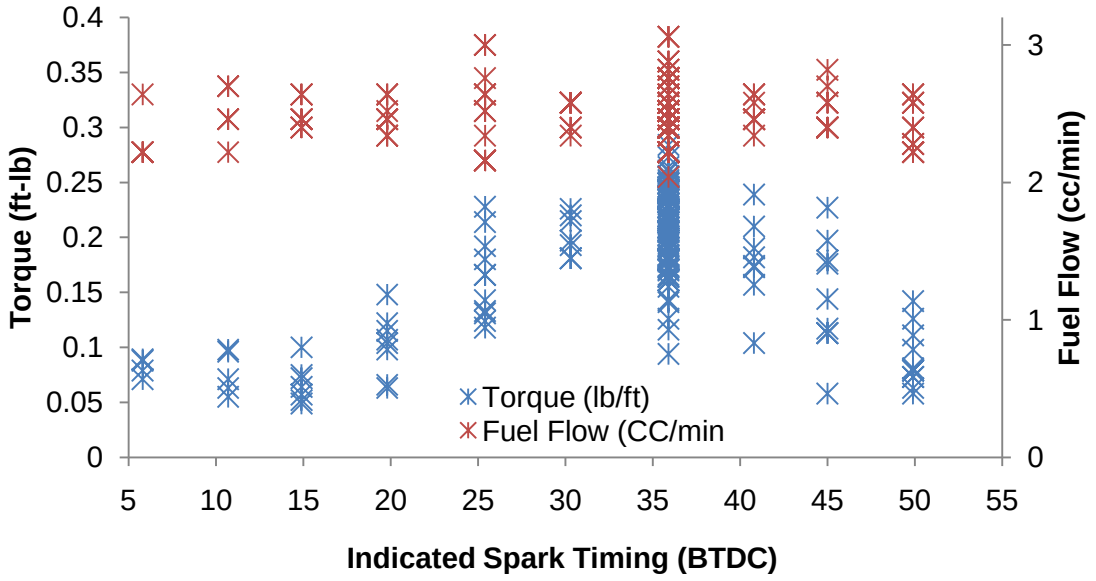

Figure 54. Raw torque and volumetric fuel flow data for variable spark timing test at 2700 RPM with n-Heptane

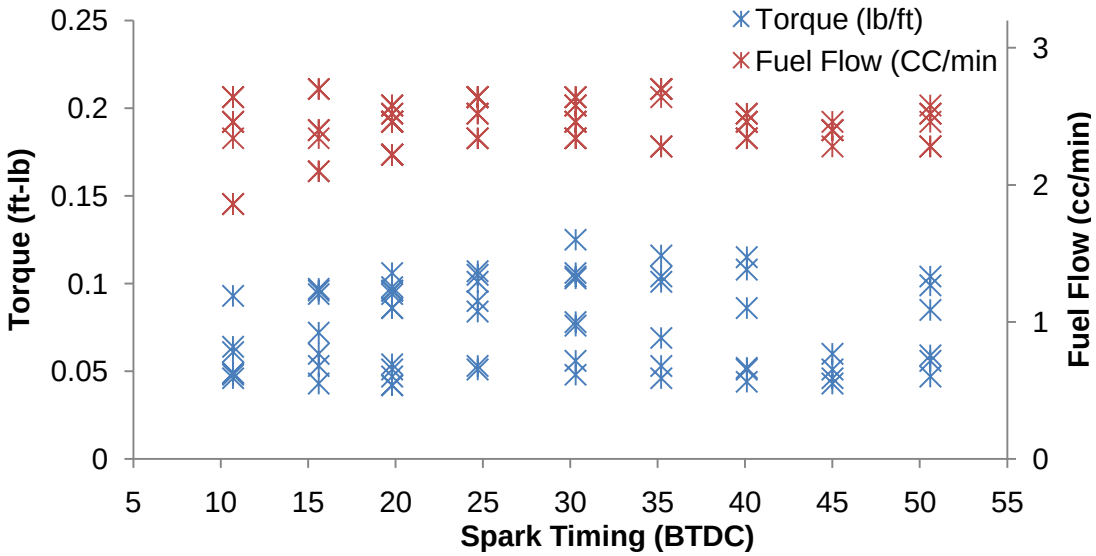

Figure 55. Raw torque and fuel flow data for varied spark timing for n-Heptane at 3000 RPM

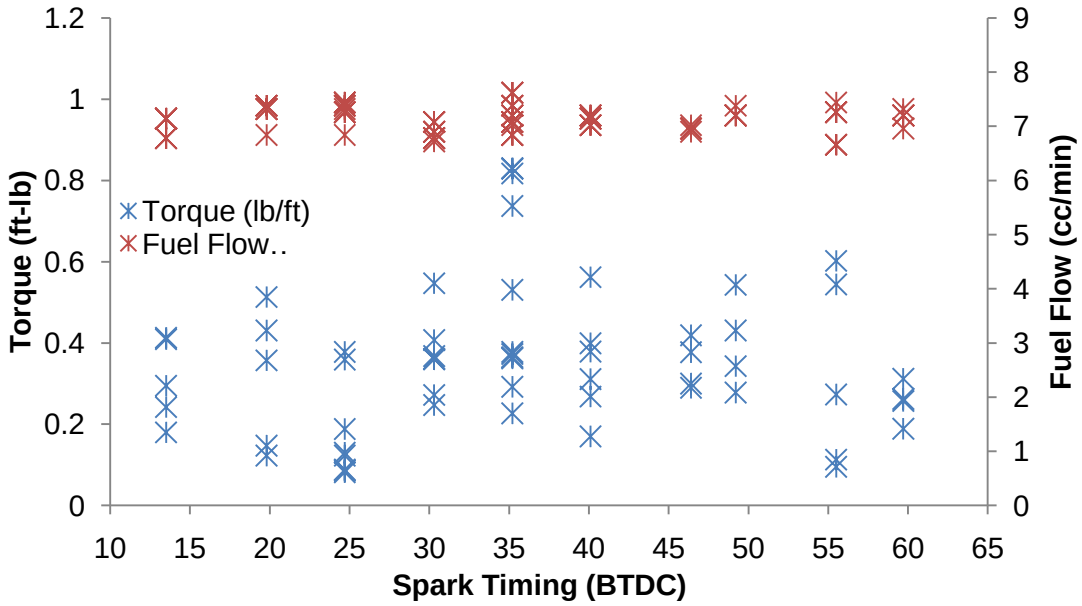

Figure 56. Raw torque and fuel flow data for varied spark timing for n-Heptane at 3500 RPM

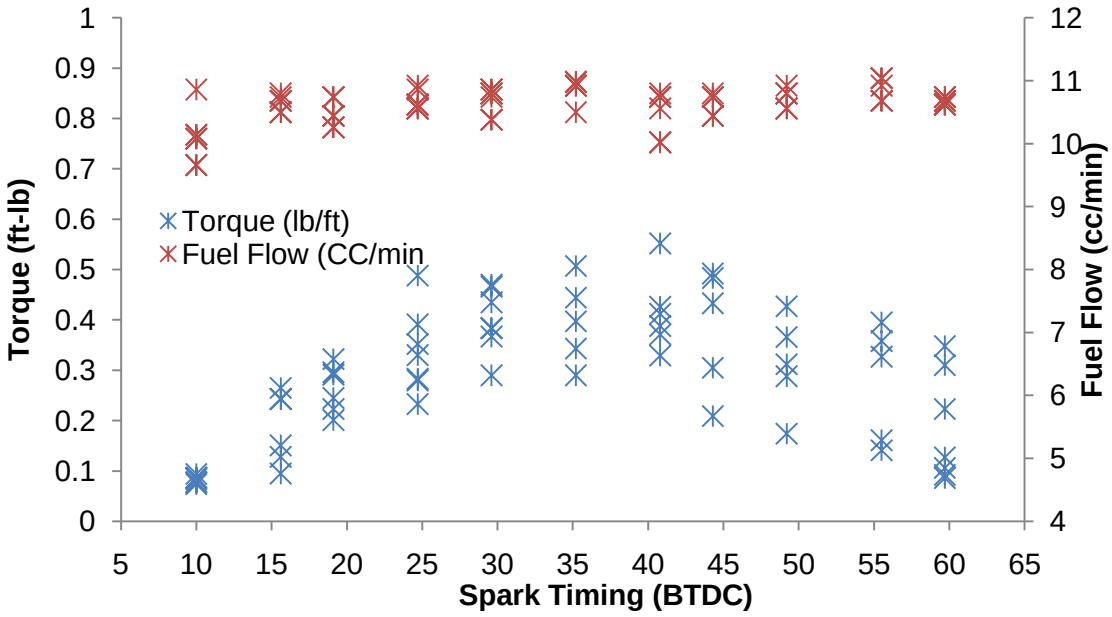

Figure 57. Raw torque and fuel flow data for varied spark timing for n-Heptane at 4500 RPM

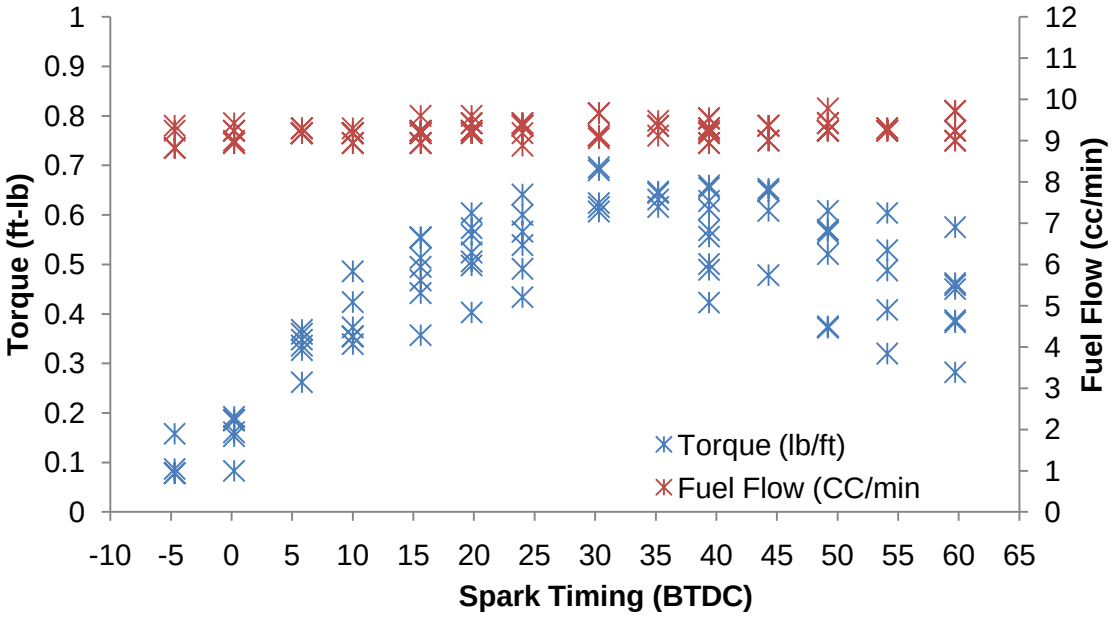

Figure 58. Raw torque and fuel flow data for varied spark timing for n-Heptane at 5000 RPM

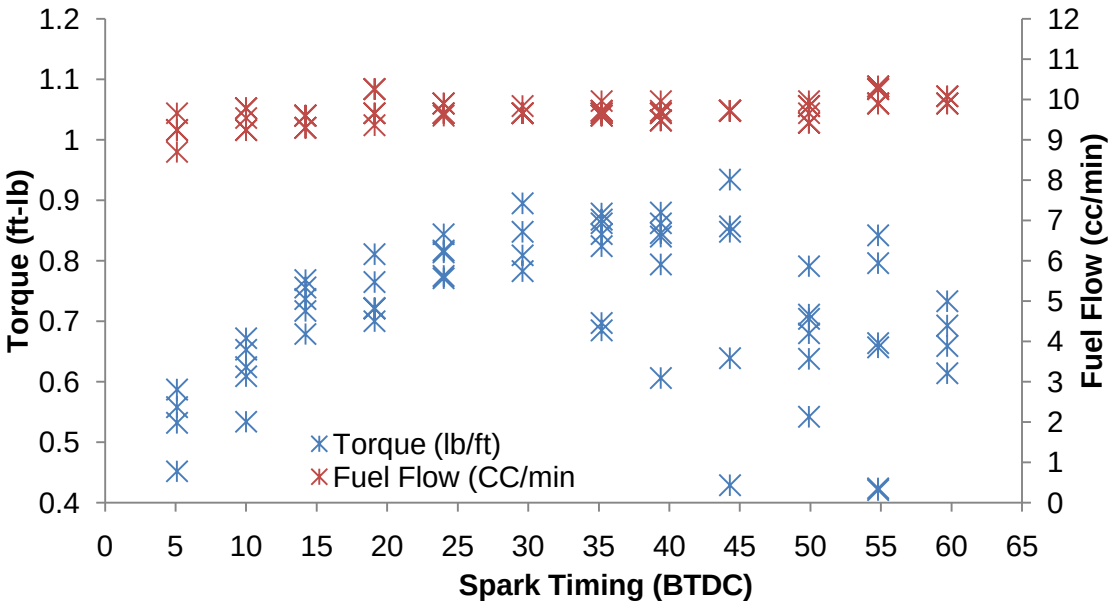

Figure 59. Raw torque and fuel flow data for varied spark timing for n-Heptane at 5500 RPM

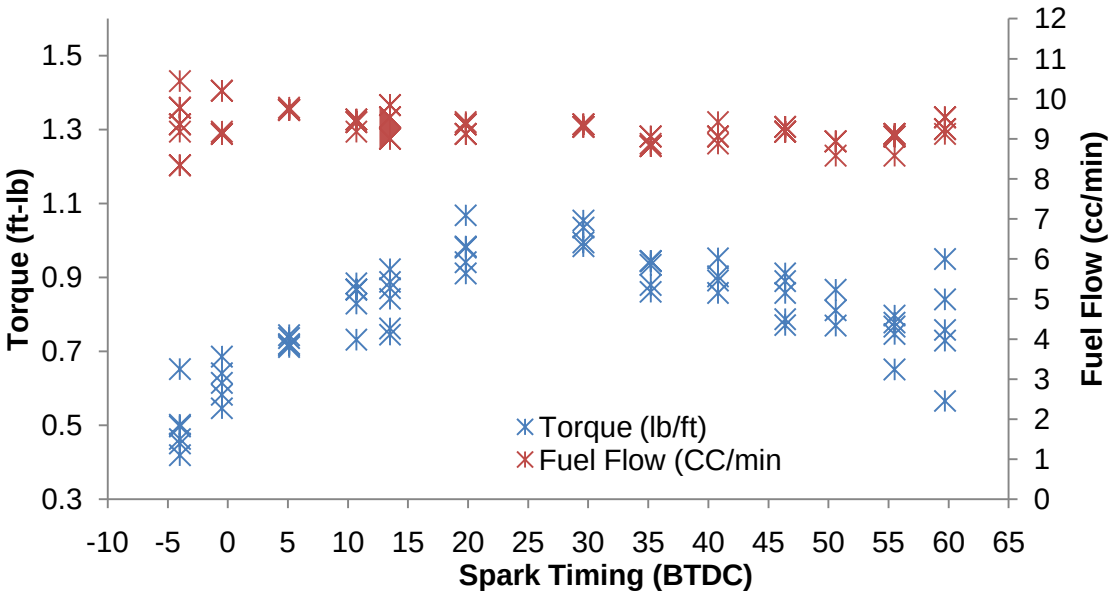

Figure 60. Raw torque and fuel flow for varied spark timing for n-Heptane at 5700 RPM

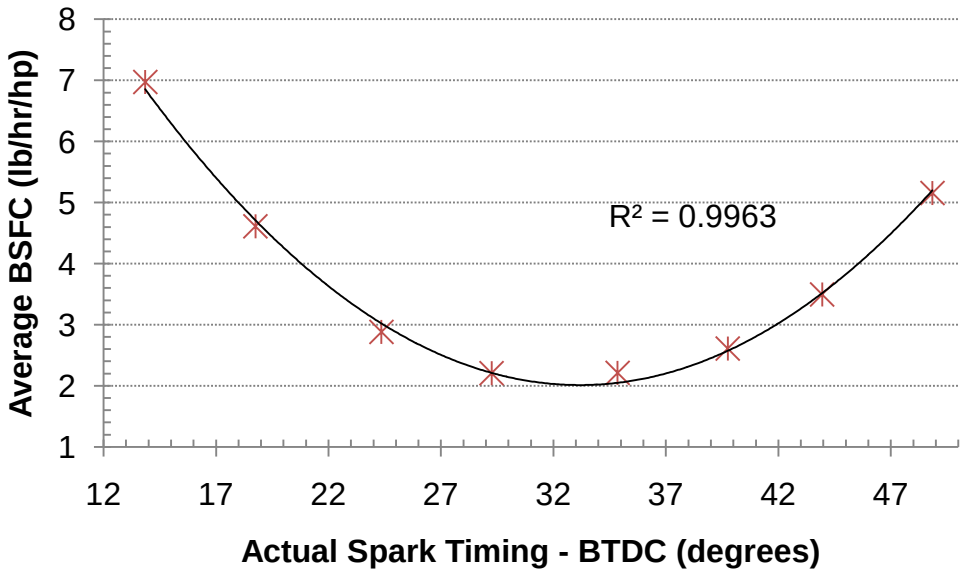

Figure 61. Average BSFC vs. spark timing for n-Heptane at 2700 RPM

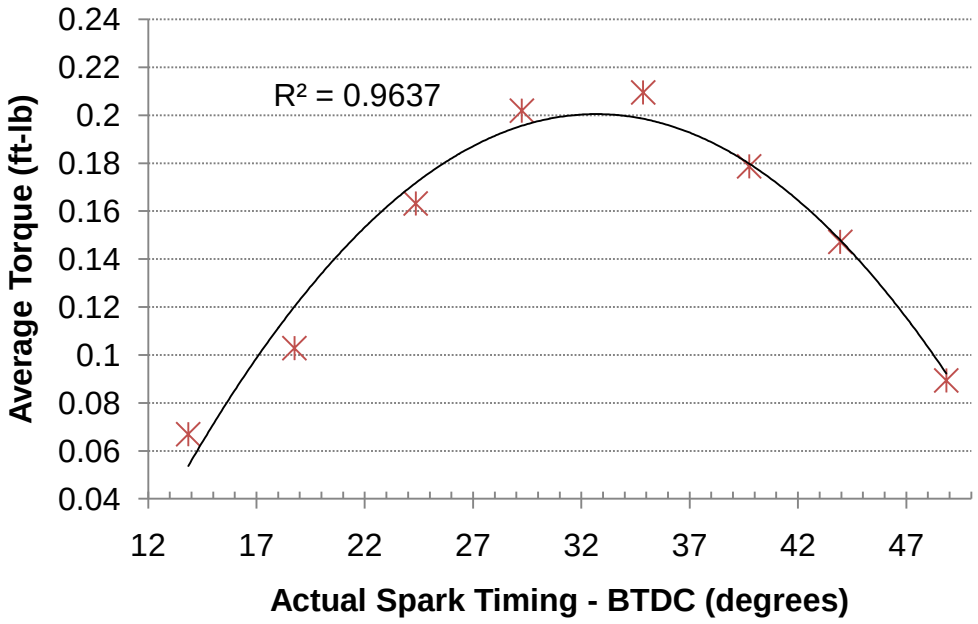

Figure 62. Average torque vs. spark timing for n-Heptane at 2700 RPM

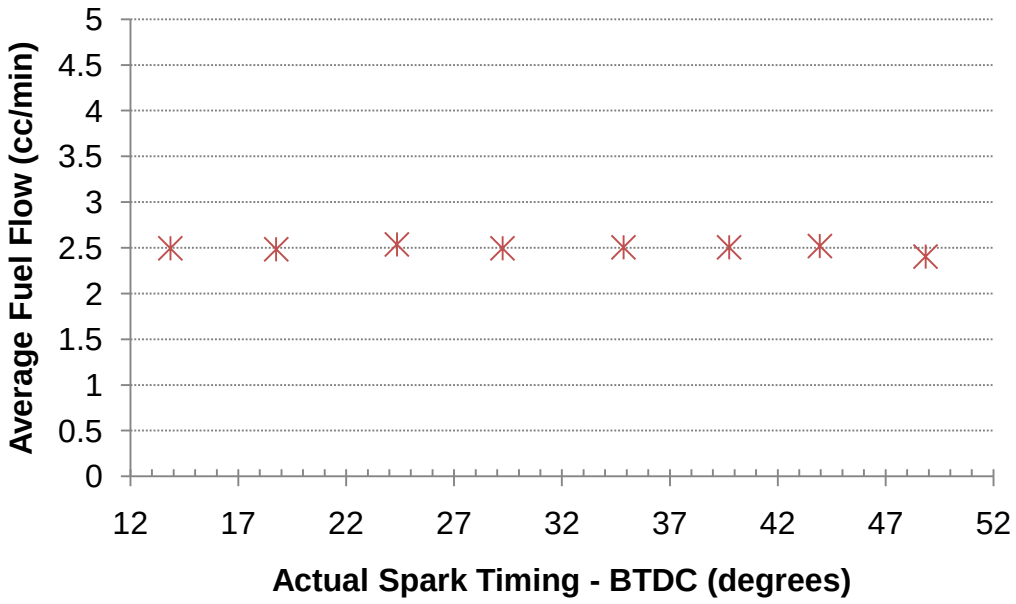

Figure 63. Average volumetric fuel flow rate vs. spark timing for n-Heptane at 2700 RPM

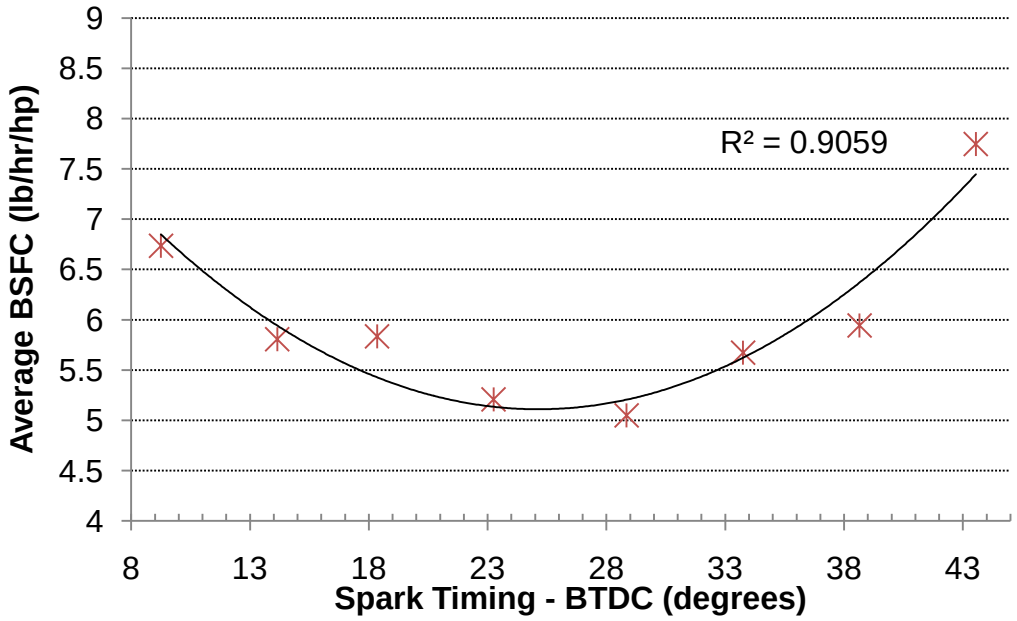

Figure 64. Average BSFC vs. spark timing for n-Heptane at 3000 RPM

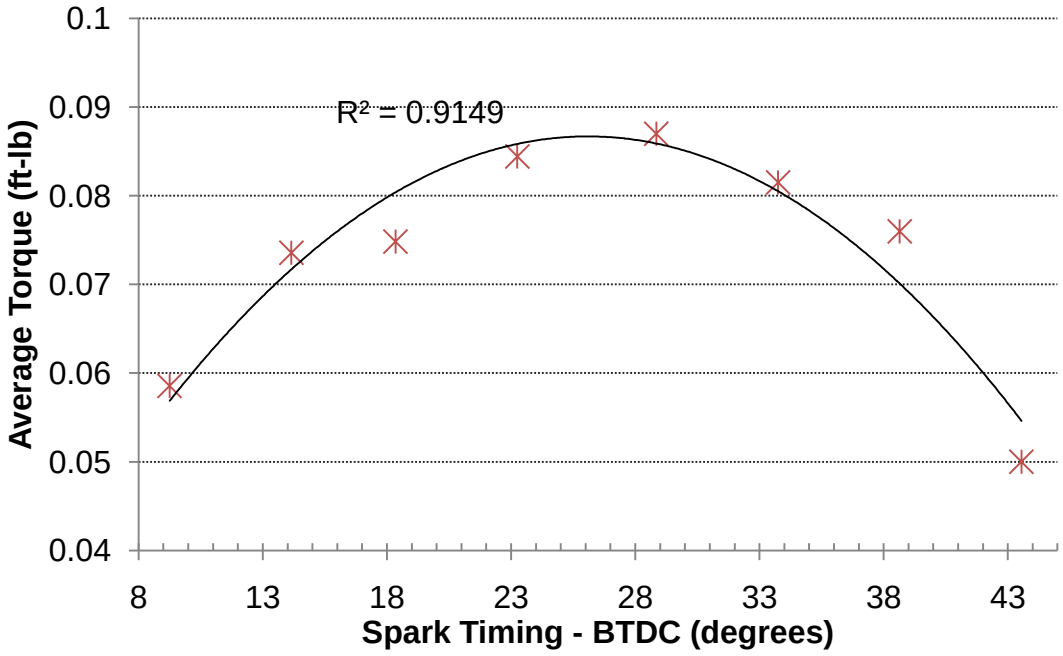

Figure 65. Average torque vs. spark timing for n-Heptane at 3000 RPM

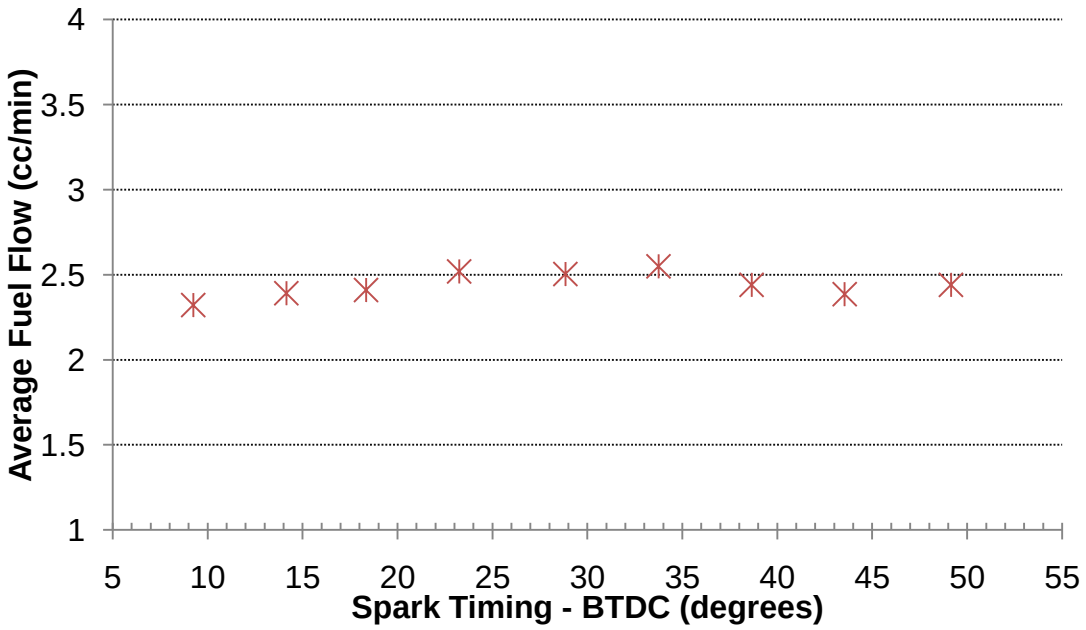

Figure 66. Average fuel flow vs. spark timing for n-Heptane at 3000 RPM

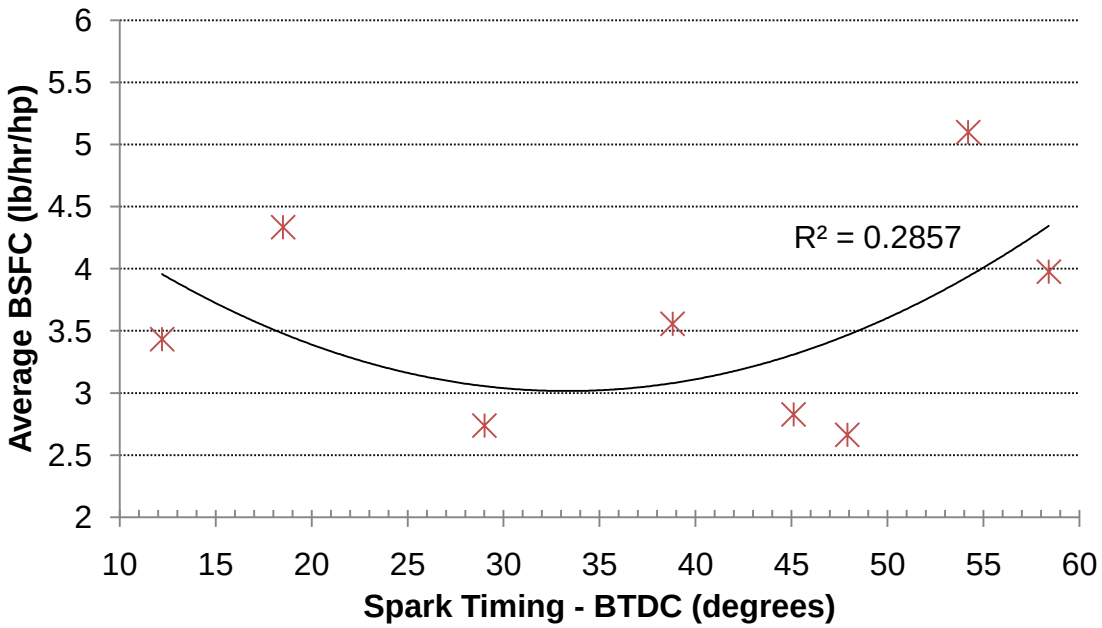

Figure 67. Average BSFC vs. spark timing for n-Heptane at 3500 RPM

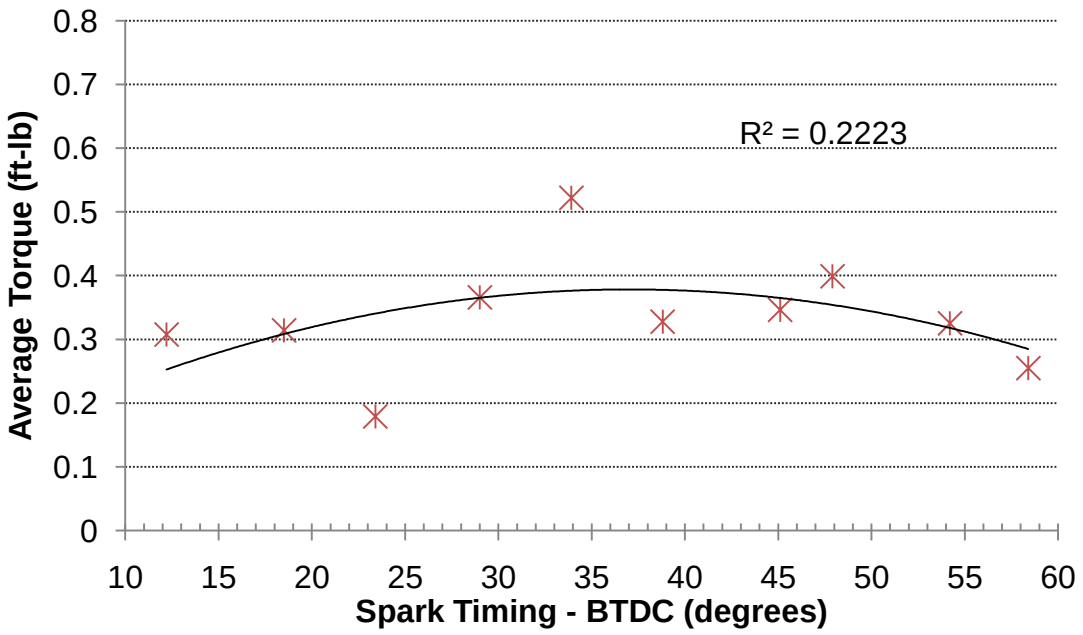

Figure 68. Average torque vs. spark timing for n-Heptane at 3500 RPM

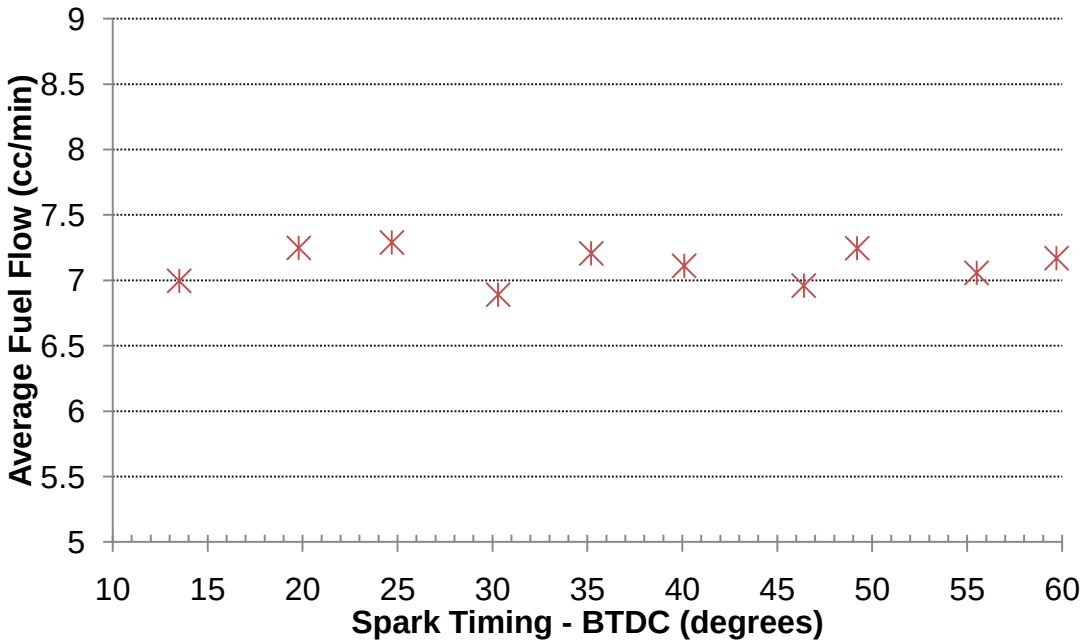

Figure 69. Average volumetric fuel flow rate vs. spark timing for n-Heptane at 3500 RPM

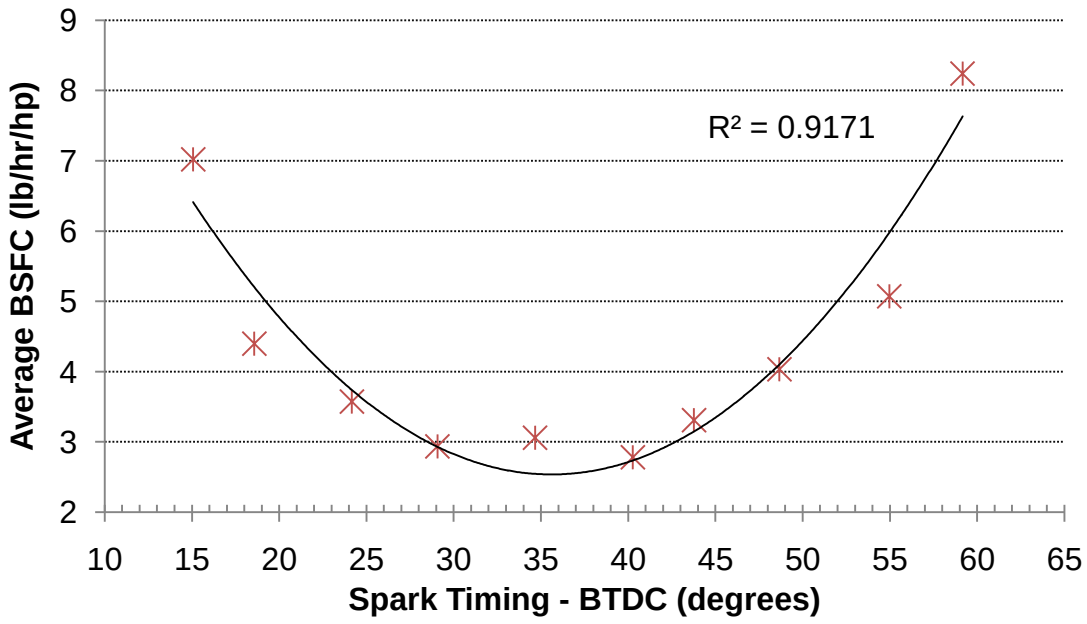

Figure 70. Average BSFC vs. spark timing for n-Heptane at 4500 RPM

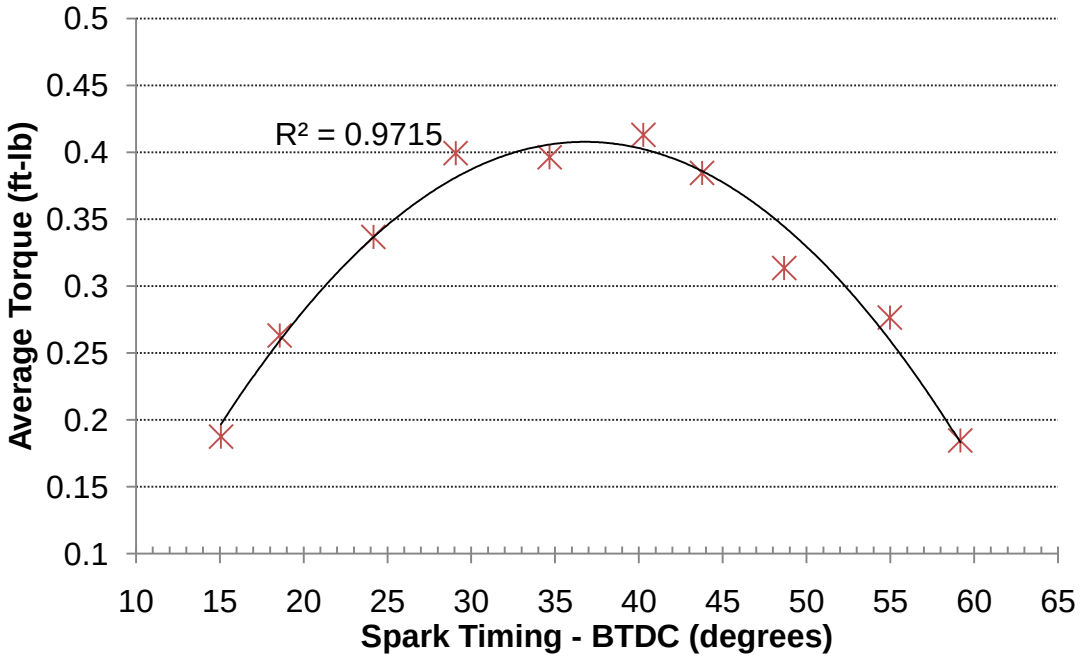

Figure 71. Average torque vs. spark timing for n-Heptane at 4500 RPM

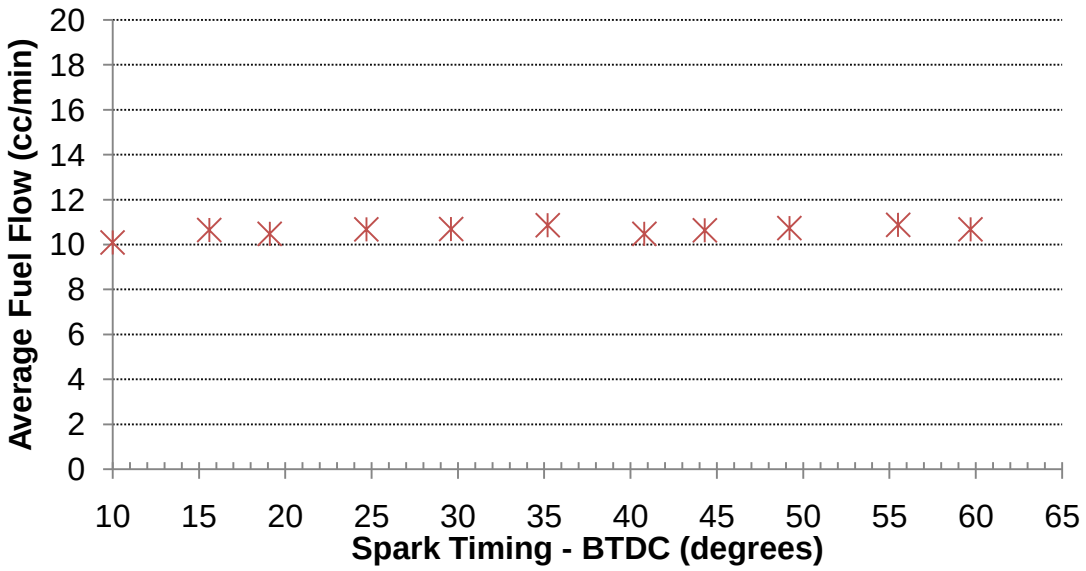

Figure 72. Average volumetric fuel flow rate vs. spark timing for n-Heptane at 4500 RPM

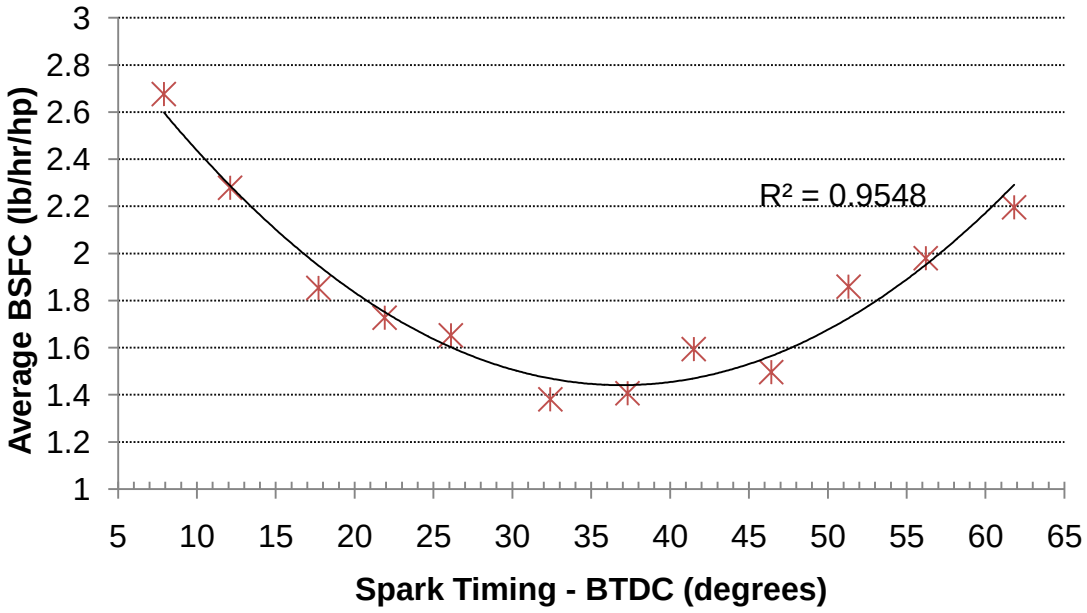

Figure 73. Average BSFC vs. spark timing for n-Heptane at 5000 RPM

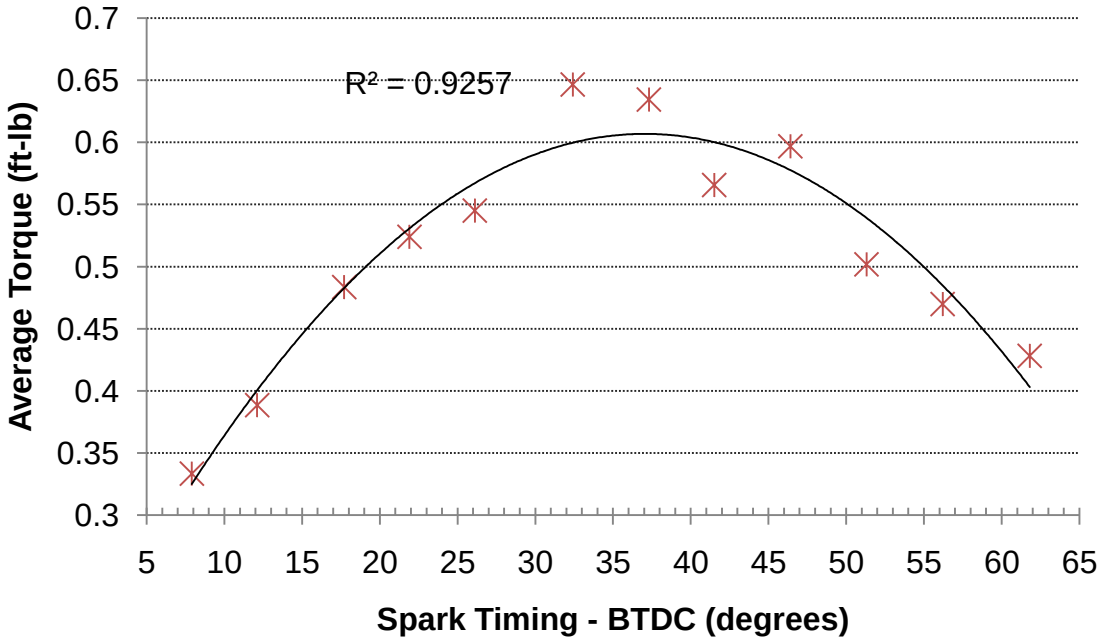

Figure 74. Average torque vs. spark timing for n-Heptane at 5000 RPM

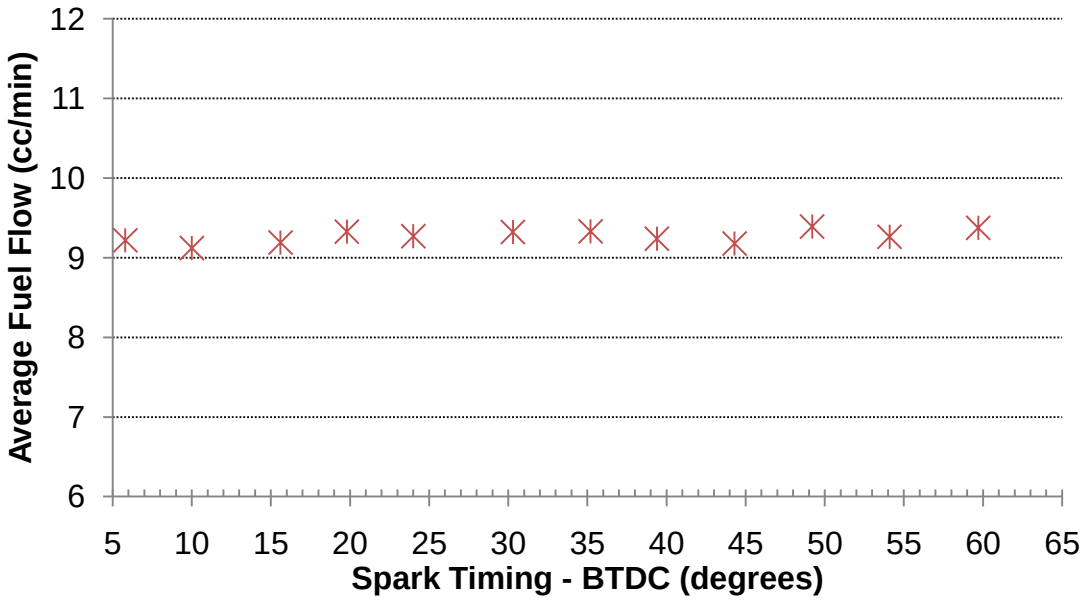

Figure 75. Average volumetric fuel flow rate vs. spark timing for n-Heptane at 5000 RPM

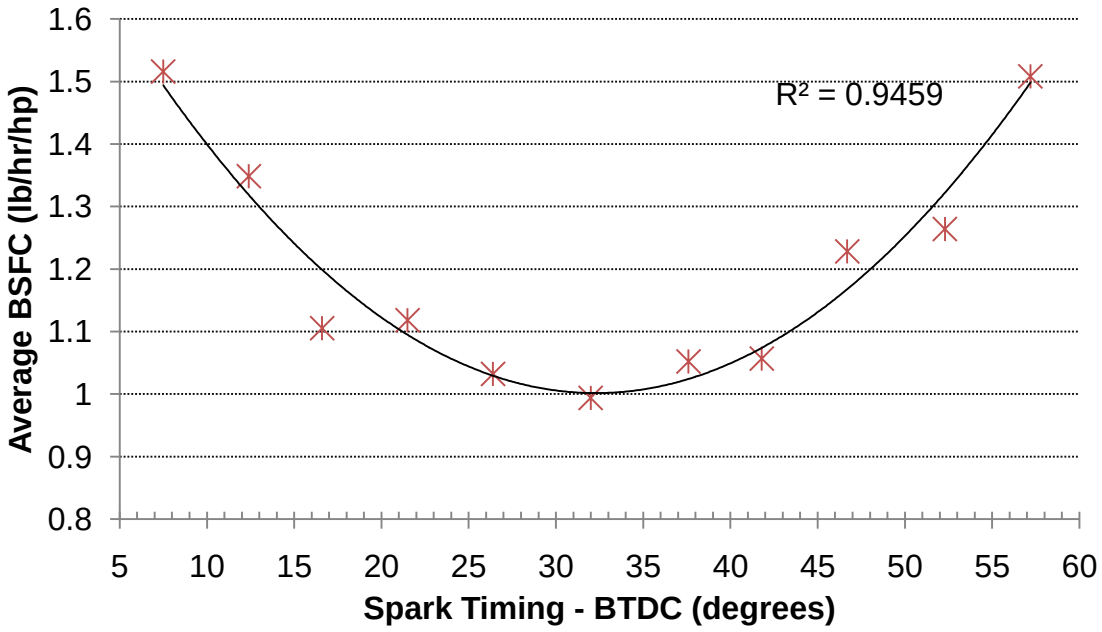

Figure 76. Average BSFC vs. spark timing for n-Heptane at 5500 RPM

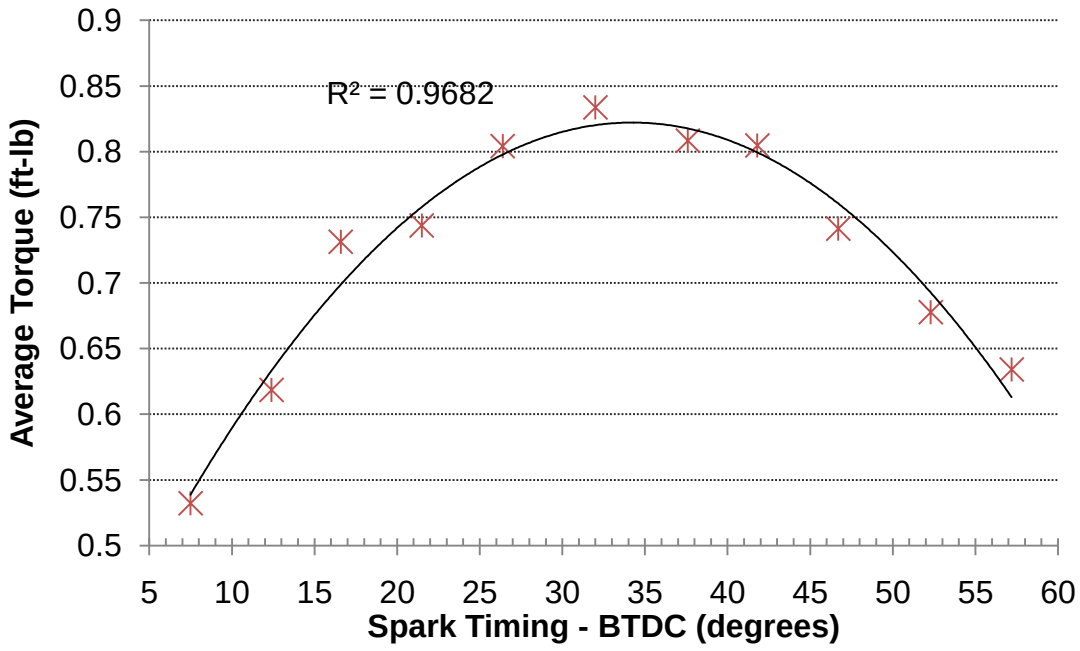

Figure 77. Average torque vs. spark timing for n-Heptane at 5500 RPM

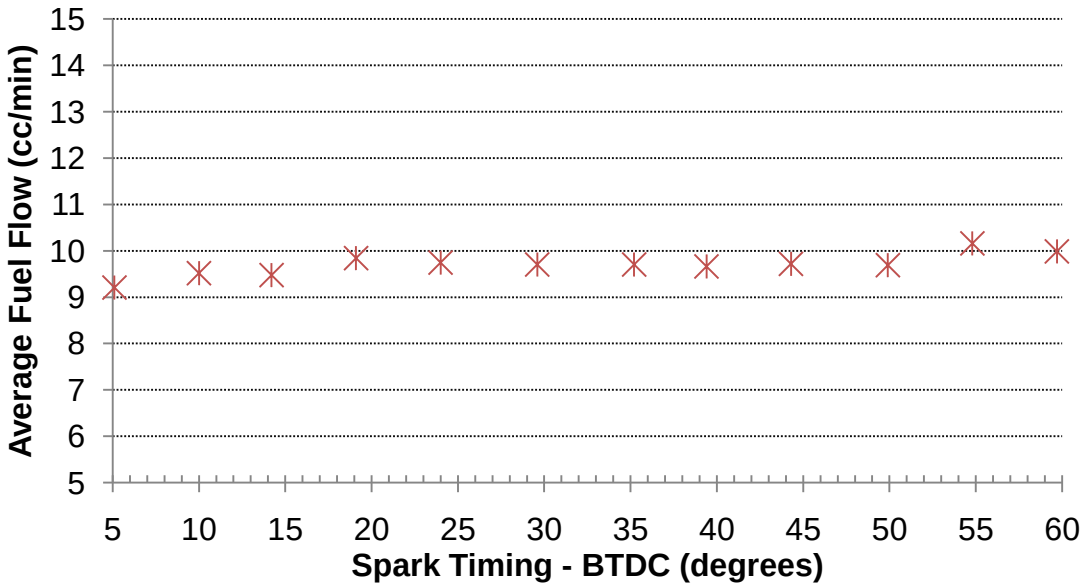

Figure 78. Average volumetric fuel flow rate vs. spark timing for n-Heptane at 5500 RPM

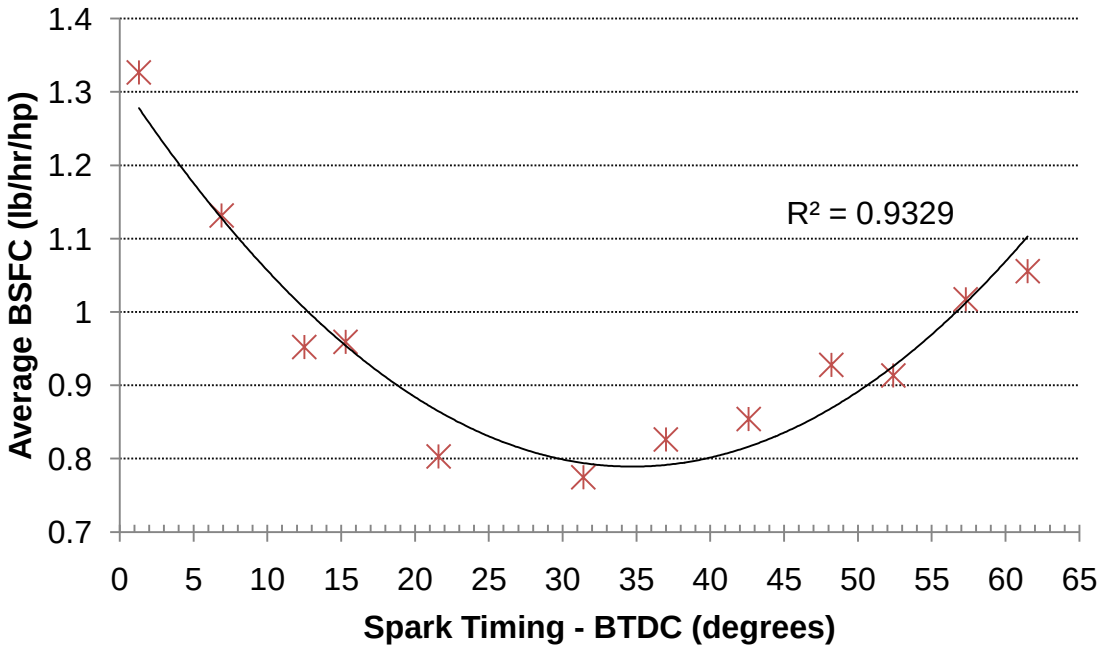

Figure 79. Average BSFC vs. spark timing for n-Heptane at 5700 RPM

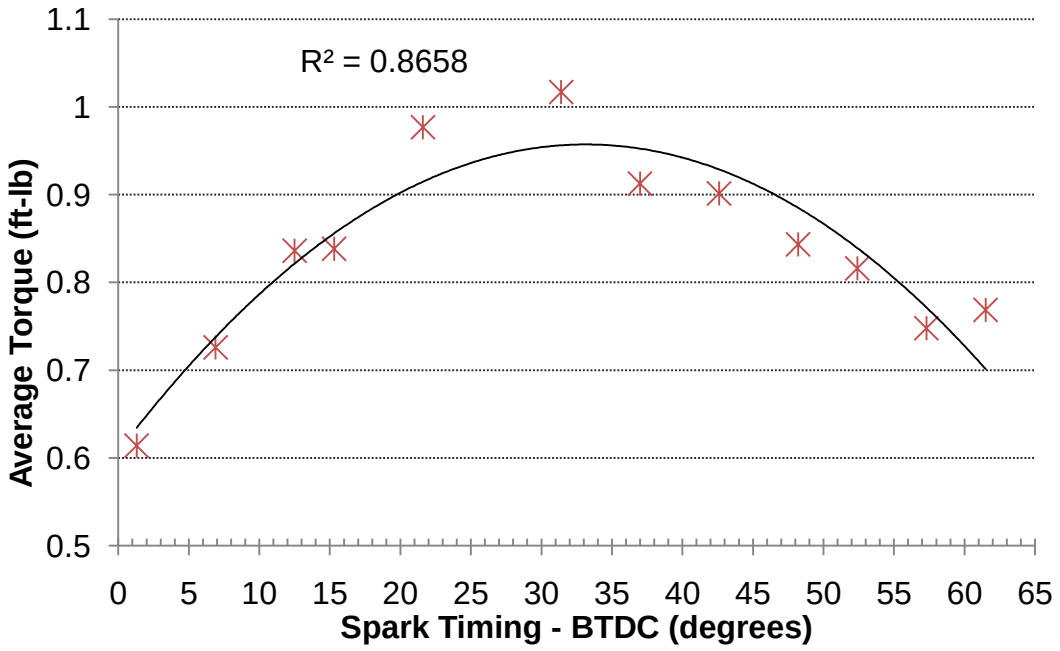

Figure 80. Average torque vs. spark timing for n-Heptane at 5700 RPM

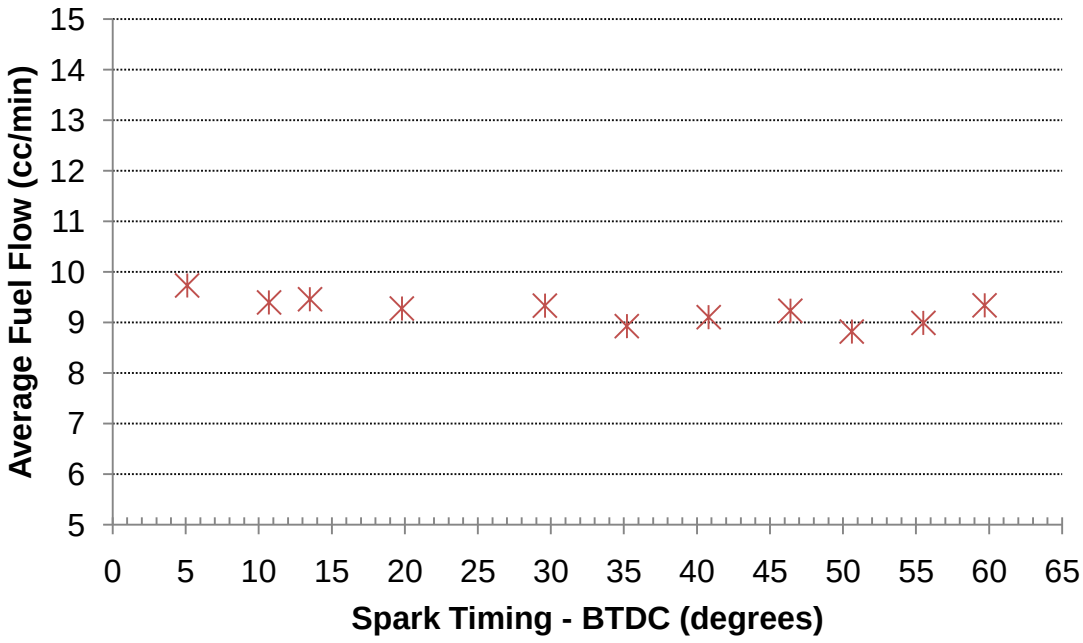

Figure 81. Average volumetric fuel flow rate vs. spark timing for n-Heptane at 5700 RPM

Heated Fuel Test #2

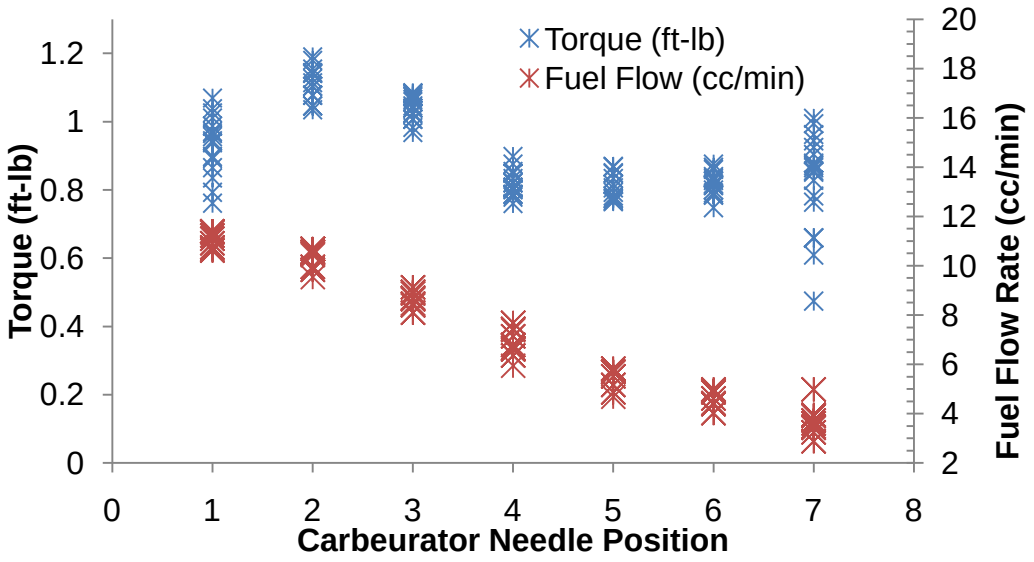

Figure 82. Raw data for varied carburetor needle position n-Heptane at ambient temperature, 4000 RPM, 85% throttle and stock timing

Heated Fuel Test #3

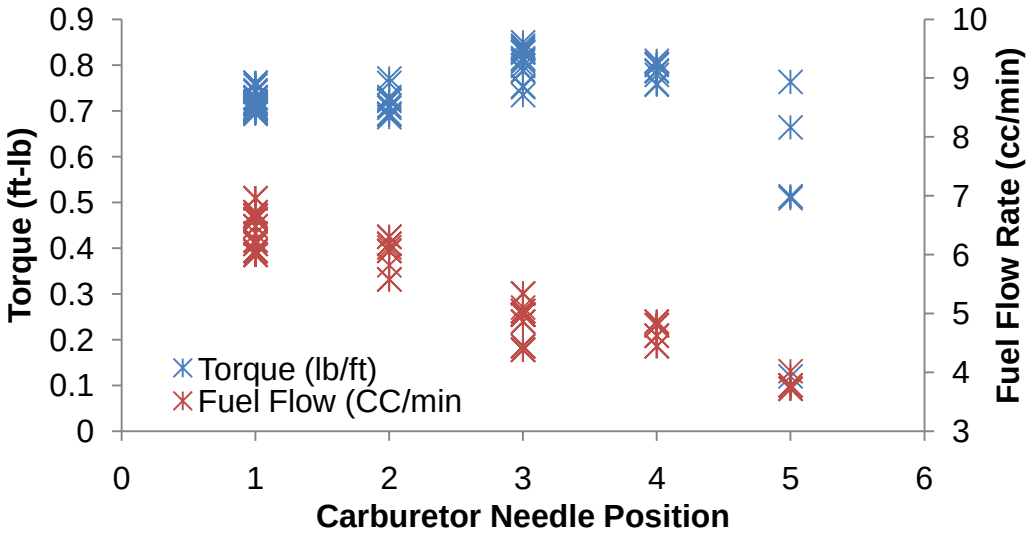

Figure 83. Raw data for varied carburetor needle position n-Heptane at 290K, 4000 RPM, 100% throttle and stock timing

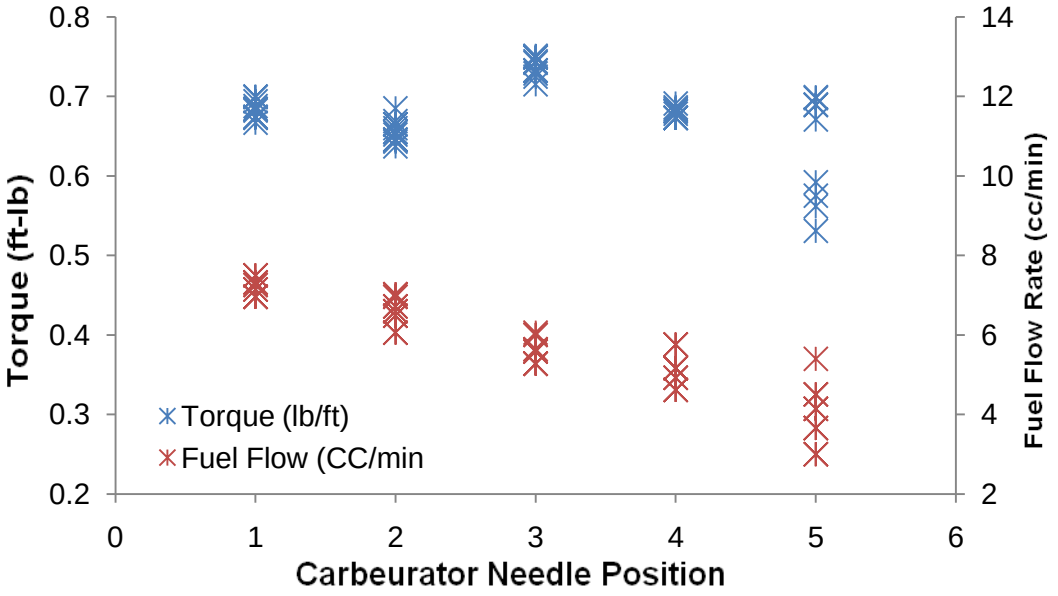

Figure 84. Raw data for varied carburetor needle position n-Heptane at 300K, 4000 RPM, 100% throttle and stock timing

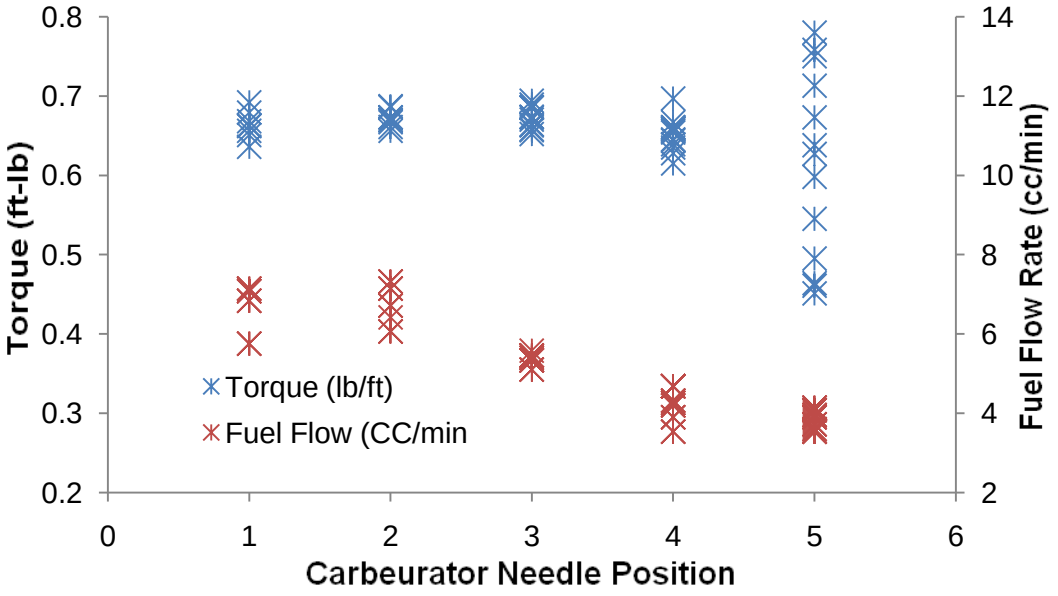

Figure 85. Raw data for varied carburetor needle position n-Heptane at 311K, 4000 RPM, 100% throttle and stock timing

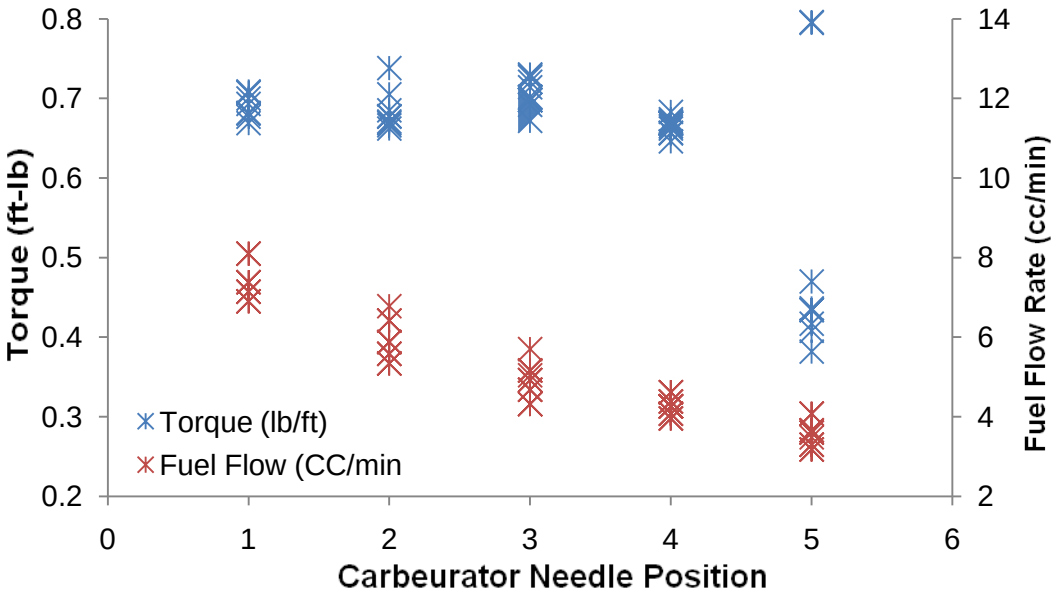

Figure 86. Raw data for varied carburetor needle position n-Heptane at 322K, 4000 RPM, 100% throttle and stock timing

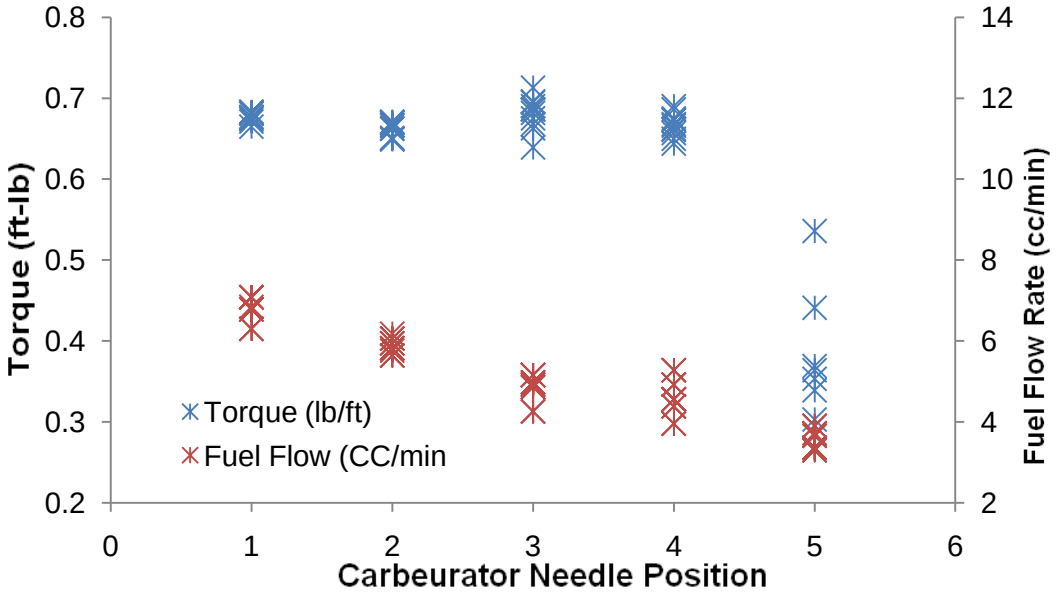

Figure 87. Raw data for varied carburetor needle position n-Heptane at 333K, 4000 RPM, 100% throttle and stock timing

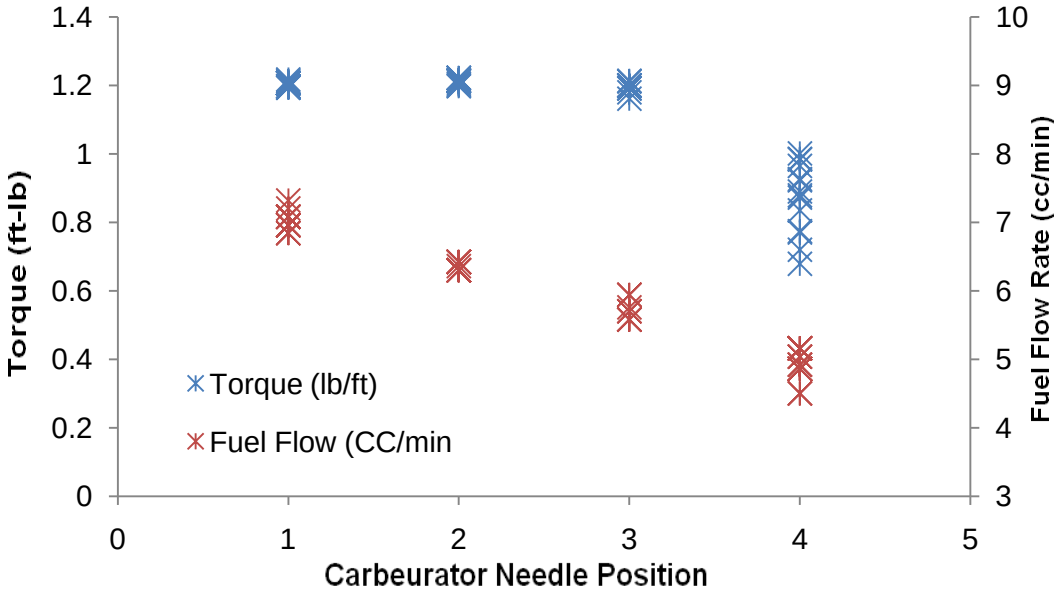

Figure 88. Raw data for varied carburetor needle position iso-Octane at 290K, 4000 RPM, 100% throttle and stock timing

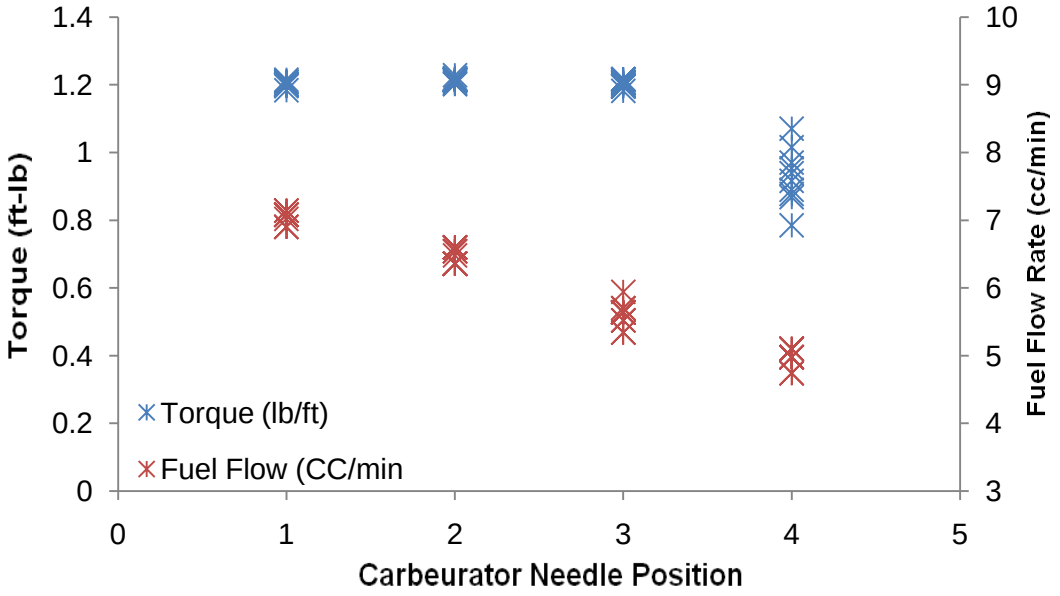

Figure 89. Raw data for varied carburetor needle position iso-Octane at 300K, 4000 RPM, 100% throttle and stock timing

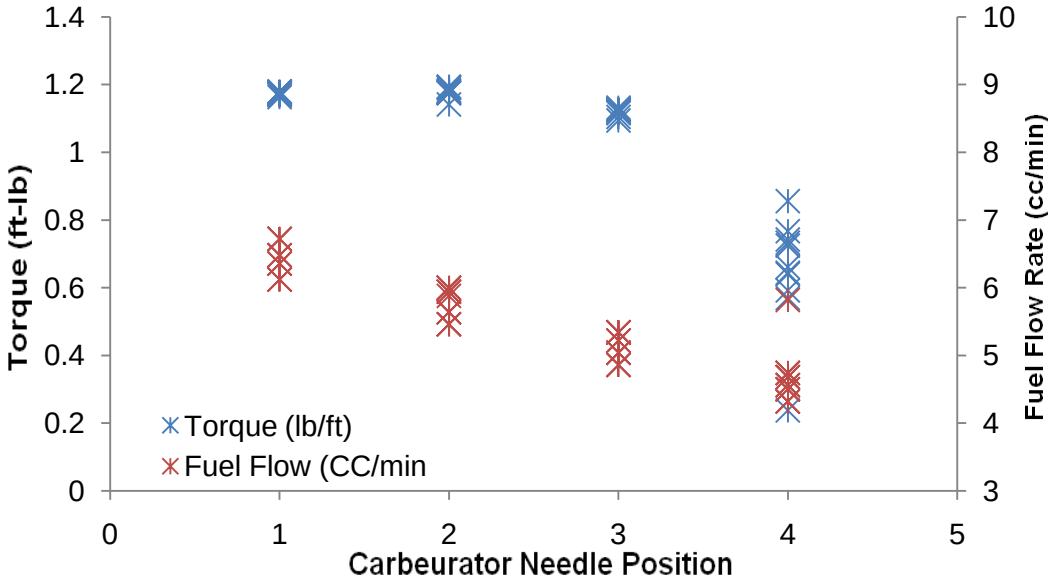

Figure 90. Raw data for varied carburetor needle position iso-Octane at 311K, 4000 RPM, 100% throttle and stock timing

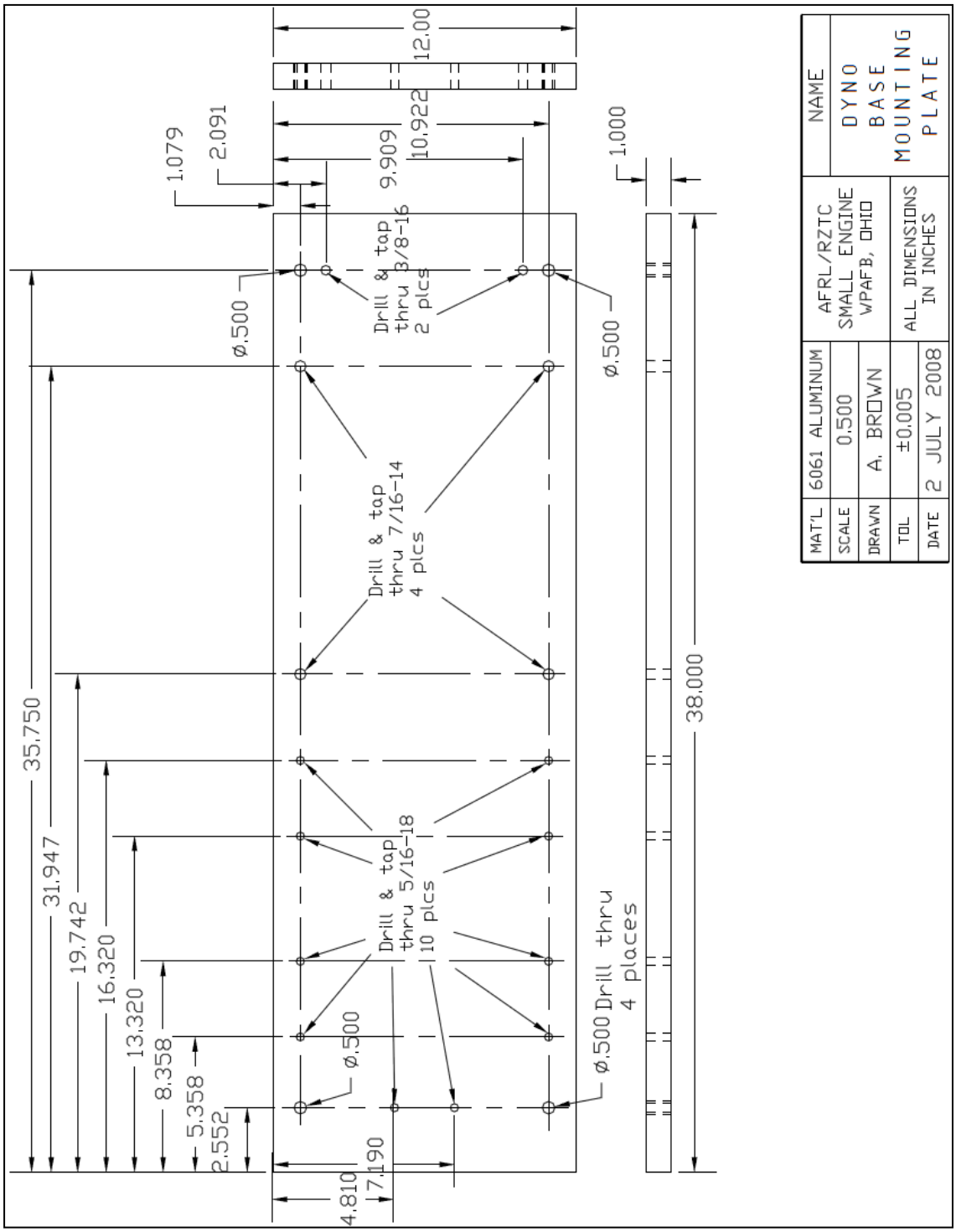
12.00
10.922
9.909
2.091
1.079
1.000
Drill & tap
thru 3/8-16
2 plcs
ø.500
ø.500
Drill & tap
thru 7/16-14
4 plcs
35.750
31.947
19.742
16.320
13.320
8.358
5.358
2.552
38.000
Drill & tap
thru 5/16-18
10 plcs
ø.500
ø.500 Drill thru
4 places
4.810
7.190
MAT'L 6061 ALUMINUM
SCALE 0.500
DRAWN A. BROWN
TOL ±0.005
DATE 2 JULY 2008
AFRL/RZTC
SMALL ENGINE
WPAFB, OHIO
ALL DIMENSIONS
IN INCHES
NAME
DYNO
BASE
MOUNTING
PLATE

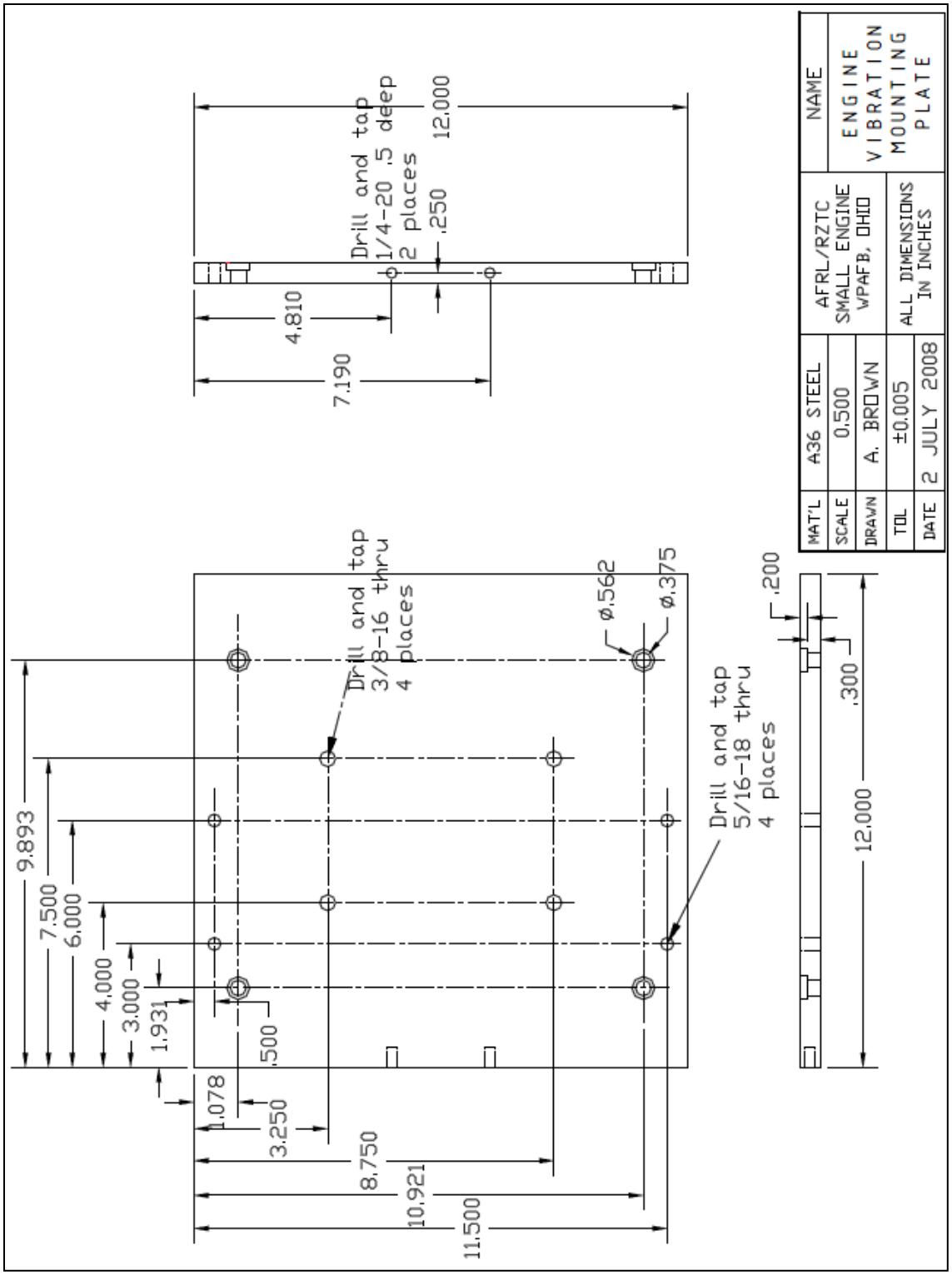
Drill and tap
1/4-20 .5 deep
2 places
.250
12.000
4.810
7.190
Drill and tap
3/8-16 thru
4 places
ø.562
ø.375
Drill and tap
5/16-18 thru
4 places
.200
.300
12.000
9.893
7.500
6.000
4.000
3.000
1.931
.500
1.078
3.250
8.750
10.921
11.500
MAT'L
A36 STEEL
SCALE
0.500
DRAWN
A. BROWN
TOL
±0.005
DATE
2 JULY 2008
AFRL/RZTC
SMALL ENGINE
WPAFB, OHIO
ALL DIMENSIONS
IN INCHES
NAME
ENGINE
VIBRATION
MOUNTING
PLATE

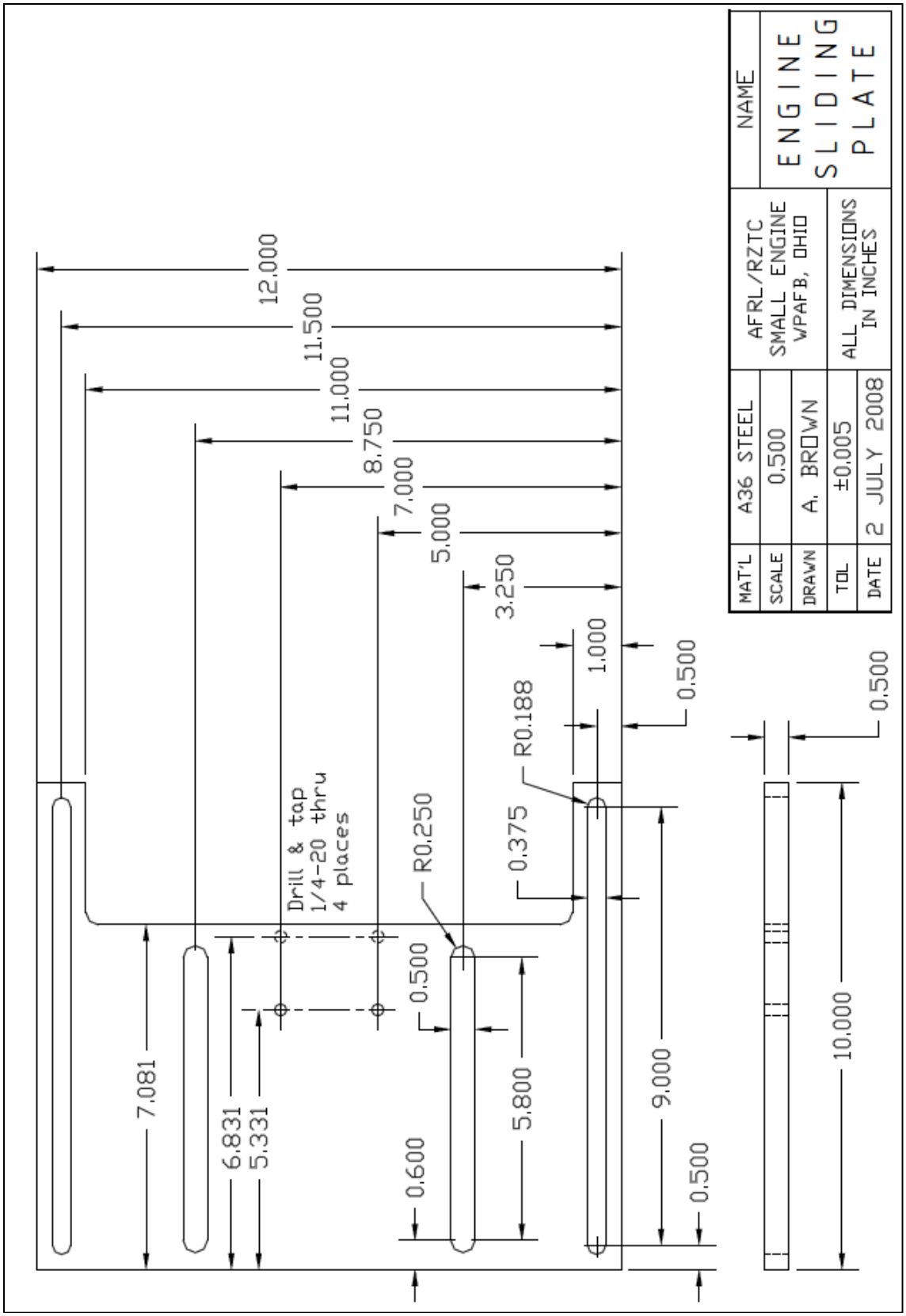
12.000
11.500
11.000
8.750
7.000
5.000
3.250
1.000
0.500
R0.188
0.375
R0.250
Drill & tap
1/4-20 thru
4 places
0.500
7.081
6.831
5.331
0.600
5.800
9.000
0.500
0.500
10.000
MAT'L
A36 STEEL
SCALE
0.500
DRAWN
A. BROWN
TOL
±0.005
DATE
2 JULY 2008
AFRL/RZTC
SMALL ENGINE
WPAFB, OHIO
ALL DIMENSIONS
IN INCHES
NAME
ENGINE
SLIDING
PLATE

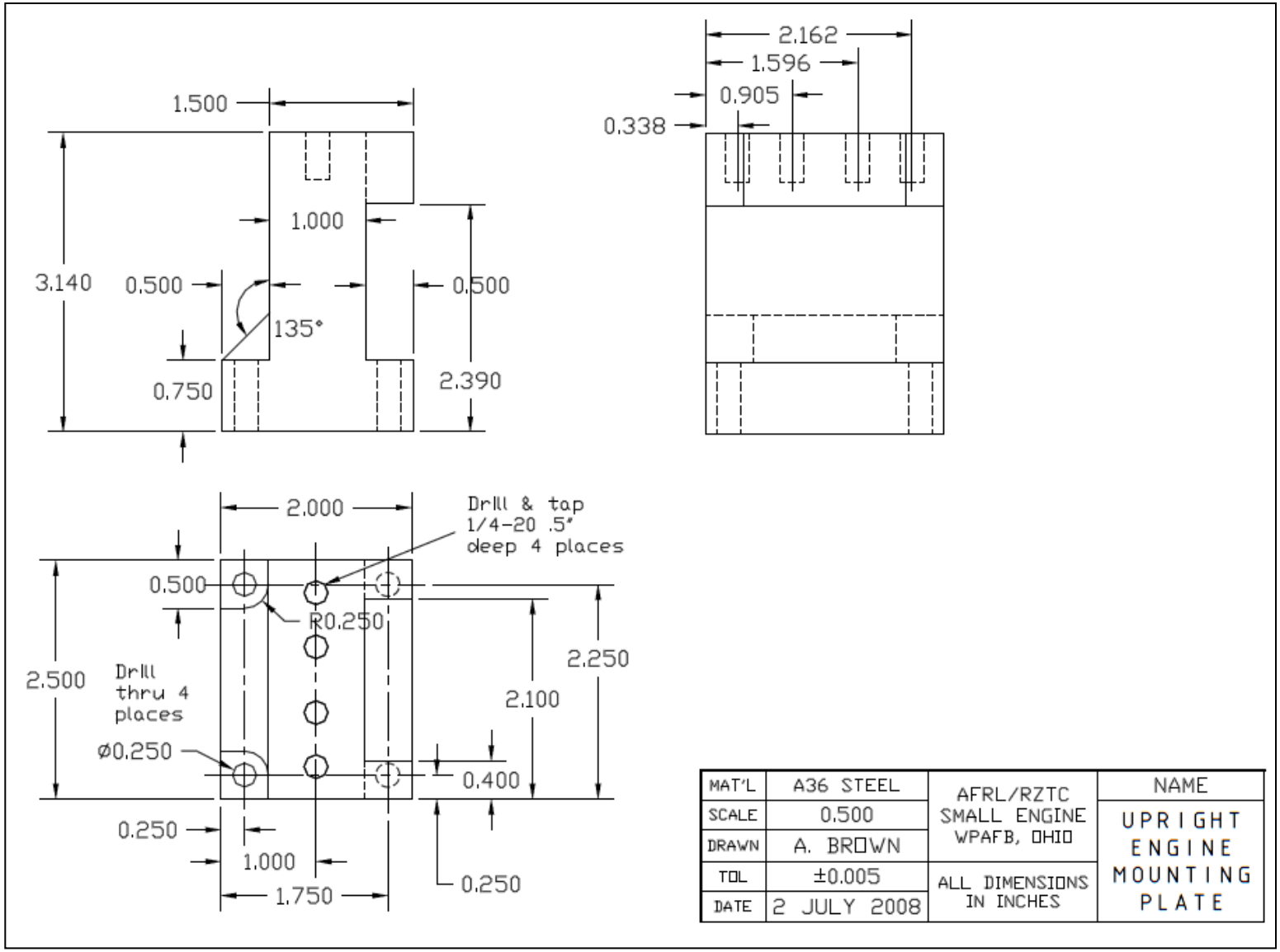

MAT'L	A36 STEEL	AFRL/RZTC SMALL ENGINE WPAFB, OHIO	NAME
SCALE	0.500		UPRIGHT ENGINE MOUNTING PLATE
DRAWN	A. BROWN		
TOL	±0.005	ALL DIMENSIONS IN INCHES	
DATE	2 JULY 2008		

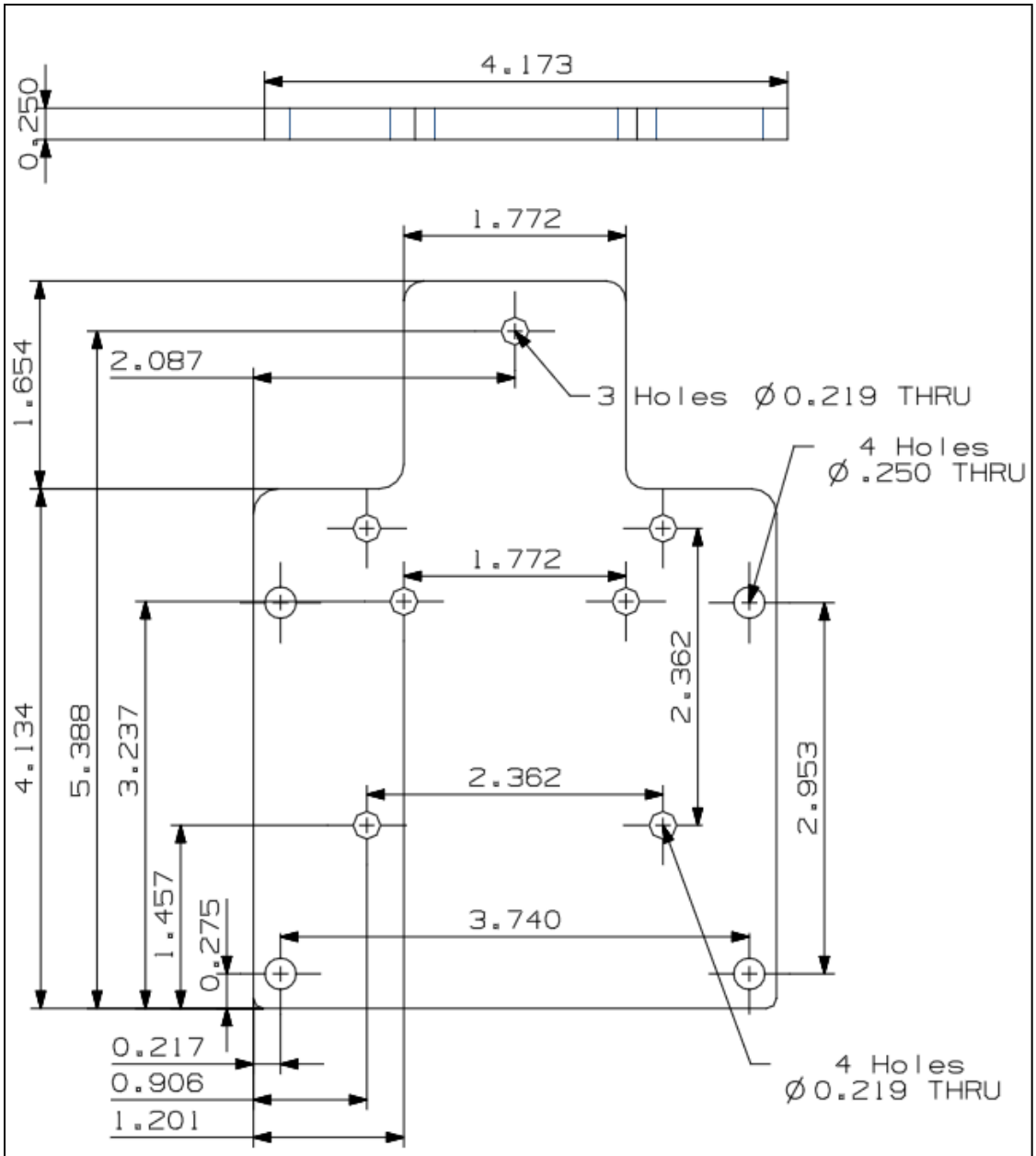

MAT'L	A36 STEEL	AFRL/RZTC SMALL ENGINE WPAFB, OHIO	NAME
SCALE	1.00		FUJI ENGINE MOUNTING PLATE
DRAWN	C. WILSON		
TOL	±0.005	ALL DIMENSIONS ARE IN INCHES	
DATE	16 NOV 2009		

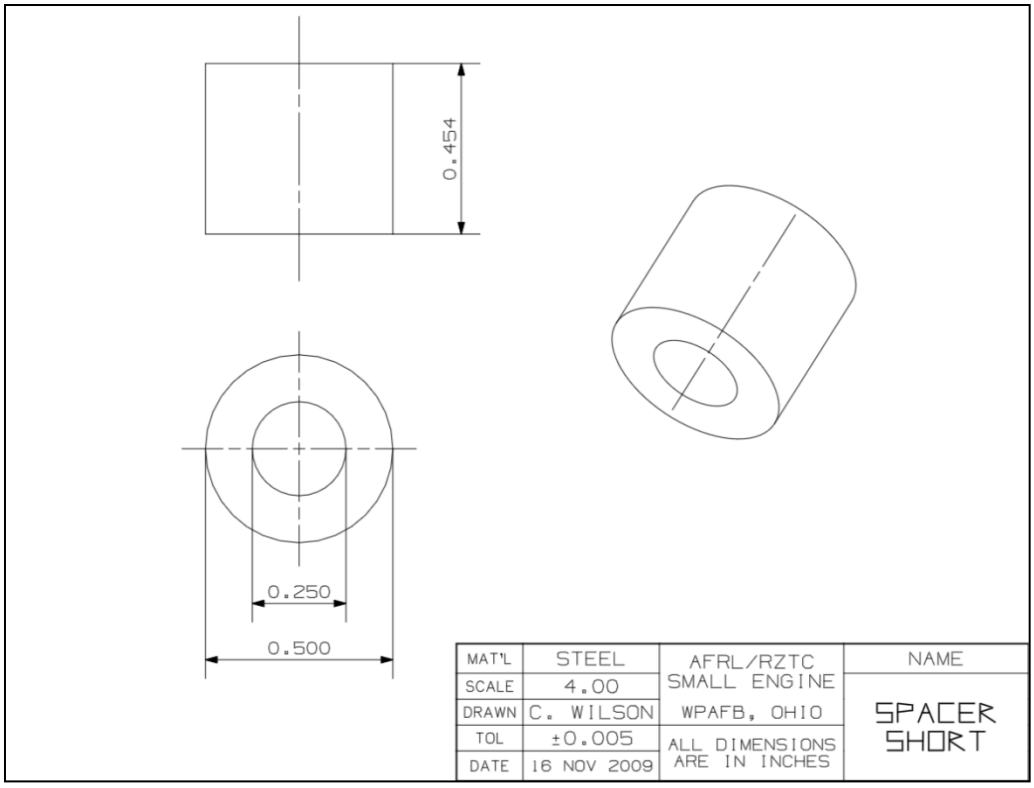

MAT'L	STEEL	AFRL/RZTC SMALL ENGINE WPAFB, OHIO	NAME
SCALE	4.00		SPACER SHORT
DRAWN	C. WILSON		
TOL	±0.005	ALL DIMENSIONS ARE IN INCHES	
DATE	16 NOV 2009		

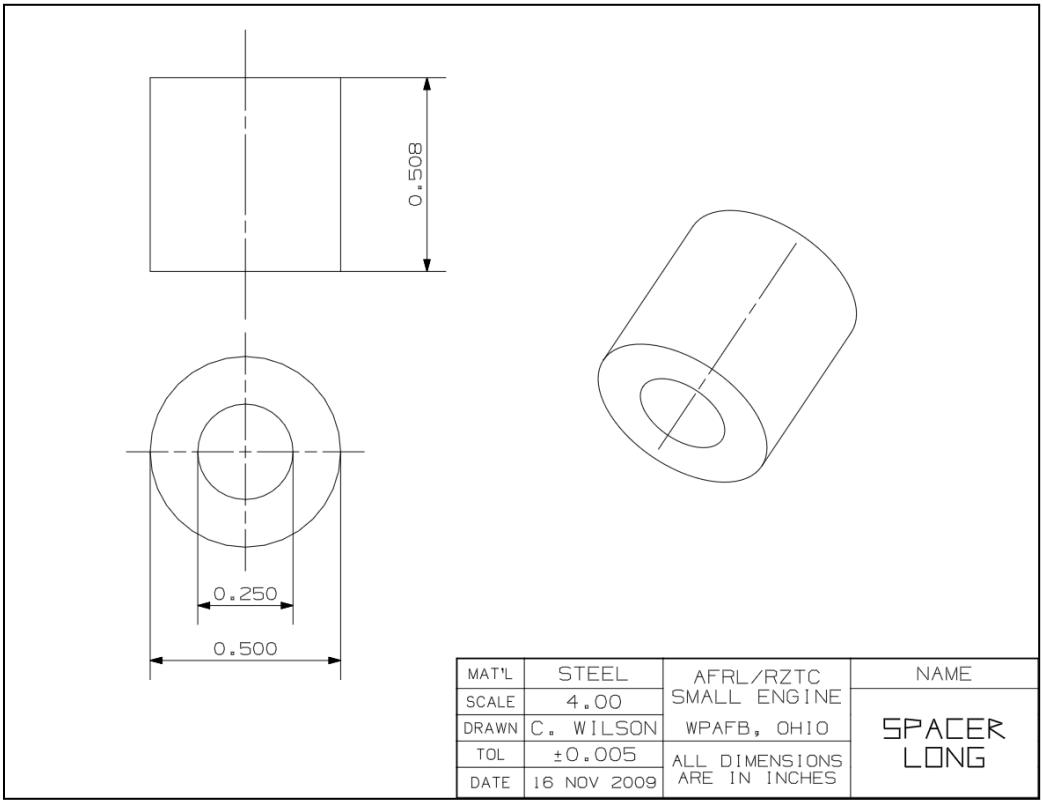

MAT'L	STEEL	AFRL/RZTC SMALL ENGINE WPAFB, OHIO	NAME
SCALE	4.00		SPACER LONG
DRAWN	C. WILSON		
TOL	±0.005	ALL DIMENSIONS ARE IN INCHES	
DATE	16 NOV 2009		

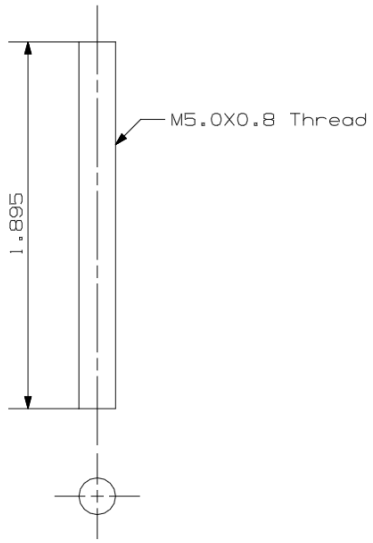

MAT'L	STEEL	AFRL/RZTC SMALL ENGINE WPAFB, OHIO	NAME
SCALE	2.00		FUJI CRANKSHAFT COVER BOLT SHORT
DRAWN	C. WILSON		
TOL	±0.005	ALL DIMENSIONS ARE IN INCHES	
DATE	16 NOV 2009		

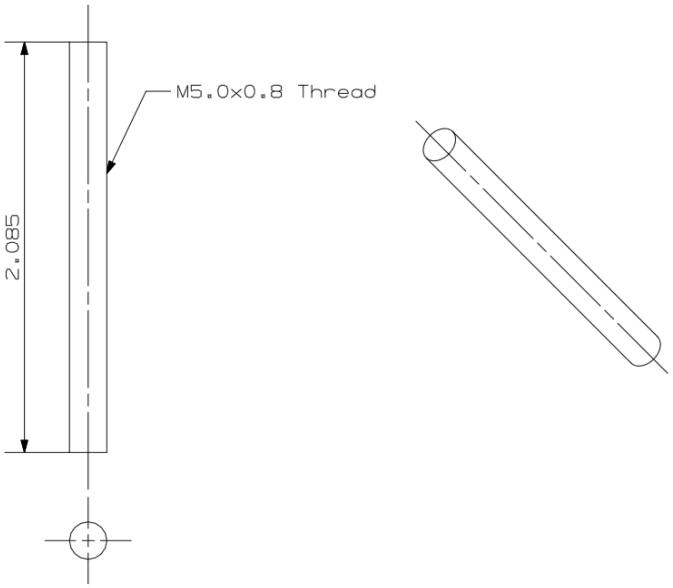

MAT'L	STEEL	AFRL/RZTC SMALL ENGINE WPAFB, OHIO	NAME
SCALE	2.00		FUJI CRANKSHAFT COVER BOLT LONG
DRAWN	C. WILSON		
TOL	±0.005	ALL DIMENSIONS ARE IN INCHES	
DATE	16 NOV 2009		

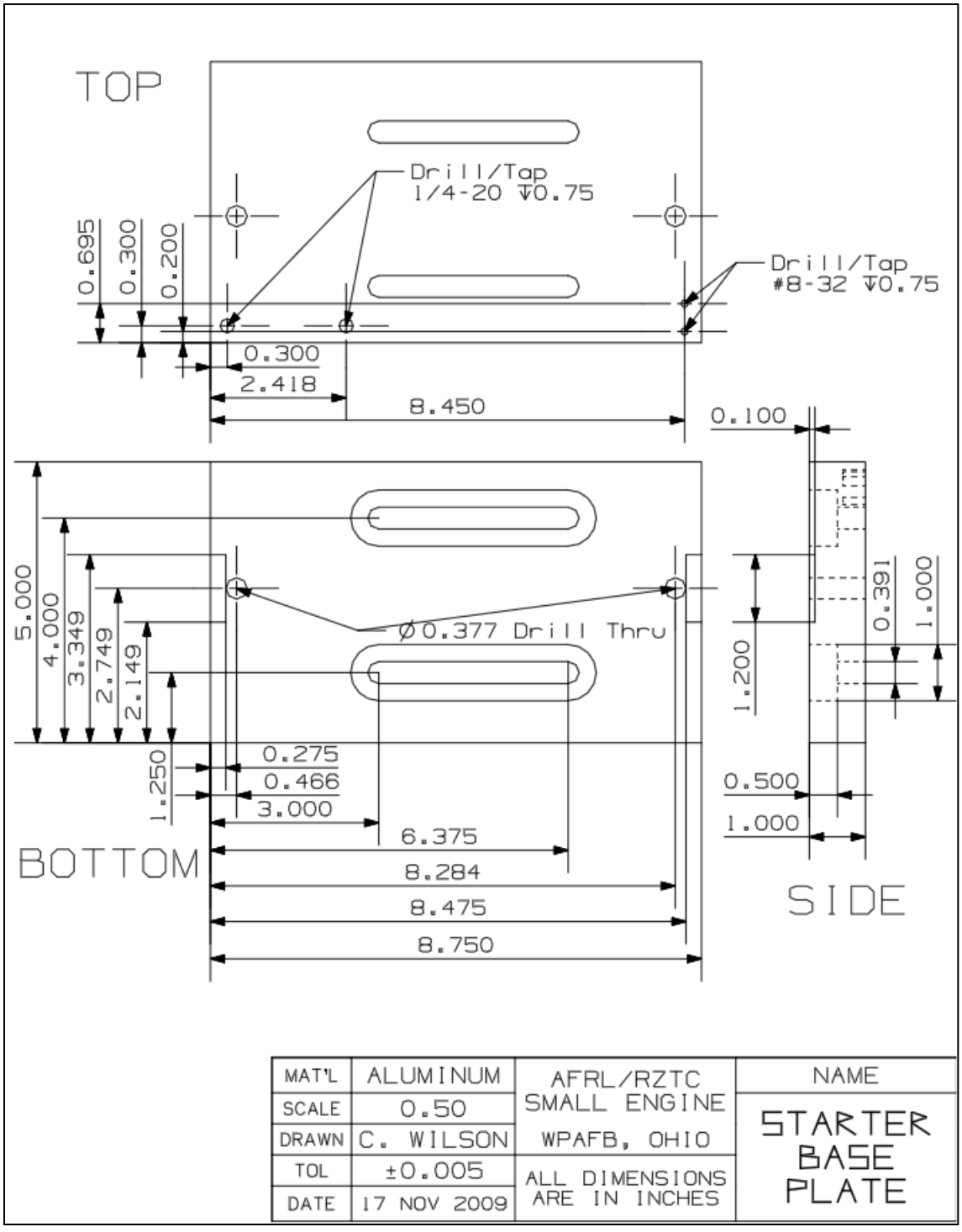

MAT'L	ALUMINUM	AFRL/RZTC SMALL ENGINE WPAFB, OHIO	NAME
SCALE	0.50		STARTER BASE PLATE
DRAWN	C. WILSON		
TOL	±0.005	ALL DIMENSIONS ARE IN INCHES	
DATE	17 NOV 2009		

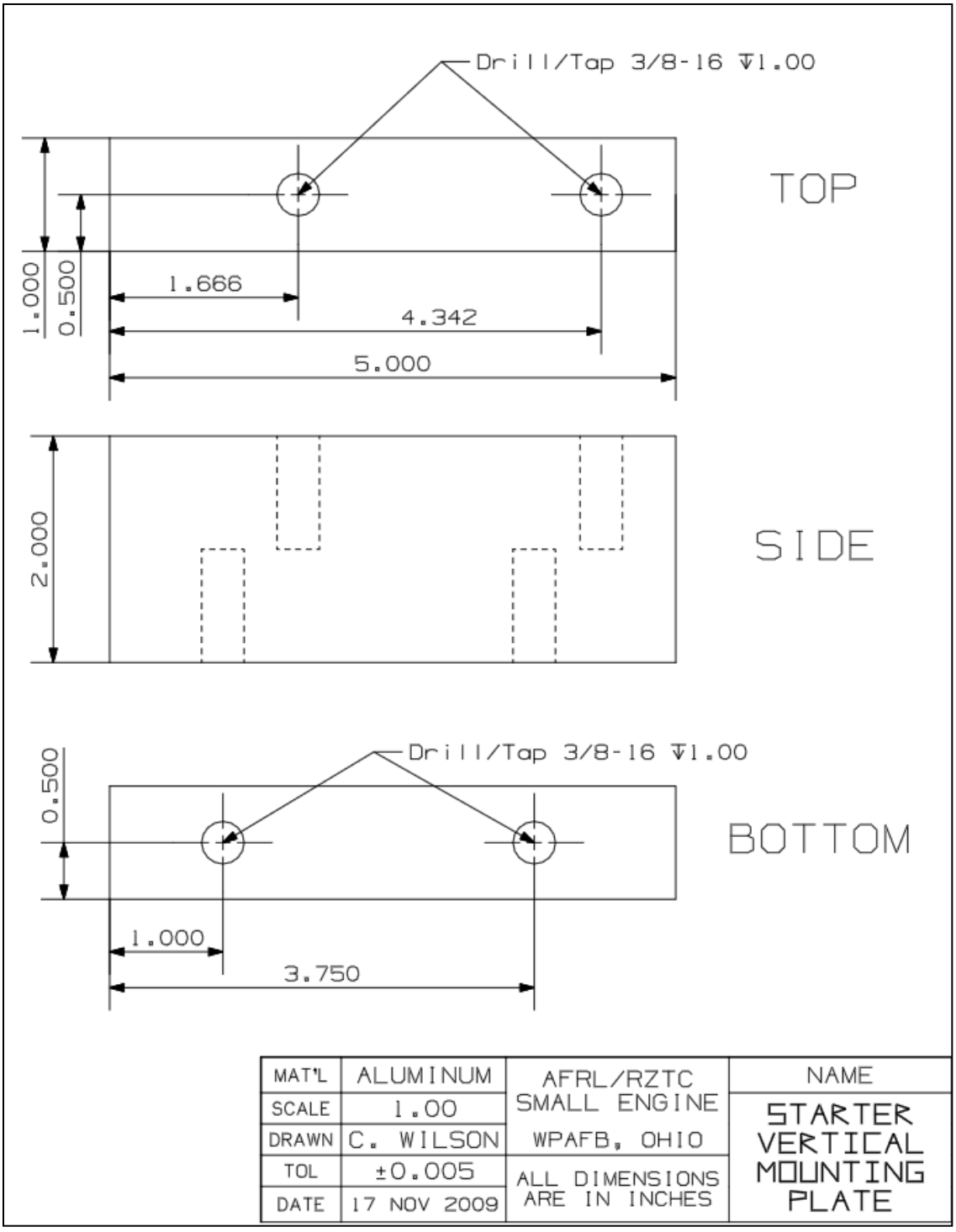

MAT'L	ALUMINUM	AFRL/RZTC SMALL ENGINE WPAFB, OHIO	NAME
SCALE	1.00		STARTER VERTICAL MOUNTING PLATE
DRAWN	C. WILSON		
TOL	±0.005	ALL DIMENSIONS ARE IN INCHES	
DATE	17 NOV 2009		

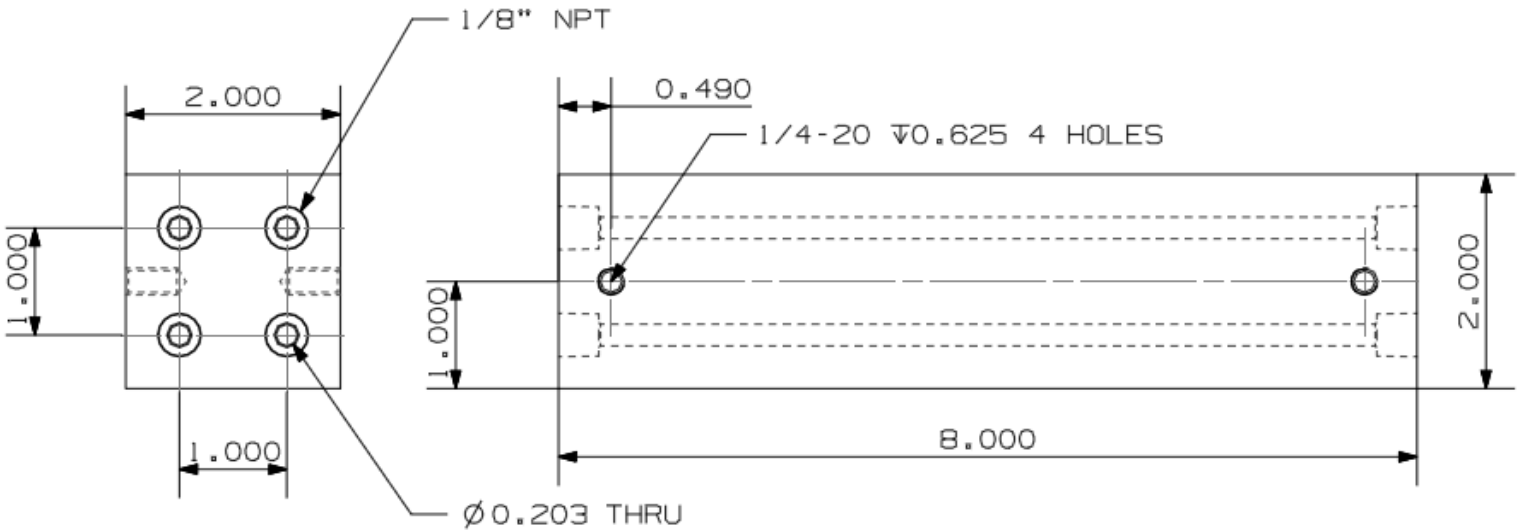

MAT'L	COPPER	AFRL/RZTC SMALL ENGINE WPAFB, OHIO	NAME
SCALE	0.75		BLOCK HEATER BODY
DRAWN	C. WILSON		
TOL	±0.005	ALL DIMENSIONS ARE IN INCHES	
DATE	10 AUG 2009		

max Max Machinery, Inc.

Model 213 Piston Flow Meter
1 to 1800 cc/min

SPECIFICATIONS

Flow Range (at 2 cP)	1 to 1800 cc/min.
Maximum Operating Pressure	70 bar or 210 bar (1000 or 3000 psi)
Displacement	0.89 cc/rev
Weight	0.6 kg
Recommended Filtration	10 micron
Port Size(s)	1/8" NPT, #4 SAE or manifold mount
Accuracy	± 0.2% of reading with a linearized transmitter ± 0.5% of reading with a non-linearized transmitter
Fluids	Most non aqueous, organic liquids

MATERIALS OF CONSTRUCTION

Body	Stainless steel, type 303
Pistons	Nitride hardened stainless steel, type 303
Crankshaft	Stainless steel
Bearings	All ball bearings, 440C stainless steel
O Rings	Viton®- standard • Teflon®, Perfluoro elastomer

DIMENSIONS

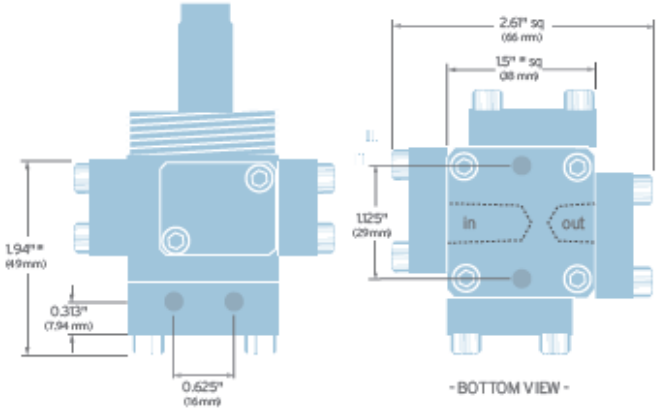

* SAE base adds 0.375" (10 mm) to height and 0.5" to face to face dimensions

MA213-000-300 • rev. 1/2009 • ©2007-9 Max Machinery, Inc.

Mineral Insulated Strip Heaters

Applications and Technical Data *(Continued)*

Specifications

Width

- 1, 1½ and 2 in. (25, 38, 51 mm), Tolerance ±1/32

Length

- 8 to 30 in. (203 to 762 mm), Tolerance ±¼

Terminations

- 1 in. (25 mm) wide—post terminals one-on-one
  1½ to 2 in. (38 to 51 mm)—post terminals two-on-one

All Widths

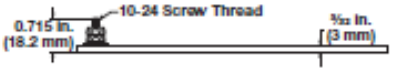

Note: In most applications mounting holes alone will not provide adequate clamping. A clamp bar should be used for each 4 in. (102 mm) of heater length.

1 in. (25 mm) Wide

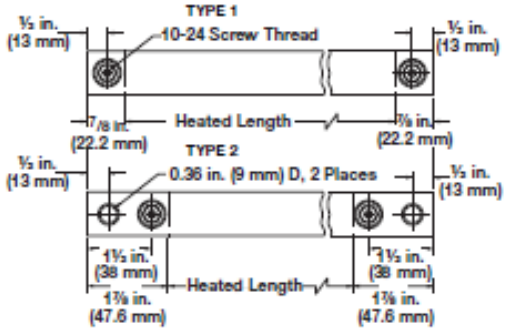

1½ in.–2 in. (38 – 51 mm) Wide

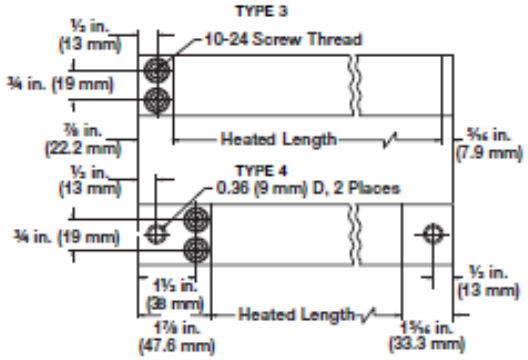

Stock Heater Code Numbers (Parallel Terminals) Type 3 and 4

Width in.	Width (mm)	Length in.	Length (mm)	Volts	Power (Watts)	Watt Density W/in²	Watt Density (W/cm²)	Approx. Net Wt. lbs.	Approx. Net Wt. (kg)	Type	Code Number
1½	(38)	8	(203)	120	500	48	(7.4)	0.3	(0.15)	3	**MS1J8AS1**
1½	(38)	8	(203)	240	500	50	(7.8)	0.3	(0.15)	3	**MS1J8AS3**
1½	(38)	12	(305)	120	350	26	(4.0)	0.5	(0.2)	4	**MS1J12AV2**①
1½	(38)	12	(305)	240	350	26	(4.0)	0.5	(0.2)	4	**MS1J12AV3**①
1½	(38)	12	(305)	120	800	49	(7.6)	0.5	(0.2)	3	**MS1J12AS1**
1½	(38)	12	(305)	240	800	49	(7.6)	0.5	(0.2)	3	**MS1J12AS2**
1½	(38)	18	(457)	120	1000	40	(6.2)	0.8	(0.3)	3	**MS1J18AS1**
1½	(38)	18	(457)	240	1000	40	(6.2)	0.8	(0.3)	3	**MS1J18AS2**

① Denotes units with mounting holes. Mounting holes are 0.36 in. (9 mm) in diameter, and are intended for use with ¼ in. (6 mm) bolts. Centers of mounting holes are located ½ in. (13 mm) from the ends of the heater.
Note: Type 1 and 2 are made-to-order only.

Vita

Captain Cary Wayne Wilson was born in Roanoke, Virginia and graduated from William Byrd High School in June 2001. He enrolled in undergraduate studies for Mechanical Engineering during the Fall of 2001 at West Virginia University in Morgantown, West Virginia. In addition he enrolled in the four year Air Force Reserve Officer Training Corps program at Detachment 915. He graduated cum lade with a B.S. in mechanical engineering and was commissioned in the United States Air Force in May 2005.

Cary's first assignment was at the 641st Combat Systems Support Squadron at Wright Patterson AFB, as an integration engineer in July 2005. In August 2006, he earned the lead engineer position for the Night Vision Cueing and Display program. Following this assignment, he enrolled in the Graduate School of Engineering and Management at the Air Force Institute of Technology in August 2008, seeking a degree in Aeronautical Engineering. Upon graduating, he will be assigned to the AFRL Propulsion Directorate at Wright Patterson AFB, continuing his research on small internal combustion engines.

REPORT DOCUMENTATION PAGE

Form Approved
OMB No. 074-0188

The public reporting burden for this collection of information is estimated to average 1 hour per response, including the time for reviewing instructions, searching existing data sources, gathering and maintaining the data needed, and completing and reviewing the collection of information. Send comments regarding this burden estimate or any other aspect of the collection of information, including suggestions for reducing this burden to Department of Defense, Washington Headquarters Services, Directorate for Information Operations and Reports (0704-0188), 1215 Jefferson Davis Highway, Suite 1204, Arlington, VA 22202-4302. Respondents should be aware that notwithstanding any other provision of law, no person shall be subject to an penalty for failing to comply with a collection of information if it does not display a currently valid OMB control number.
PLEASE DO NOT RETURN YOUR FORM TO THE ABOVE ADDRESS.

1. REPORT DATE *(DD-MM-YYYY)*	2. REPORT TYPE	3. DATES COVERED *(From – To)*
25-03-2010	Master's Thesis	September 2008 – March 2010

TITLE AND SUBTITLE

PERFORMANCE OF A SMALL INTERNAL COMBUSTION ENGINE USING N-HEPTANE AND ISO-OCTANE

5a. CONTRACT NUMBER

5b. GRANT NUMBER

5c. PROGRAM ELEMENT NUMBER

6. AUTHOR(S)

Cary W. Wilson, Captain, USAF

5d. PROJECT NUMBER

5e. TASK NUMBER

5f. WORK UNIT NUMBER

7. PERFORMING ORGANIZATION NAMES(S) AND ADDRESS(S)
Air Force Institute of Technology
Graduate School of Engineering and Management (AFIT/ENY)
2950 Hobson Way, Building 640
WPAFB OH 45433-8865

8. PERFORMING ORGANIZATION REPORT NUMBER

AFIT/GAE/ENY/10-M28

9. SPONSORING/MONITORING AGENCY NAME(S) AND ADDRESS(ES)
AFRL/RZTC
ATTN: Dr. Frederick R. Schauer
Building 71A, D-Bay, 7th Street
Wright Patterson AFB, OH 45433 DSN: 785-6462

10. SPONSOR/MONITOR'S ACRONYM(S)

11. SPONSOR/MONITOR'S REPORT NUMBER(S)

12. DISTRIBUTION/AVAILABILITY STATEMENT
APPROVED FOR PUBLIC RELEASE; DISTRIBUTION UNLIMITED.

13. SUPPLEMENTARY NOTES

14. ABSTRACT

With the sustained interest in Unmanned Aircraft Systems (UAS) and Micro Air Vehicles (MAV), the military services have a real need for vehicles powered by an internal combustion (IC) engine that can run efficiently on heavy hydrocarbon fuels, especially JP-8 due to established logistics. This thesis concerns the results of running a two horsepower, 4-stroke, spark-ignition engine (FUJI BF34-EI) with both iso-Octane and n-Heptane. Results include the knocking characteristic of this engine with n-Heptane, a comparison of the brake specific fuel consumption (BSFC) of the two fuels in a factory delivered engine configuration over a 17x10 APC propeller loading, a comparison of the heated fuel effects on BSFC and torque of the two fuels and the effects of varied spark timing with n-Heptane on BSFC and torque. It is shown with stock ignition timing and fuel at ambient temperature, n-Heptane exhibits on average less specific fuel consumption than iso-Octane; specifically, an average of 4.1% over the entire engine loading and 12.61% over the stock propeller engine loading. It is concluded that the knocking characteristic of a zero octane number (ON) fuel using a stock configuration in this engine is negligible, thus allowing the USAF to run any ON fuel for this particular engine. Additionally, with spark timing advanced or retarded beyond the stock setting, it is shown to decrease BSFC on average 9.4% with n-Heptane. Lastly, the performance effects of heating n-Heptane up to 344K and iso-Octane up to 311K are shown to be negligible.

15. SUBJECT TERMS
Small engine, Fuji, BSFC, heptane, octane, JP-8, UAS, spark ignition, knock, combustion

16. SECURITY CLASSIFICATION OF:			17. LIMITATION OF ABSTRACT	18. NUMBER OF PAGES	19a. NAME OF RESPONSIBLE PERSON
a. REPORT	b. ABSTRACT	c. THIS PAGE			Dr. Paul I. King
U	U	U	UU	147	19b. TELEPHONE NUMBER *(Include area code)* (937) 255-3636, ext 4628 (paul.king@afit.edu)

Standard Form 298 (Rev. 8-98)
Prescribed by ANSI Std. Z39-18